SRESA's International Journal of

LIFE CYCLE RELIABILITY AND SAFETY ENGINEERING

Vol.1 **Issue No.4** **Oct – Dec 2012** **ISSN – 2250 0820**

Special Issue :

on Papers Presented at "International Symposium on Engineering under Uncertainty: Safety Assessment and Management – ISEUSAM-2012" Part - 2

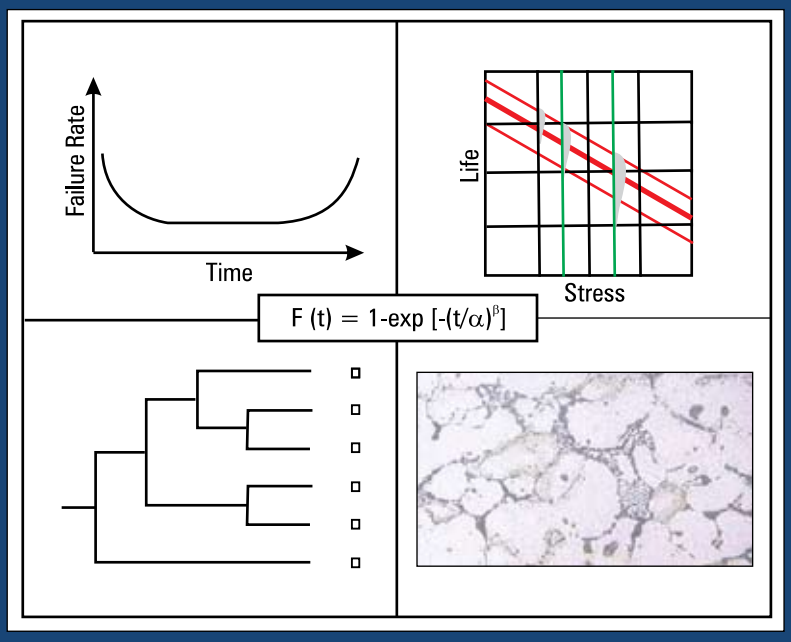

Guest-Editors
Subrata Chakrab
Sankaran Mahad

Chief-Editors
P.V. Varde
A.K. Verma
Michael G. Pecht

Society for Reliability and Safety

website : http://www.sresa.org.in

SRESA Journal of Life Cycle Reliability and Safety Engineering

Extensive work is being performed world over on assessment of Reliability and Safety for engineering systems in support of decisions. The increasing number of risk-based / risk-informed applications being developed world over is a testimony to the growth of this field. Here, along with probabilistic methods, deterministic methods including Physics-of-Failure based approach is playing an important role. The International Journal of Life Cycle Reliability and Safety Engineering provides a unique medium for researchers and academicians to contribute articles based on their R&D work, applied work and review work, in the area of Reliability, Safety and related fields. Articles based on technology development will also be published as Technical Notes. Review articles on Books published in the subject area of the journal will also form part of the publication.

Society for Reliability and Safety has been actively working for developing means and methods for improving system reliability. Publications of quarterly News Letters and this journal are some of the areas the society is vigorously pursuing for societal benefits. Manuscript in the subject areas can be communicated to the Chief Editors. Manuscript will be reviewed by the experts in the respective area of the work and comments will be communicated to the corresponding author. The reviewed final manuscript will be published and the author will be communicated the publication details. Instruction for preparing the manuscript has been given on inside page of the end cover page of each issue. The rights of publication rest with the Chief-Editors.

SCOPE OF JOURNAL

System Reliability analysis	**Structural Reliability**	**Risk-based applications**
Statistical tools and methods	Remaining life prediction	Technical specification optimization
Probabilistic Safety Assessment	Reliability based design	Risk-informed approach
Quantitative methods	Physics-of-Failure methods	Risk-based ISI
Human factor modeling	Probabilistic Fracture Mechanics	Risk-based maintenance
Common Cause Failure analysis	Passive system reliability	Risk-monitor
Life testing methods	Precursor event analysis	Prognostics & health management
Software reliability	Bayesian modeling	Severe accident management
Uncertainty modeling	Artificial intelligence in risk and reliability modeling	Risk-based Operator support systems
Dynamic reliability models	Design of Experiments	Role of risk-based approach in Regulatory reviews
Sensitivity analysis	Fuzzy approach in risk analysis	Advanced electronic systems reliability modeling
Decision support systems	Cognitive framework	Risk-informed asset management

SRESA AND ITS OBJECTIVES

a) To promote and develop the science of reliability and safety.

b) To encourage research in the area of reliability and safety engineering technology & allied fields.

c) To hold meetings for presentation and discussion of scientific and technical issues related to safety and reliability.

d) To evolve a unified standard code of practice in safety and reliability engineering for assurance of quality based professional engineering services.

e) To publish journals, books, reports and other information, alone or in collaboration with other organizations, and to disseminate information, knowledge and practice of ensuring quality services in the field of Reliability and Safety.

f) To organize reliability and safety engineering courses and / or services for any kind of energy systems like nuclear and thermal power plants, research reactors, other nuclear and radiation facilities, conventional process and chemical industries.

g) To co-operate with government agencies, educational institutions and research oganisations

SRESA Journal of

LIFE CYCLE RELIABILITY AND SAFETY ENGINEERING

Vol.1 Issue No.4 Oct–Dec 2012 ISSN – 2250 0820

SOCIETY FOR RELIABILITY AND SAFETY

Typeset & Printed

EBENEZER PRINTING HOUSE
Unit No. 5 & 11, 2nd Floor, Hind Services Industries,
Veer Savarkar Marg,
Dadar (west), Mumbai -28
Tel.: 2446 2632/ 3872
E-mail: outwork@gmail.com

Life Cycle Reliability and Safety Engineering
Vol.1 Issue 3 (2012) iv-v

Guest Editorial

International Symposium on Engineering under Uncertainty: Safety Assessment and Management (ISEUSAM - 2012) was organised during January 4 to 6 to facilitate the discussion for a better understanding and management of uncertainty and risk, encompassing various aspects of safety and reliability of engineering systems. Thirteen Selected papers were selected to be compiled in two special issues of *Society for Reliability and Safety (SRESA) Journal of Life Cycle Reliability and Safety Engineering* to provide a snapshot of the various papers discussed during ISEUSAM - 2012. Six papers were already published in the third issue. All the seven papers included in this fourth issue are revised versions of those presented in the symposium. *The first paper* deals with a novel approach to obtain the seismic fragility curves for a primary containment structure using incremental dynamic analysis. The seismic fragility curves obtained by using the proposed approach are found to be more realistic than those obtained using the conventional approach considering an elastic response spectrum and a linear elastic seismic analysis of the structure. *The second paper* deals with computational studies of pressurized air flow through cracks in concrete. The statistical crack model available in the literature has been refined to incorporate local tortuosity of the crack due to the smallest material inhomogeneity that can affect the airflow rates. The local tortuosity is introduced using fractal geometry based curves. *The third paper* deals with estimating the rain-flow fatigue damage in wind turbine blades using the polynomial chaos expansion approach. The turbine blade is modelled as a two-dimensional airfoil and is subjected to stationary Gaussian loading. The fatigue damage due to this loading is described through the rain-flow cycle counting method. *The fourth paper* deals with safety evaluation of a pressure vessel made of titanium alloy based on the data collected during manufacturing and operation. An attempt has also been made to carry out multi objective design analysis to suggest optimum design parameters for design operating conditions taking into account the effect of variation of design parameters. *The fifth paper* focuses on the stochastic response surface method to evaluate the reliability index. The implicit limit state is modelled using a series expansion of standard normal random variables. Once the order of the polynomial and subsequently the coefficients are evaluated, the reliability index is obtained by a gradient- based approach. *The sixth paper* is the inaugural keynote paper that presents the author's perspective of engineering under uncertainty. The past, present and future trends of reliability assessment methods, applicable to many branches of engineering including reliability evaluation of very large structures are discussed, covering cases with both explicit and implicit limit state functions. The necessity of estimating risks for both strength and serviceability limit states isdiscussed. Risk management in the context of decision analysis framework is also brieflypresented. The use of artificial neural networks and soft computing, incorporation of cognitive sources of uncertainty, developing necessary computer programs, and education-related issues are discussed towards future directions. *The last paper* summarizes the growth in the area of structural health assessment from infancy (i.e. hitting something with a hammer and listening to sound) to the most recent development of wireless sensors and the associated advanced signal processing algorithms. Studies by the authors are also discussed, and some of the future challenges in structural health assessment are identified. Since this is a relatively new multi-disciplinary area, the education component is also highlighted at the end.

The Guest Editors would like to express their deep gratitude to all authors for their time and efforts devoted to the completion of their contributions. We also would like to specially thank Professor Achintya Haldar, Chair, Scientific Committee of ISEUSAM 2012 for his in-depth reviews and recommendations. In addition, we are most appreciative of the Editors of *SRESA Journal of Life Cycle Reliability and Safety Engineering*, for their kind invitation to edit this Special Issue.

Guest Editors

Subrata Chakraborty Department of Civil Engineering, Bengal Engineering and Science University, Shibpur Howrah - 711103 INDIA Ph:03326684561-63(ext 281) Fax:03326682916 Email: schak@civil.becs.ac.in	Sankaran Mahadevan Department of Civil & Environmental Engineering, 272 Jacobs Hall Vanderbilt University VU Station B 356077 Nashville, TN 37235-6077 Ph:615-322-3040 Fax:615-322-3365Email: sankaran. mahadevan@vanderbilt.edu

Dr. Subrata Chakraborty, a fellow of the Indian National Academy Engineering, is currently a Professor at Bengal Engineering and Science University, Shibpur. He did his bachelor of Civil Engineering at Bengal Engineering College, Shibpur, M. Tech. and PhD at IIT Kharagpur. He visited RWTH, Aachen, Germany in 2009, 2010 as a Humboldt Fellow, University of Arizona, Tucson, USA in 2005 as a BOYSCAST Fellow and was a Research Associate at University of Cambridge, UK in 2003. Prof. Chakraborty's research interests include Stochastic Finite Element and Sensitivity Analysis, Dynamic Analysis under Seismic, Wind and Blast load, Seismic Vulnerability Assessment, Reliability under Hybrid Uncertainty, Robust and Reliability Based Optimization, Fibre Reinforced Concrete, Structural Control and Health Monitoring, etc. He has completed a number of research projects funded by DST, UGC, CSIR etc. and international collaborative research in Indo-Italian Cultural Exchange Programme of UGC and CP-STIO programme of DST etc. Prof. Chakraborty has supervised four doctoral and forty master theses. He has authored more than hundred technical articles including international and national journals, conference proceedings, book and book chapters. Prof. Chakraborty has served as a managing editor, associate editor and member of the editorial board of national and international journals. In recognition of his contribution in Engineering Science, Prof Chakraborty has received several awards and laurels as honourable as the Humboldt Fellowship for Experienced Researchers, the INAE Young Engineer Award, the BOYSCAST Fellowship, the Young Faculty Research Award etc.

Dr. Sankaran Mahadevan is John R. Murray Sr. Professor of Engineering at Vanderbilt University, and founder-director of NSF-funded IGERT multidisciplinary doctoral program in Reliability and Risk Engineering and Management at Vanderbilt University. He has twenty five years of research and teaching experience in the areas of reliability and risk analysis, uncertainty quantification, design optimization, materials durability, and structural health monitoring. His research has been funded by many U.S. agencies such as NSF, NASA, FAA, DOD, DOE, DOT, NRC, and private industry such as GM, Chrysler, Union Pacific, and American Association of Railroads. He has directed 34 Ph.D. dissertations and 22 M.S. theses, taught many industry short courses on risk and reliability methods, and authored more than 350 technical publications, including two textbooks and 150 peer-reviewed journal articles.

Professor Mahadevan has served as Technical and General Chair of the AIAA SDM conference and the AIAA Non-Deterministic Approaches Conference. In addition, he has served as Chair of several ASCE committees and is on the Editorial Board of several journals.

Professor Mahadevan obtained his B.Tech from Indian Institute of Technology, Kanpur, M.S. from Rensselaer Polytechnic Institute, Troy, NY, and Ph.D. from Georgia Institute of Technology, Atlanta, GA.

Life Cycle Reliability and Safety Engineering
Vol.1 Issue 4 (2012) 01-09

Seismic Fragility Analysis of a Primary Containment Structure Using IDA

Tushar K. Mandal[1], Siddhartha Ghosh[1], Ajai S Pisharady[2]
[1]*Department of Civil Engineering, Indian Institute of Technology Bombay, Mumbai, India*
[2] *Siting & Structural Engineering Division, Atomic Energy Regulatory Board, Mumbai, India*
E-mail: sghosh@civil.iitb.ac.in

Abstract

The seismic fragility of a structure is the probability of exceeding certain limit state of performance given a specific level of hazard. This fragility is typically estimated for multiple hazard levels considering monotonically increasing intensity measures, such as peak ground acceleration (PGA). The seismic safety of the primary/inner containment structure, which is the most important civil engineering structure in a nuclear power plant (NPP) housing the reactor and other major safety related components, is of utmost concern for both old and new NPP. This paper presents a novel approach of obtaining the seismic fragility curves for a primary containment structure using incremental dynamic analysis (IDA). The limit state of performance selected for these fragility estimations is based on the collapse of the structure. In order to reduce the computation involved, a simple 'stick model' of the containment structure is used for the nonlinear response-history analyses in the multi-earthquake IDA. The seismic fragility curves obtained using the proposed approaches are compared with those obtained using the conventional approach considering an elastic response spectrum and a linear elastic seismic analysis of the structure. The IDA based fragilities are found to be more realistic than those obtained using conventional methods.

***Keywords:** fragility analysis, probabilistic seismic risk analysis, nuclear containment, inner containment, incremental dynamic analysis*

1. Introduction

The objective of seismic probabilistic safety assessments (PSA) for nuclear power plants is to examine the existence of vulnerabilities against postulated earthquake hazards [1]. It involves assessing the plant's (or, its components') safety numerically, in a probabilistic framework, so that appropriate measures can be taken to enhance a NPP's safety level, if needed. One of the major components in the seismic PSA of a NPP, is the seismic fragility evaluation. Seismic fragility is defined as the conditional probability of failure for a given seismic intensity level. These fragilities are typically expressed using fragility plots, where these conditional probabilities are plotted against varying values of seismic intensity. Seismic fragility can be defined both at the component level and at the system level in a NPP. Fragility definitions also depend on how failure is defined while estimating the probability of failure.

India has 20 operational nuclear reactor units, 18 of which are pressurized heavy water reactor (PHWR) with the earliest dating back to 1973. All of these are located in moderate seismic zones (Zones 2 and 3 as per the current seismological intensity map of India), except for those in Narora, UP, which is in Zone 4 (IS 1893-2002). Seismic re-evaluation of these reactors, including those in moderate seismic zones, is an extremely important task, considering several factors, such as:

(i) A change in the seismicity of the site based on newer information.

(ii) Requirement of checking the safety level for greater seismic hazard than the original design basis.

(iii) Lack of seismic design or, more commonly, poor seismic design and detailing not meeting current standards.

(iv) Low level analysis adopted in the original qualification (many a times owing to a lack of computational tools necessary to perform high level analyses)

2. Conventional Seismic Fragility Analysis

Seismic fragility analyses of nuclear power plant structures and other critical components typically

adopt the method proposed by Kennedy and Ravindra [2]. In their pioneering work on seismic fragility analysis, they stated that the objectives of a seismic PSA were to estimate the frequencies of occurrence of earthquake-induced accidents and to identify the key risk contributors, so that necessary risk reductions could be achieved. They identified the component fragility analysis to be a major part of the seismic PSA (other parts being seismic hazard analysis, system-level analysis, accident sequence identification, etc.). Among many others, two major achievements of this work were in the identification of different levels of damage, and in the treatment of system-level fragilities separately from component-level fragilities.

In this fragility analysis approach, the conditional probability of failure is computed as:

$$P_f = \Phi\left(\frac{ln(a/A_m)+\beta_U \Phi^{-1}(Q)}{\beta_R}\right) \quad (1)$$

where, P_f is the conditional probability of failure for an earthquake intensity given by its peak ground acceleration (PGA) = a, A_m = median ground acceleration capacity of the structure/component, Q = confidence level in terms of non-exceedance probability. A_m is related to the actual ground acceleration capacity parameter, $A = A_m\, \varepsilon_R\, \varepsilon_U$, where $A_m = A_{RBGM}\, F_m$

A_{RBGM} is the PGA of review basis ground motion (RBGM) or review level earthquake (RLE). ε_R the random variable representing the aleatory uncertainties, i.e. inherent randomness associated with ground acceleration capacity. ε_U the random variable representing epistemic uncertainty in the determination of median value, A_m, i.e. the uncertainty associated with data, modelling, methodology etc. F_m is the median value of factor of safety, F. ε_R and ε_U are taken as lognormally distributed random variables, with logarithmic standard deviations of β_U and β_R, respectively, and both having unit median.

Once A_{RBGM} is known, determination of median factor of safety, F_m, is the key to derive A_m. Generic expression of 'F' can be written as [3]:

$$F = F_1 F_2 F_3 \quad (2)$$

F_1 is a factor representing ratio of capacity to demand, and is a strength factor. F_2 corresponds to the level of conservatism in assessing the capacity; it depends primarily on the energy absorption capacity of structure, system or component (SSC) beyond elastic limit. F_3 represents the conservatism associated with calculating demand. Different methodologies for fragility analysis are all about determining the median values of F_1, F_2 and F_3, and selection of corresponding β.

There are numbers of components of a NPP which should remain functional during a seismic event, so it is very difficult to check the seismic qualification of each component individually. So all the components the NPP are grouped in number of categories and different methods are recommended for their seismic qualification [3].

2.1 Drawbacks of conventional methods

The conventional methodologies for seismic fragility analysis have the following drawbacks [4, 5]:

i) Though these methods are easy to implement, but they require considerable engineering judgement especially in case of selecting of parameters for aleatory and epistemic uncertainties.

ii) The use of a double lognormal model is mathematically feasible but doesn't have too strong theoretical basis/background.

iii) The use of response spectrum based methods introduces epistemic uncertainties:

(a) Response contribution from different modes depends on the accuracy of different modal combination rules.

(b) In case of nonlinear system modal analysis are not applicable.

Thus fragility estimated using conventional methods are not very realistic specifically for nonlinear response of structure.

3. The Proposed Method of Fragility Analysis

This paper presents a novel approach of obtaining the seismic fragility curves for a primary containment structure using incremental dynamic analysis (IDA). The response of the IC structure, modelled as a 2-D stick, is studied for different types of ground motions.

The important assumptions made for fragility analysis are:

i) Randomness associated with the seismic forces is much more compared to that for structural parameters [6]. Hence, the randomness in seismic forces is considered only and structural parameters are considered to be deterministic. The reason behind it is as we are considering the

IC structure and a better quality control is done for these kind of important structures.

ii) The structure will behave linearly in shear even while it behaves non-linearly in flexure. It is done as we don't want the stick-model to be failed in shear.

iii) Pre-stressing forces are considered as uniaxial compression for the simplified stick-model.

iv) Reinforcement orientation in the dome portion is taken vertical for each element though it is not the case in actual, assuming that this will not affect too much in final result of the analysis as maximum strain and inter-storey-drift ratio usually occurs at the base of the cantilever kind of structure.

v) Openings are not considered for the stick-model though it can be done by manually selecting some equivalent reduced sectional properties at the location opening. The reason behind that procedure of taking reduced section will work well during Linear behaviour of structure but it will not work beyond that as non-linear behaviour depends largely on the actual section geometry which cannot be resembled using equivalent reduced section and our main motive is to do nonlinear response history analysis (NLRHA).

3.1 The basic steps of fragility analysis are:

i) Choose the ground motion data comparing its response spectrum with the design spectrum of the site and the seismological location of the site i.e. either intra-plate or at plate boundary.

ii) Prepare the mathematical model appropriate for NLRHA.

iii) Do the incremental dynamic analysis which is basically a set of NLRHA, for all ground motion data.

iv) Calculate the probability of exceedance of particular limit states from the output of IDAs and plot it to obtain fragility plot.

4. Modelling of the Structure

4.1 Description of structure

The IC structure considered for this study consists of a prestressed concrete cylindrical wall capped by a segmental pre-stressed concrete dome through a massive ring beam. The containment shell is supported on a circular raft. The typical containment structure considered for the study is depicted in Fig. 1(A). The containment structure responds to seismic excitation like a cantilever beam with a circular cross-section. The segmental dome along with the ring beam acts to stiffen the circular cross section and also adds to the mass of the system.

4.2 Mathematical model

The inner containment structure is idealized as a system of lumped masses at elevations of mass concentrations, connected by 2-dimensional Beam Column elements with actual section geometry other than the zone of openings. The structure is assumed to be fixed at the top of the raft foundation. The earthquake excitation is constrained along a single horizontal direction only. The stick model of a containment structure so developed is also shown in Fig. 1(B). Nonlinearity of the system is modelled in the program *OpenSees* [7] using *NonLinearBeamColumn* element. Concrete is modelled using *Concrete01* and reinforcing steel as *steel01* in *OpenSees*. Sections at

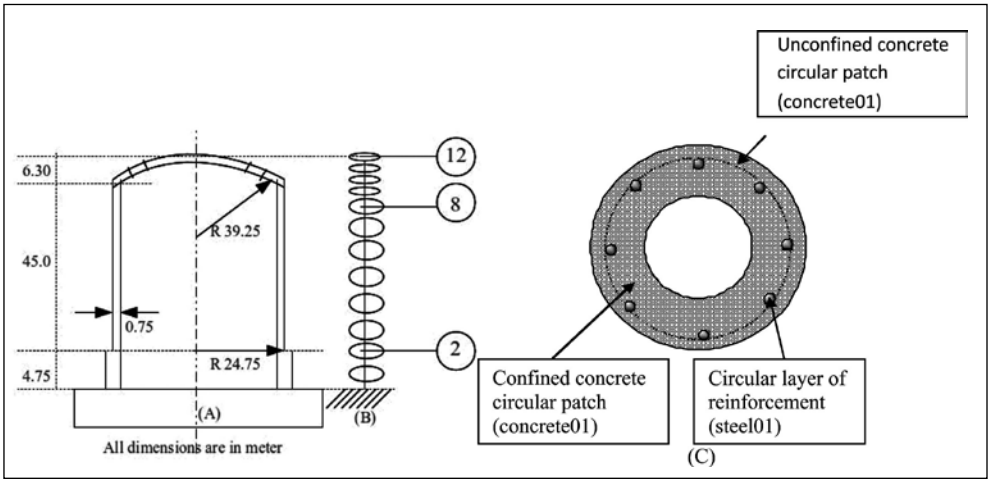

Fig. 1: (A) Containment Structure and (B) its stick model, (C) sample fiber section (not to scale)

Table 1: Summary of ground motion data considered

Record name	No. of records	Event	Component	Epicentral distance, km	PGA-range, g
GM-1 to 2	2	Bhuj, 2001	Horizontal	unknown	0.08-0.08
GM-3	1	Koyna, 1967	Horizontal	unknown	0.474
GM-4 to 25	22	Saguenay, 1988	Horizontal	45-167	0.002-0.174
GM-26 to 32	7	Miramichi, 1982	Horizontal	11-23	0.125-0.575

Table 2: Limit States

Damage Measure	LS-1	LS-2	LS-3	Reference
Drift	0.004	0.006	0.0075	FEMA-356
Plastic Rotation (θ_p)	0.0015	0.005	0.005	FEMA-356
Curvature (obtained from θ_p)	0.00015	0.00025	0.00025	FEMA-356 and Priestley (1997)
Compressive Strain	0.002	0.0035	0.005	IS-456 and Priestley (1997)
Tensile Strain	0	0.00014	0.013	OpenSees Concrete02 model

different level are defined as *fiber* sections (Fig. 1(C)) with circular concrete patch and circular layer of reinforcements. As stick-model made of single *fiber* section at each level cannot directly take the shear deformation, the shear deformation behaviour is incorporated using *SectionAggregator* command. A different uniaxial elastic material is defined as the slope of stress-strain plot as GA_s, where, G is the shear modulus of concrete and A_s is the shear area of the containment cross section. The *Section Aggregator* command is used to combine this material with *fiber* section previously defined with actual geometrical properties. This section is used to model the element at that level. The gravity load is calculated for each element and applied as nodal load on the upper node of each 2-noded element. The average prestress is taken as 10 MPa. Total prestressing force is calculated by multiplying the prestress with the average cross section area and it is applied as compressive force at top-most and bottom-most node.

5. Incremental Dynamic Analysis

Incremental dynamic analysis is an emerging analysis method offering detailed seismic demand and capacity prediction capability through a series of NLRHA for multiple scaled ground motion. Results of IDA are presented as IDA plots. A single IDA plot is basically the variation of maximum structural response at different intensity of a scaled ground motion. Maximum structural response is known as damage measure (DM) and intensity of ground motion is known as intensity measure (IM). After analyzing the structure for multiple ground motion data, the results are plotted on a single paper and the generated plot is known as multi-IDA plot.

5.1 Ground motions considered

The containment is assumed to be in the stable continental region of Indian peninsula. Considering this, ground motion records selected for performing a multi-IDA of this containment structure are sourced from recorded earthquakes in similar seismic regions across the world. 5% damped elastic response spectra of these records are compared with the design spectrum of the site, and those varying significantly from this design spectrum are filtered out. Details of ground motions considered for study are provided in Table 1. The PGA of a ground motion data is adopted to be the intensity measure (IM) for the IDA. Based on previous literature on fragility analysis of nuclear containment structures, a maximum PGA of 5.0g is considered. For successive NLRHA the PGA is incremented by 0.075g on a trial basis. For numerical convergence this increment is modified as discussed later.

5.2 Structural limit states considered

The limit states of the containment structure subjected to seismic loading considered in the study are tensile cracking of concrete, crushing of concrete in compression, interstorey drift ratio (IDR) and plastic rotation of section.

i) The tensile and compressive strains developed at the inner-most and the outer-most fiber of

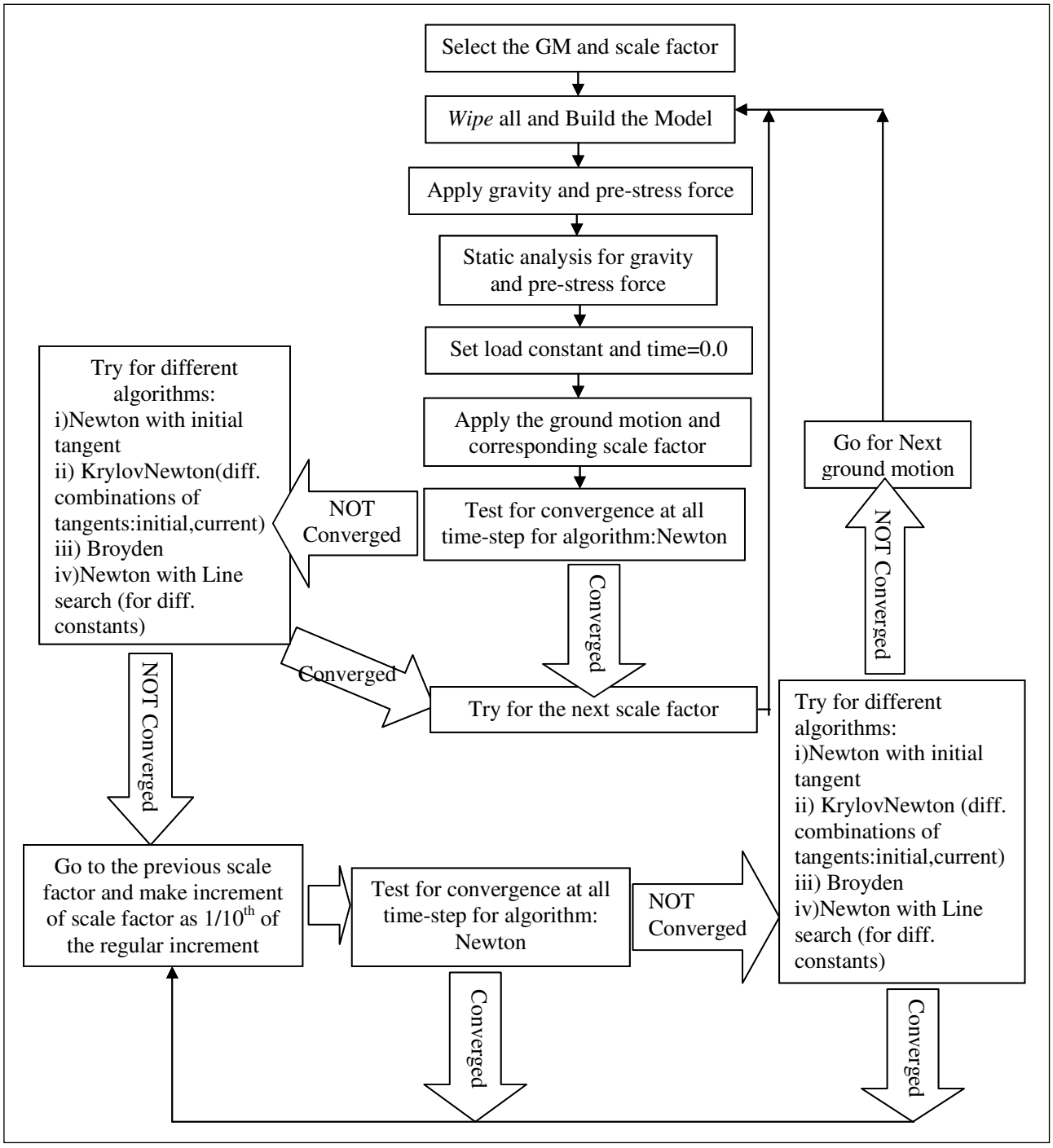

Fig. 2: IDA flow-chart

each section are stored for each scale factor of ground motion and compared with limiting valued specified by FEMA-356 [8]. As FEMA-356 doesn't consider any tensile strength of concrete, the limiting values for tensile strain are adopted from the material model *Concrete02*.

ii) The allowable total (elastic and plastic) IDR values are adopted from Table 6-19 of FEMA-356.

iii) The allowable plastic rotation values are adopted from Table 6-7 of FEMA-356. Using Preistley's equation [9] limiting values in terms of curvature is calculated since *Opensees* provides curvature as output not plastic rotation.

5.3 Numerical convergence of IDA

As stated by Vamvatsikos and Cornell [10, 11] numerical convergence is a very critical issue in

performing IDA especially in the zone of higher PGA levels when the structure may reach a state of global dynamic instability. To deal with this following steps are adopted:

1. The structure is modelled with nonlinear *NonLinearBeamColumn* element which has capability to track the distributed plasticity across the member section and the length of the member.
2. Instead of single algorithm for solving nonlinear equations, a number of algorithms in sequence are tried. The following algorithms are used in sequence if one fails next one is used:
   i) Newton-Raphson
   ii) Modified Newton-Raphson
   iii) KrylovNewton -with different combinations of tangents: initial and current.
   iv) Broyden
   v) Newton with Line search (for different constants)
3. For a specific ground motion if all algorithm fails at a particular PGA, it may be due to: i) global dynamic instability or ii) Numerical failure. Here, if all the algorithm fails at any particular scale factor, it is assumed that it is global dynamic instability situation not only numerical failure and the control is sent back to the previous scale factor with updated increment of scale factor equal to $1/10^{th}$ of the regular increment of scale factor. The procedure of obtaining multi-IDA is illustrated in detail in Fig. 2.

6. Results and Discussion

Eigen value analysis is done only to get an overview of the dynamic properties of the primary containment structure (Table 3).

Table 3: Natural period and frequencies of different modes

Mode	T, s	f, Hz
Mode-1	0.1826	5.48
Mode-2	0.0988	10.12
Mode-3	0.0595	16.82
Mode-4	0.0473	21.13
Mode-5	0.0385	25.96

6.1 IDA plots from raw data and its correction

If the raw data obtained from a IDA are plotted it is sometimes found that there are unexpected large rebounds at high PGA level. Such a rebound is due to single data point being located far off from the other data points of the same IDA (Fig. 3(C)). This is inconsistent even with the previous and the next data points from structural perspective. Such problematic data points are considered to be points of numerical failure, which has not been detected by the algorithm. The IDA is replotted by removing these points causing large rebounds by placing some limiting conditions on rate of change in slope of the IDA plot (Fig. 3(C-1)). The other plots (Fig. 3(A), 3(B)) are quiet normal as per literature review.

6.2 Fragility Plots

Seismic Fragility of a structure, which is the probability of a pre-defined damage measure (DM) exceeding certain pre-defined limit states (LS) for a given intensity measure (IM), is calculated as the fraction of IDA curves exceeding the LS at the selected PGA. Fragility analysis results in a set of $P(\text{DM} > \text{LS} \mid \text{IM})$ vs. IM plots. All the fragility plots so obtained are stepped since a discrete number of ground motion data are used for multi-IDA. The stepped plots are smoothened using weighted cubic spline approximation. By increasing the number of ground motion records and reducing the PGA increment for each IDA.

Fig. 4 shows fragility plots based on various performance limit states as mentioned earlier in Table 2. Fig. 4(B) and 4(D) also show fragility curves based on Eq. (1). Some major observations from these fragility plots are:

i) Based on IDR, the fragility is zero up to PGA = 5g (Fig. 4(A)).

ii) The fragility, based on plastic rotation (or curvature) limits, is zero up to 2g for LS-1 and up to 3g for LS-2 and LS-3 (Fig. 4(B)).

iii) The fragility based on tensile strain at the inner-most fiber, which indicates a through crack along the thickness, is almost zero up to PGA = 0.5g for LS-1(zero tensile strain) & LS-2 (cracking strain) and up to PGA = 5g for LS-3. It reaches almost 0.95 for LS-1 & LS-2 at PGA = 5g (Fig. 4(C)).

iv) Fragility curve for concrete crushing is almost zero up to PGA = 5g for all limit states.

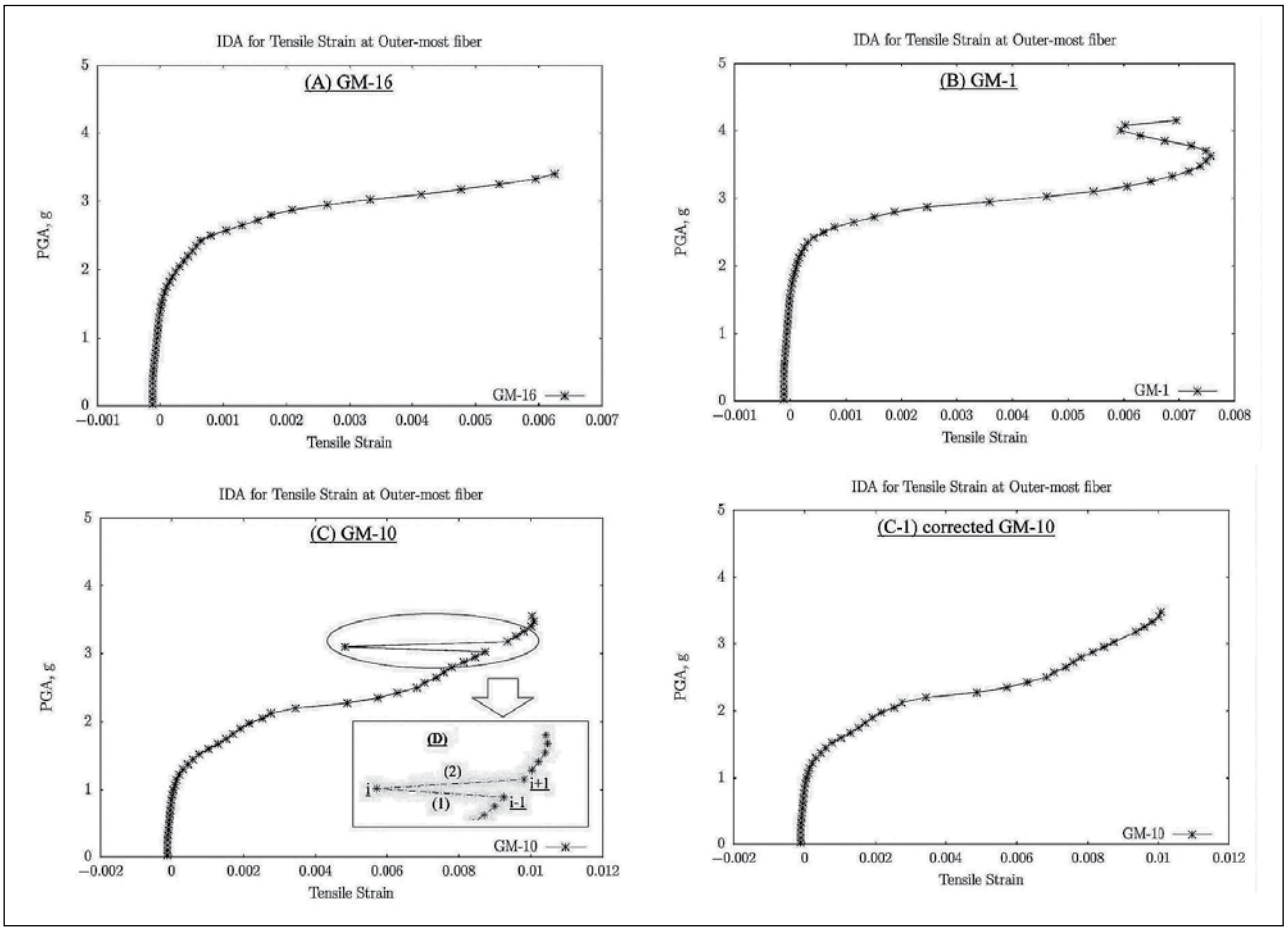

Fig. 3: Sample IDA plots: (A) without any rebound (B) with realistic rebound (C) with unrealistic sharp rebound (C-1) corrected IDA plot with rebound removed

Fragilities are also computed for the same containment using Eq. (1). A_{RBGM} is adopted as 0.214g for this PHWR. The median value of F_1 is obtained from a linear elastic analysis. The standard deviations for uncertainties and randomness are based on the recommendations of Pisharady and Basu [3]. The fragility plots obtained this way are significantly different from those obtained using multi-IDA (e.g. Fig. 4(B), 4(D)). Since the linear elastic analysis shows no tensile strain at the RBGM or design PGA level, the through crack fragility based on conventional method is zero even at PGA = 5g. This shows the unrealistic nature of the fragility curves using the conventional method.

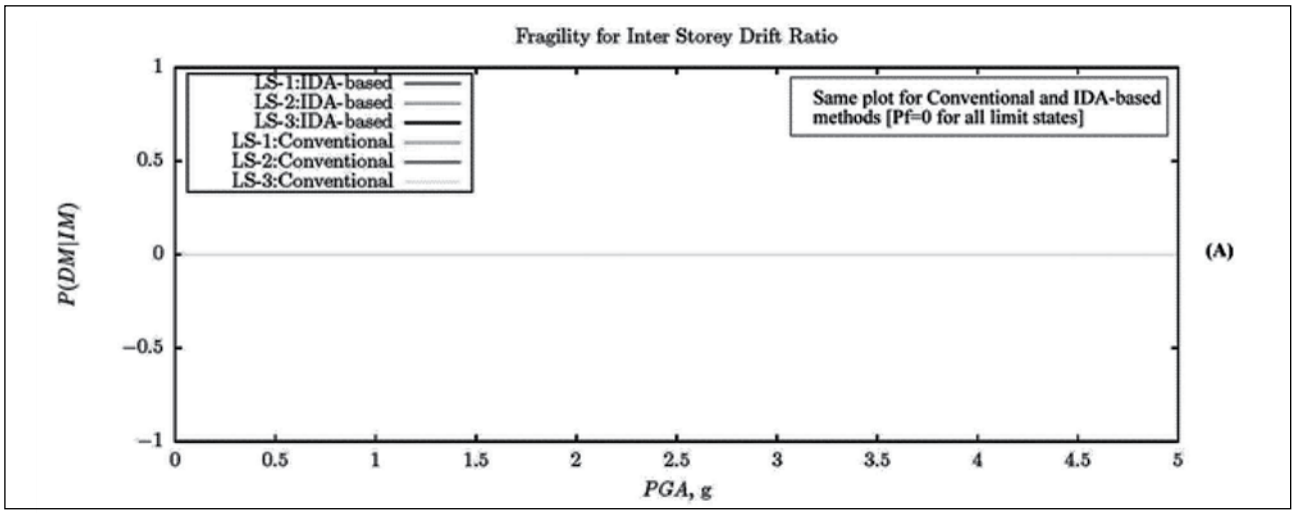

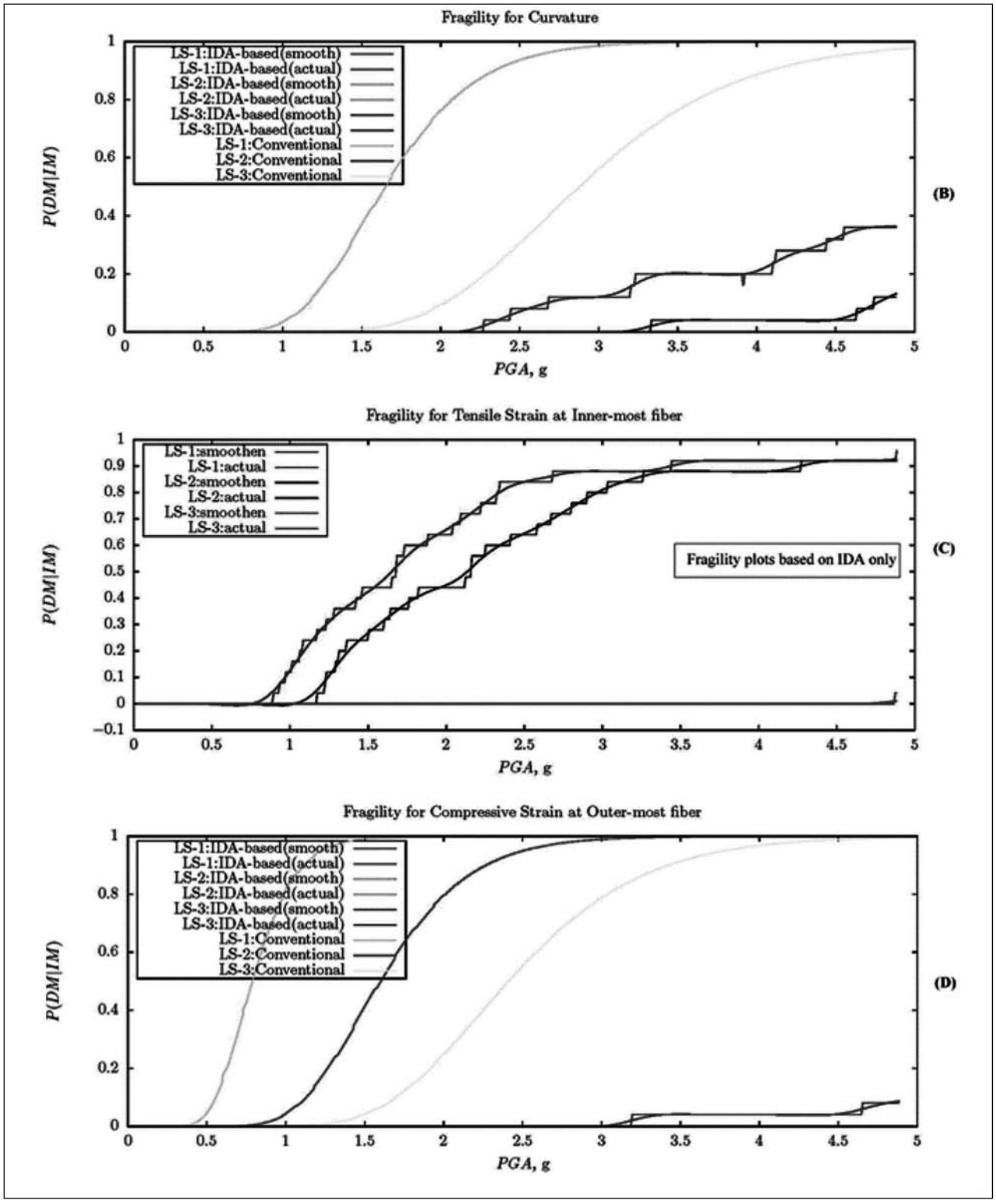

Fig. 4: Fragility Plots (IDA-based and conventional methods)

7. Conclusions

Primary containment structures are found to have almost zero fragility considering limit states based on IDR and crushing of concrete. But these structures have very high probability of failure in terms of through crack formation, which results in radiation leakage. The IDA based fragility curves are found to be more realistic than fragility curve obtained using conventional method. This is primarily due to

the fact that the effect of nonlinearities are directly incorporated in IDA based estimation of fragility. However, it should be noted that the IDA based fragilities shown here do not include uncertainties associated with structural modelling. Future works in this area should focus on reducing the model uncertainty by using detailed structural model, soil-structure interaction and larger number of earthquake records.

References

1. Hari Prasad, Dubey P N, Reddy G R, Saraf R K, Ghosh A K (2006), Seismic PSA of nuclear power plants : a case study, BARC/2006/015, BARC.
2. Kennedy, R. P. and Ravindra, M. K. (1984), 'Seismic fragilities for nuclear power plant risk studies', Nuclear Engineering and Design 79(1), 47–68. 38
3. Pisharady, A. S. and Basu, P. C. (2010), 'Methods to derive seismic fragility of npp components: A summary', Nuclear Engineering and Design 240(11), 3878–3887.
4. Gupta, S. and Manohar, C. S. (2006a), 'Reliability analysis of randomly vibrating structures with parameter uncertainties', PhD thesis at Indian Institute of Science, Bangalore 297, 1–407.
5. Gupta, S. and Manohar, C. S. (2006b), 'Reliability analysis of randomly vibrating structures with parameter uncertainties', Journal of Sound and Vibration 297(3-5), 1000– 1024.
6. Ellingwood, B. R., Celik, O. C. and Kinali, K. (2007), 'Fragility assessment of building structural systems in mid-America', Earthquake Engineering and Structural Dynamics 36(3-5), 1935–1952.
7. Mazzoni S, McKenna F et al. (2007) Opensees command language manual
8. FEMA-356 (2000), 'Prestandard and commentary for the Seismic rehabilitation of buildings', Federal Emergency Management Agency, Washington D.C.
9. Priestley, M. J. N. (1997), 'Displacement-based seismic assessment of reinforced concrete buildings', Journal of Earthquake Engineering 1(1), 157–192. Cited By (since 1996): 62.
10. Vamvatsikos, D. and Allin Cornell, C. (2002), 'Incremental dynamic analysis', Earthquake Engineering and Structural Dynamics 31(3), 491–514.
11. Vamvatsikos, D. and Cornell, C. A. (2004), 'Applied incremental dynamic analysis', Earthquake Spectra 20(2), 523–553.
12. Bhargava, K., Ghosh, A. K., Agrawal, M. K., Patnaik, R., Ramanujam, S. and Kushwaha, H. S. (2002), 'Evaluation of seismic fragility of structures - a case study', Nuclear Engineering and Design 212(1-3), 253–272.
13. Bhargava, K., Ghosh, A. K. and Ramanujam, S. (2005), 'Seismic response and failure modes for a water storage structure - a case study', Structural Engineering and Mechanics 20(1), 1–20.
14. Rizkalla, S. H., Lau, B. L. and Simmonds, S. H. (1984), 'Air leakage characteristics in reinforced concrete.', Journal of Structural Engineering 110(5), 1149–1162.

Life Cycle Reliability and Safety Engineering
Vol.1 Issue 4 (2012) 10-16

Refined Modeling of Crack Tortuousness to Predict Pressurized Air Flow Through Concrete Cracks

L.R. Bishnoi[1], R.P. Vedula[2], S.K. Gupta[3]
[1]*Siting & Structural Engineering Division, Atomic Energy Regulatory Board, Mumbai,*
[2]*Mechanical Engineering Department, Indian Institute of Technology Bombay, Mumbai*
[3]*Safety Analysis & Documentation Division, Atomic Energy Regulatory Board, Mumbai*
Email: lr.bishnoi@gmail.com

Abstract

Cracks may appear in the pressurized concrete containment of a nuclear power plant during a severe accident and provide leak paths for release of radioactive aerosols dispersed in the contained air. In this study, numerical results for air leakage through concrete cracks are reported for a range of pressure gradients and crack widths relevant to containment atmosphere during a severe accident scenario. Crack geometry in 2D is generated using statistical crack model to account for crack tortuousness. While airflow predictions through such models provide good agreement with experimental results reported in literature, the computational results generally provide over-prediction of airflow. The statistical crack models account for the gross tortuousness of the concrete cracks based on experimental studies. The local tortuousness of the order of grain size that can deflect the crack from straight path is not accounted in these models. In this study, fractal geometry based curves are used to introduce the local tortuousness within the global crack segments represented by straight lines in the statistical models. Comparison of pressurized airflow rates obtained from such refined crack model with the experimental values reported in literature for plain concrete shows very good agreement. The effect of local tortuousness on the pressurized airflow rates was accounted indirectly in 3D crack models for reinforced concrete with modified crack morphology due to reinforcing steel. The computational results with corrections due to local tortuousness compared well with the experimental values for pressurized airflow through cracks in reinforced concrete panels reported in literature.

Keywords: severe accident; containment; concrete cracks; tortuousness; fractal geometry; airflow

1. Introduction

A major fraction of the airborne radioactivity within nuclear reactor containment, consequent to a postulated severe accident involving reactor core meltdown, consists of aerosols generated by condensation of volatile fission products. The containment envelope becomes pressurized during a severe accident and there is a possibility of cracks through concrete shell of the containment, which can provide leak paths for pressurized air and aerosol release to the outside atmosphere.

Rizkalla et al. [1] reported experimental data for leakage rate through cracks in reinforced concrete test panels and suggested correlations. Riva et al. [2] performed finite element analysis of reinforced concrete test panels to calculate equivalent average single crack width for evaluating leakage rate with different correlations and reported good match of the test leakage rate with the calculated rate using correlation of Rizkalla et al. [1]. Gelain and Vendel [3] performed experiments on plain concrete panels and computed crack geometry as an equivalent rectangular channel, which would have the same flow rate as the experimental data. Boussa et al. [4] generated cracks in a large number of test specimens of different concrete grades, modeled the crack profile in terms of statistical parameters and reported good agreement of the crack profile obtained from the statistical model with the experimental data. Bishnoi et al. [5] conducted computational studies for airflow and aerosol transport through cracks in plain concrete using statistical crack model of Boussa et al. [4] and reported good match between the computational and experimental results. Bishnoi et al. [6] studied effect of reinforcing steel on air flow through cracks in reinforced concrete using

computational models incorporating modified crack morphology due to reinforcing steel derived from stress analysis of reinforced concrete panels.

In this study, numerical results for air leakage through concrete cracks are reported for a range of pressure gradients and crack widths relevant to containment atmosphere during a severe accident scenario. Crack geometry is generated using statistical crack model of Boussa et al. [4] to account for crack tortuousness. While airflow predictions using such computational model provide good agreement with experimental results reported in literature, the numerical results generally provide over-prediction of airflow. The Boussa crack model defines gross tortuousness of the concrete cracks in statistical terms derived from experimental studies. Local tortuousness of the order of grain size that can deflect the crack from straight path is not accounted in these models.

The Boussa crack model is refined in this study by using fractal geometry based curves to introduce the local tortuousness within the global crack segments represented by straight lines. The airflow study results from such refined model are compared again with the experimental values. The comparison shows very good agreement between computational values from the refined crack model and the experimental values of Gelain and Vendel [3] for cracks in plain concrete. The computational airflow studies through cracks in reinforced concrete also shows very good agreement with experimental results of Rizkalla et al. [1] when the effect of local tortuousness is accounted along with the effect of reinforcing steel on the crack morphology.

Statistical crack model including refinement of the crack morphology to represent the local tortuousness using fractal geometry methods were implemented in MATLAB. FLUENT (version 6.2.16, 2005) was used for airflow computations through the crack models.

2. Numerical Procedure

The crack model parameters were chosen to represent concrete grade in the range of M50-M60, typically used to construct containment structures. The range of pressure gradients and crack widths for the study has been reported in Bishnoi et al. [5]. These parameters were chosen to be representative of air leakage through containment leak paths, which are likely to exist under postulated severe accident conditions in water-cooled reactor based nuclear power plants.

The 2D crack profile is defined in terms of straight segments and deviation of these segments from horizontal line by specifying mean value and standard deviation separately for these two parameters as per the approach suggested by Boussa et al. [4]. Two identical profiles placed at a constant spacing equal to the crack width represent two lips of the crack in 2D. Details of statistical crack model in 2D are reported in Bishnoi et al. [5]. Refinement of the 2D crack model was done to represent roughness due to local tortuousness, introduced by crack tip deflecting material grains using fractal geometry, for each of the straight segments. Random midpoint displacement method [7] was used to approximate local deflection of the crack due to micrometer size concrete material grains as approximate fractal Brownian motion representation.

A typical statistical crack model geometry representing global tortuousness of the crack is shown in Fig. 1. Typical global tortuousness and local tortuousness in portion 'A' of the global crack model geometry, derived using random midpoint displacement method, are depicted in Fig. 2.

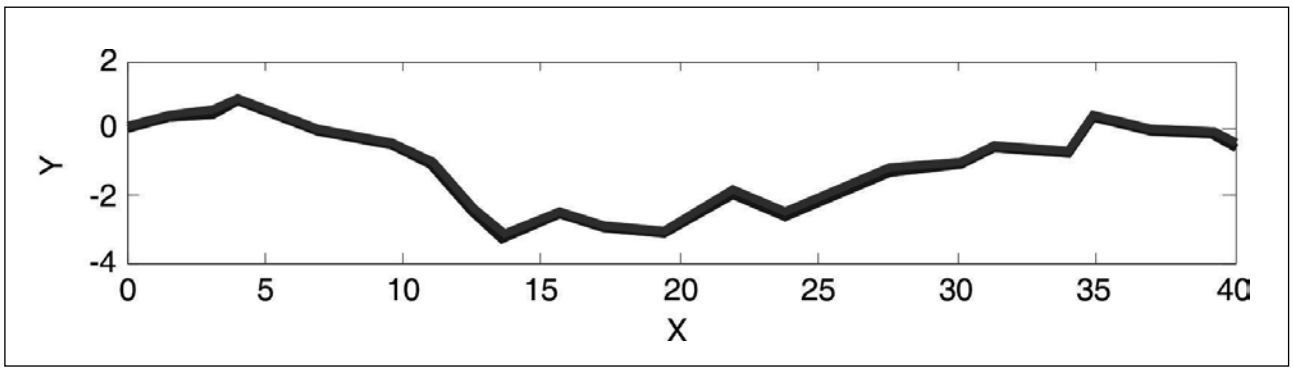

Figure 1: Typical 2D crack model representing global tortuousness (all dimensions in mm)

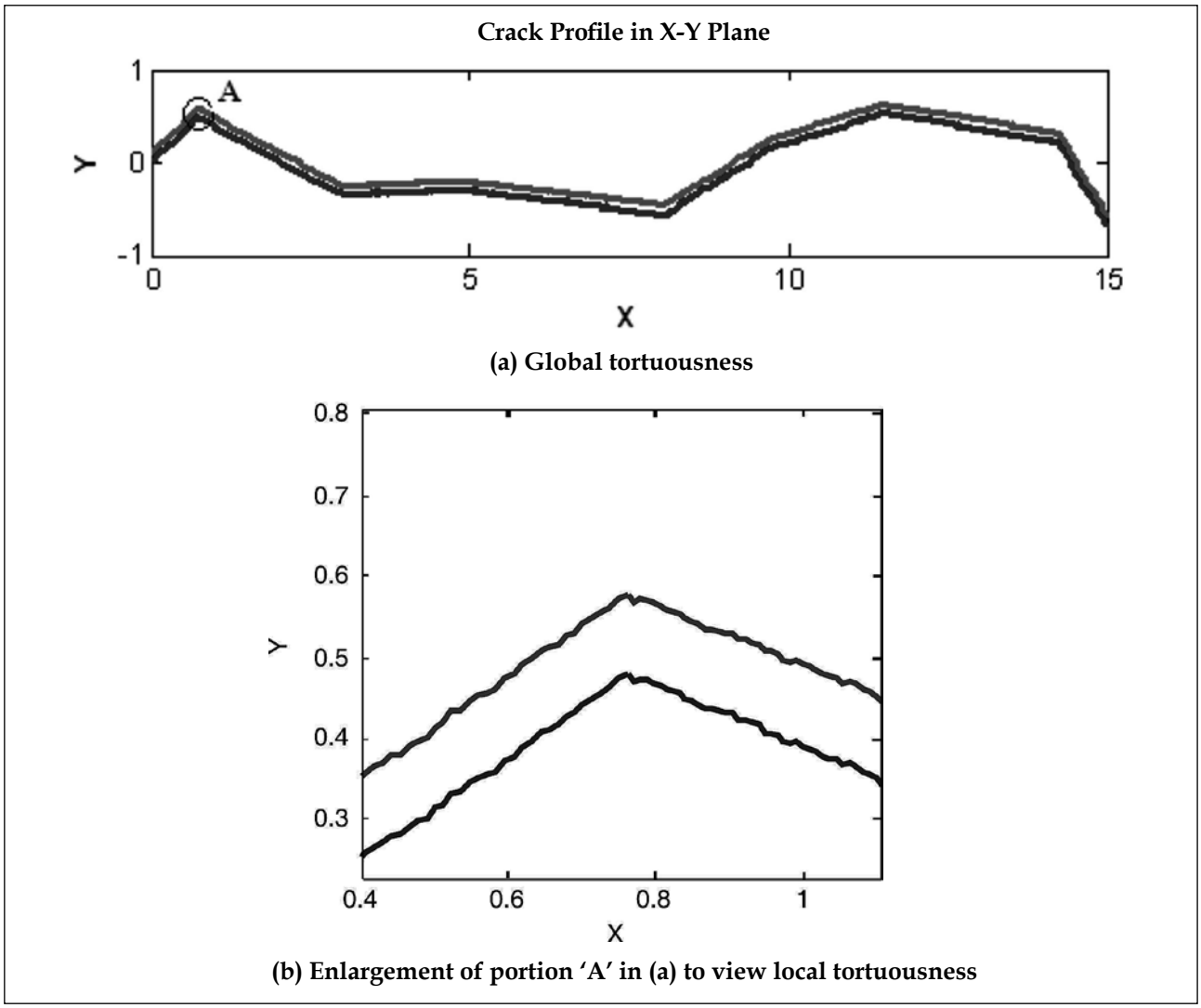

Figure 2: Depiction of typical global and local tortuousness (all dimensions in mm)

To construct the fractal geometry representing local tortuousness in a straight segment of the crack, displaced y-value of the midpoint (based on x-coordinates of the end points) of the straight line is calculated as the average of the y-values of the endpoints plus a random offset. The process is repeated by calculating a displaced y-value for the midpoint of each half of the subdivided line. The subdivision is continued until the subdivided line segments are less than a preset value, s_{lim}.

The random offset, r, is calculated as follows:

$$r = sr_g \langle L \rangle \quad (1)$$

Where, s is a selected 'surface roughness' factor, r_g is a Gaussian random value with mean zero and variance one, and L is the length of the straight line.

Nominal diameter of the capillary pores in cement paste varies from about 0.3 to 3 μm [8]. Assuming water cement ratio of 0.45, porosity of cement paste works out to be about 11.5% [8]. Considering average size of capillary pores in the range of 1 to 1.5 μm, the material inhomogeneity affecting crack path (i.e. effective grain size for crack deflection) was taken in the range of 7.5 to 15 μm. The surface roughness (i.e. deviation from straight path) was considered to be in the range of ¼ to ½ of the grain size, the actual variation was approximated to be 2.5 to 5 μm. The values adopted in the current study are 3 micron and 10 micron for s and s_{lim} respectively, which were arrived at from parametric airflow computations on crack models with varying values of s and s_{lim} in the size ranges stated above.

Stress analyses were performed on finite element (FE) model of a reinforced concrete experimental

test specimen (L4) from Rizkalla et al. [1] to derive morphology and extent of crack surfaces to be used for airflow calculations. Specimen L4 was selected because complete details of geometry, reinforcement, cracking and airflow results are reported for this specimen only. Uniaxial tensile load was applied to reinforcing steel bars in the stress analysis models as was done in the experimental study. Two nonlinear analyses were conducted; one with reinforcing steel and another with plain concrete without reinforcement to see the effect of reinforcing steel on crack surface pattern growth compared to the plain concrete. These analyses indicated sudden spread of the concrete damage in plain concrete from exterior faces to the entire cross section whereas the reinforcement does not allow spread of the damage over the entire cross section even at ultimate load, though the extent of damage keep increasing with load increments. Typical damage spread over the cross section of the test specimen for plain concrete and reinforced concrete are shown in Fig. 3 (a) and (b) respectively.

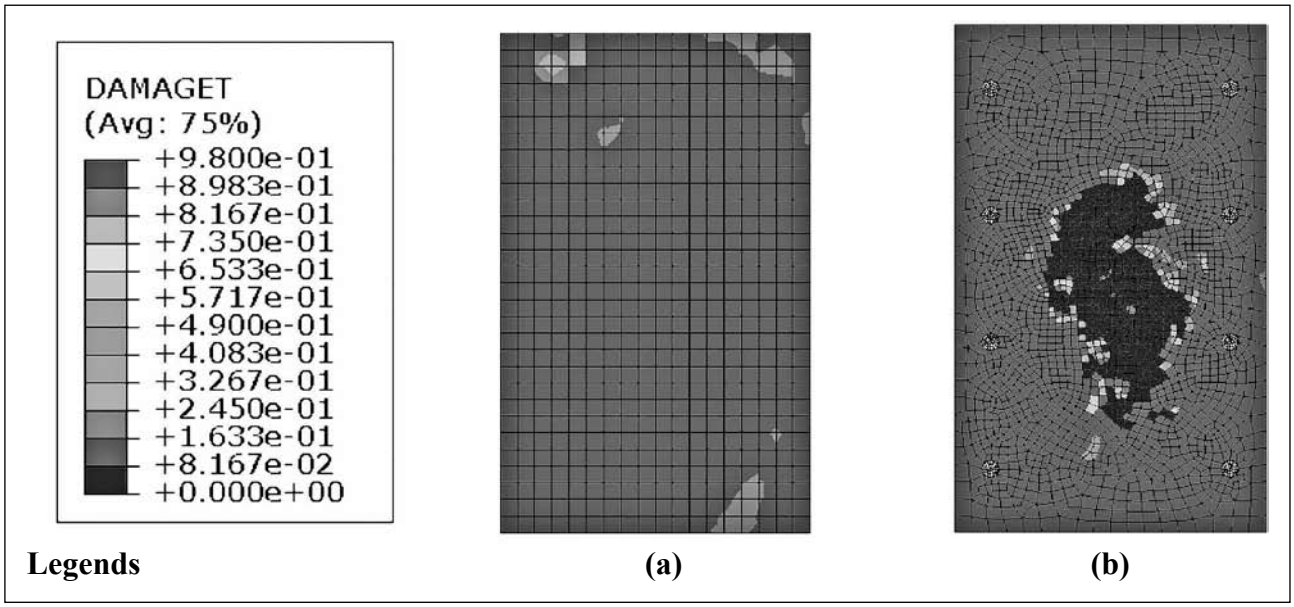

Figure 3: Concrete damage spread over the X-sections of plain and reinforced concrete specimen models at typical load steps

Linear stress analysis was conducted with a priori crack in the form of a slit of finite width to obtain the likely morphology of the crack around reinforcing steel bars under uniaxial tensile load. Typical crack surface contours due to the effect of reinforcing steel are depicted in Fig. 4. Details of these analyses and the modified 3D crack geometry are reported in Bishnoi et al. [6].

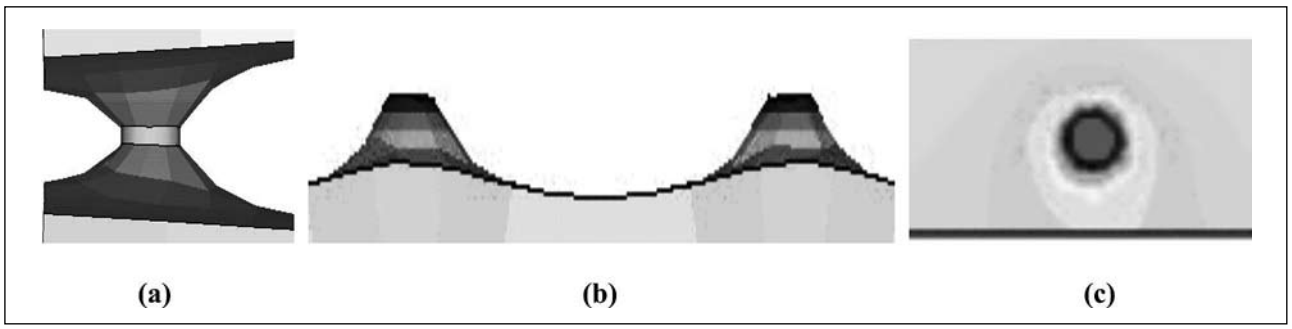

Figure 4: Crack surface contours around rebar (a) cross section along crack path through rebar (b) typical crack profile across the flow path between two rebar at the edge (c) typical crack surface contour in plan around a rebar.

The standard Navier-Stokes and continuity equations are solved for the flow domain defined by the crack morphology using the finite volume method (FVM) with SIMPLEC algorithm for pressure-velocity coupling and second order upwind scheme with under relaxation factor of 0.5 for discretization of momentum

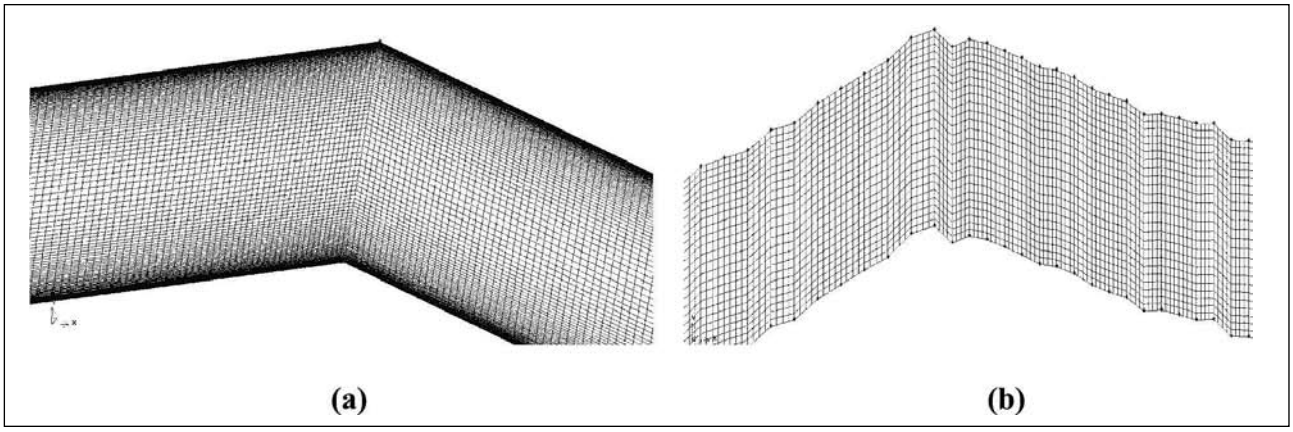

Figure 5: Typical grids used for numerical computation of pressurized airflow using FVM

equations. Atmospheric pressure was assumed at outlet and inlet pressure was calculated according to the specified pressure gradient. No-slip condition was imposed at crack wall boundaries. All case studies were conducted for a constant temperature of 300 K. Since the pressure drop across the crack is not large the flow is assumed incompressible and confirmed by checking the flow Mach numbers, which remained much below unity for all the cases. The constant air density was assumed to be 1.225 kg/m^3. Details of optimized computational grid and validation of the crack model for 2D airflow computations are reported in Bishnoi et al. [5]. Typical grids for numerical computation of pressurized airflow in the crack model with (a) the global tortuousness alone and (b) the refined crack model incorporating the local tortuousness are depicted in Fig. 5.

Numerical procedure established for airflow through 2D crack path was extended to 3D crack surfaces for airflow computations through cracks in reinforced concrete.

3. Results and Discussion

3.1 Airflow Through Cracks In Plain Concrete

Considering enormous computational resources and convergence issues associated with large size models, a comparative study of flow rate was conducted for crack lengths of 15mm, 40mm and 70mm and crack widths of 0.1mm 0.2mm and 0.3 mm with same model parameters to explore feasibility of restricting crack length for computational model. The study confirms that a crack length as small as 15 mm could also be considered as a representative sample for air flow studies. In view of this, an intermediate crack length of 40mm was chosen for airflow computations with the global tortuousness. The crack length was restricted to 15 mm for the refined model incorporating the local tortuousness because of computational constraints arising due to model size.

The results in terms of friction factor (f) as a function of Reynolds number (Re) for the Boussa crack model representing the global tortuousness of the crack are shown in Fig. 6 (a). Several different pressure gradients (0.25-1 bar/m) were used in the computations to generate the plot. The results reported by Gelain and Vendel [3] for plain concrete are superposed in the figure and the comparison is noticed to be within 25% for majority of the data points. Fig. 6 (b) depicts f versus Re along with a curve fit.

The computational study was repeated with the refined crack model incorporating the local tortuousness besides the global tortuousness. The results are shown in Fig. 7 (a) along with the experimental results of Gelain and Vendel [3].

While most of the data points from refined model computation and experimental values are within 9%, the maximum difference in friction factor (f) values is within 16%. Fig. 7 (b) depicts f versus Re along with a curve fit for the results from the refined model.

3.2 Airflow Through Cracks In Reinforced Concrete

Airflow calculations were performed, with the same flow parameters as used in the experimental study by Rizkalla et al. [1], for pressure difference of 106 kPa across the specimen thickness of 178 mm (i.e. pressure gradient of 5.96bar/m) and specified average crack width of 0.06 mm, using the computational model generated for 3D crack morphology of the test specimen (L4) of Rizkalla et al. [1] as well as with refined 2D crack model. Details

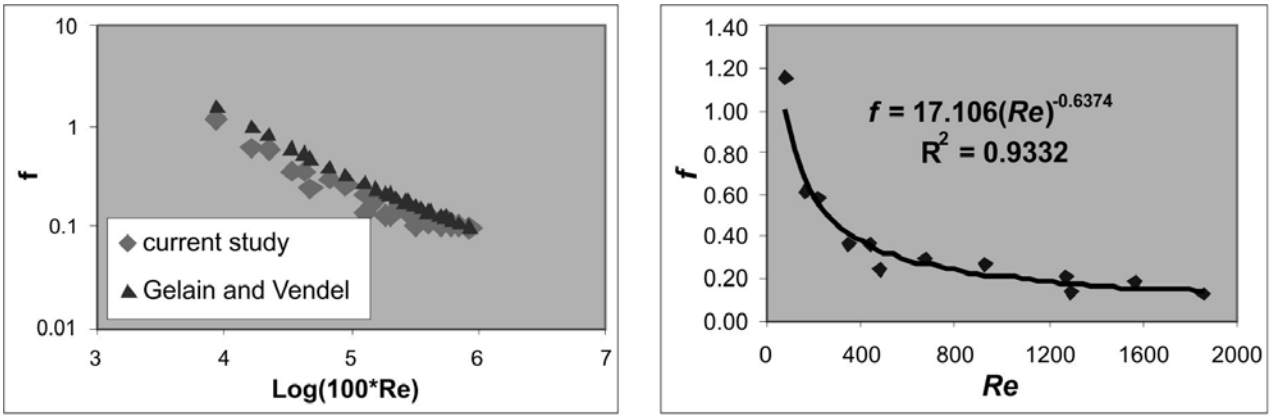

(a) **(b)**

Figure 6: Plot of f versus Re for the crack model with global tortuousness alone

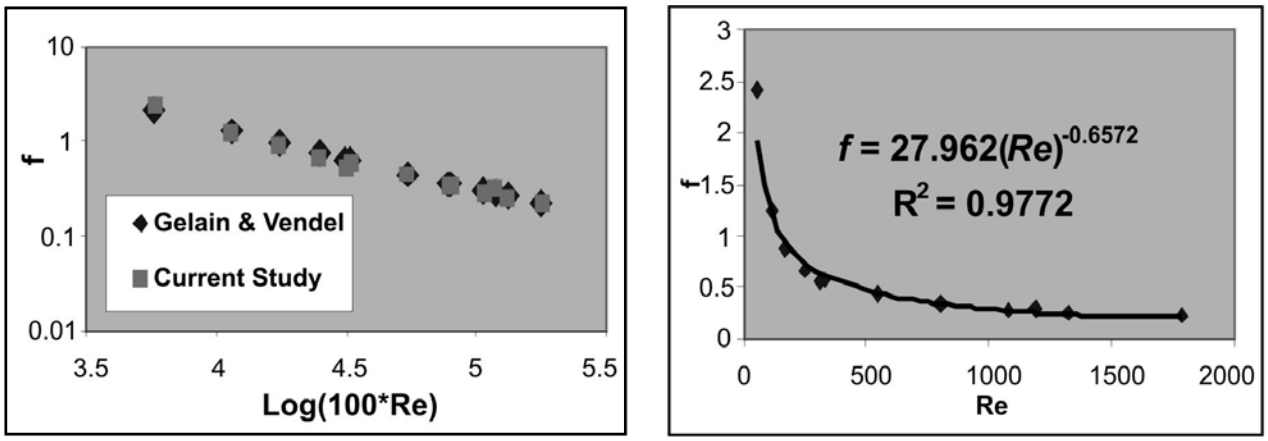

Figure 7: Plot of f versus Re for the refined crack model incorporating local tortuousness

Table-1: Experimental and computational air flow rates through cracks in RC

Measured flow through reinforced concrete test specimen L4 (m^3/s)	Flow calculated from 2D plane crack Model (m^3/s)	3D plane crack model without modified morphology due to rebar		3D plane crack model with modified morphology due to rebar			
		Calculated flow (m^3/s)	diff. w.r.t. (2) (%)	Calculated flow (m^3/s)	diff. w.r.t. (1) (%)	diff. w.r.t. (2) (%)	diff. w.r.t. (3) (%)
(1)	(2)	(3)	(4)	(5)	(6)	(7)	(8)
5.18e-4	10.68e-4	11.05e-4	+ 3.46	5.7e-4	+10	-46.63	-48.42

of the airflow computational models are reported in Bishnoi et al. [6].

Parametric study was conducted on three crack models of 0.06 mm crack width with different 2D crack morphologies derived using Boussa model [4] and the morphology was refined by introducing the local tortuousness (slim and s as 10 µm and 3 µm respectively) in all the three cases. The study was conducted for pressure gradients of 1.5-10 bar/m. There was a reduction of mass flow rate computed from the refined models with respect to the Boussa model [4] for all three sample cases. The flow reduction varied from 29% to 35% for all the pressure gradients and all three sample cases considered in the study. The average flow reduction was about 32% for pressure gradient of 5.96 bar/m representing airflow test parameters of specimen L4 of Rizkalla et al. [1]. A comparison of the airflow rate

through a plane crack and the three sample crack morphologies incorporating the global tortuousness based on the Boussa model [4] for pressure gradients of 1.5-10 bar/m was also carried out. The air flow rate through all the three crack samples with the global tortuousness was lower by about 7.5% with respect to the plane crack model for crack width of 0.06 mm.

The flow rate computed from the 3D crack model for RC test specimen (L4) with modified morphology around reinforcing bars was compared with flow rate through another 3D plane crack model in which two plane surfaces were separated by the average crack opening of 0.06 mm throughout without incorporating the actual crack morphology around reinforcing bars. The computed airflow from the 3D crack model with the modified morphology around the reinforcing steel was corrected to account for the global and the local tortuousness based on the parametric studies mentioned above as these effects could not be accounted directly in the 3D crack model. Airflow calculated from a 2D plane crack channel (without any tortuousness) is also included for comparison. Air density was assumed to be a constant value of 1.225 kg/m3. The comparison of flow rates from different models is provided in Table-1.

From the above comparison, it is seen that the 3D crack model incorporating the crack morphology derived by considering the local constriction effect of rebar provide very good comparison with the flow obtained experimentally. The difference in the computed and the experimental values of flow rates is about 10%. This difference is well within the statistical variation among different crack samples based on Boussa model with the same model parameters. There is also a very good comparison between the 2D and the 3D models of a plane concrete channel without any tortuousness, the difference being only about 3.5%. It is seen that for the present case of a crack width of 0.06 mm and pressure gradient of 5.96 bar/m, the crack tortuousness together with the effect of the reinforcing steel causes flow rate reduction of about 50% through cracks in RC elements compared to flow through a plane channel.

4. Conclusions

Results of computational studies for pressurized airflow through cracks in concrete are reported. The statistical crack model available in the literature has been refined to incorporate local tortuousness of the crack due to the smallest material inhomogeneity that can affect the airflow rates. The local tortuousness is introduced using fractal geometry based curves. The computational results for pressurized airflow through refined crack models are compared with the experimental values reported in the literature for cracks in plain concrete and reinforced concrete. The comparison shows very good agreement between the computational results and the experimental values.

These studies have certain limitations. The parameters considered for fractal curve approximation of the crack tortuousness are the surface roughness and the limiting value of straight crack segment, which are considered to be functions of the level of material inhomogeinity affecting the crack propagation and its deflection from the straight path. These parameters have been approximated from the knowledge of cement paste properties and parametric studies for airflow were conducted to arrive at the most appropriate values. Further studies are required to establish these parameters for different grades of concrete and sensitivity of the airflow results to these parameters. Additional studies are also required in case of reinforced concrete to establish the effect of reinforcing bar spacing on leakage rates.

References

1. Rizkalla, S.H., La u, B.L., Simmonds, S.H., 1984. "Air leakage characteristics in reinforced concrete," Jnl. St. Eng. (ASCE) **110**(5), 1149-1162.
2. Riva, P., Brusa, L., Contri, P., Imperato, L., 1999. "Prediction of air and steam leak rate through cracked reinforced concrete panels," Nucl. Eng. Des. **192**, 13-30.
3. Gelain, T., Vendel, J., 2008. "Research works on contamination transfers through cracked concrete walls," Nucl. Eng. Des. **238**, 1159-1165.
4. Boussa, H., Tognazzi-Lawrence, C., La Borderie, C., 2001. "A model for computation of leakage through damaged concrete structures," Cem. Concr. Composites **23**, 279-287.
5. Bishnoi, L.R., Vedula, R.P., Gupta, S.K., 2010. "Characterization of pressurized air leakage and aerosol transport through cracks in concrete," Proceedings of the 37th International & 4th National Conference on Fluid Mechanics and Fluid Power (FMFP2010). Paper ID: 311, 16-18 December, Indian Institute of Technology Madras, Chennai, India.
6. Bishnoi, L.R., Vedula, R.P., Gupta, S.K., 2010. "Effect of reinforcing steel on pressurized air leakage through cracks in concrete," Transactions, SMiRT21. Div-III: Paper ID# 496, 6-11 November, 2011, New Delhi, India.
7. Hearn, D., and Baker, M. (1994), Computer Graphics, 2nd edition.
8. Neville, A.M., (2000), Properties of Concrete, Pearson Education Asia Pte. Ltd.

Life Cycle Reliability and Safety Engineering
Vol.1 Issue 4 (2012) 17-25

Estimating the Rain-Flow Fatigue Damage in Wind Turbine Blades Using Polynomial Chaos

N Ganesh[1], Sayan Gupta[2]
[1]*Department of Applied Mechanics, Indian Institute of Technology Madras, Chennai 600036, India,*
[2]*Department of Applied Mechanics, Indian Institute of Technology Madras, Chennai 600036, India,*
e-mail: nganesh22@gmail.com

Abstract

Modern wind turbine blades are slender structures whose increased flexibilities have led to unforeseen aero-elastic instabilities leading to failures. In this study, the turbine blade is modeled as a two-dimensional airfoil and is subjected to random loading. The airfoil is assumed to oscillate only in the rotational degree of freedom. The loading is assumed to be stationary and Gaussian. The fatigue damage due to this loading is described through the rain-flow cycle counting method. An approach based on polynomial chaos expansion is used to obtain the response of the nonlinear oscillator.

Keywords: Wind turbine, air foil, rain-flow

1 Introduction

The increased pace of economic development throughout the world has led to an enormous increase in the demand for energy. Consequently, the focus in recent times has been on exploring alternative sources of clean energy. Among these, wind energy being a clean, renewable form of energy, has gained popularity. The focus has been on increasing the efficiency in harnessing wind energy. This has led to the construction of wind turbines of enormous dimensions. However, the increased flexibility of the wind turbine blades, which are of enormous dimensions, has led to unforeseen failures. These failures have been attributed to aero-elastic instabilities. To develop robust designs to withstand these instabilities, a thorough understanding of the fluid-structure interaction mechanisms of these turbine blades is necessary.

The modeling of the turbine blade leads to a set of highly nonlinear differential equations. It has been observed that beyond a critical value of the mean wind velocity, known as the flutter velocity, the system exhibits self-sustained oscillations. These oscillations significantly contribute to fatigue damage. From the design perspective, it is therefore desirable that the system be designed such that the operating conditions do not lead to self-sustained oscillations. The critical wind speed beyond which the system exhibits self-sustained oscillations is referred to as the bifurcation point. However, in real life situations, the wind flow has random fluctuations about a mean value. This implies that the bifurcation point cannot be quantified in deterministic terms. Instead, the bifurcation point needs to be characterized in a probabilistic sense. To have a robust design, these random effects must be realistically represented in the modeling stage itself. However, doing so would increase the complexity in the mathematical model as these random fluctuations enter as model parameters in the governing equations of motion for the dynamical system.

Traditionally, Monte-Carlo simulations(MCS) have been used in the analysis of dynamical systems with stochastic uncertainties wherein a large number of realizations of response are obtained for a given distribution of the random process. However, MCS is a computationally expensive approach, especially for problems involving significant non-linearity and high dimensions.

2 Problem Statement

We consider a two dimensional model for the wind turbine blade. The wind turbine blade is modeled as an airfoil with two degrees of freedom in the pitch and heave directions. The schematic diagram of the two-dimensional airfoil is shown in Fig. 2. The governing equations of motion for the airfoil can be expressed as [3]

$$\begin{aligned} m\ddot{h} + S\ddot{\alpha} + K_h h &= Q_h, \\ S\ddot{h} + I_\alpha \ddot{\alpha} + K_\alpha \alpha &= Q_\alpha. \end{aligned} \tag{1}$$

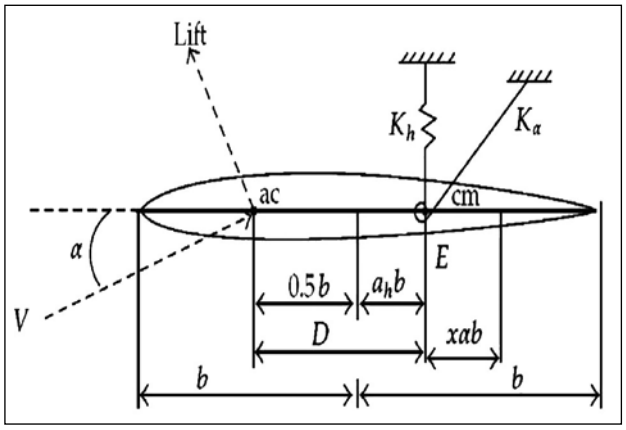

Figure 1: Schematic diagram of the wind-turbine blade modeled as a 2-D airfoil

Here, h is the heave displacement, α is the pitch angle, m is the total mass per unit span, S is the mass static moment, I_α is the mass moment of inertia, K_h is the heaving stiffness co-efficient, K_α is the pitching stiffness, $a_h b$ denotes the distance of the elastic axis from the mid chord and $x_\alpha b$ is the distance of the center of mass from the elastic axis; see Fig.1 for a schematic. The non-homogeneous terms Q_α and Q_h represent the forcing terms and are usually represented as a set of coupled second order differential equations which are functions of α and h [2]. Thus, these equations constitute a set of fluid-structure interaction problems. The over-dots represent differentiation with respect to time. Here, the coefficients K_α and K_h could be nonlinear functions of α and h. If only the pitching motion is considered a simplified form for the above system could be represented in the form of the differential equation

$$\ddot{x} + 2\eta\omega_n\dot{x} + {\omega_n}^2 x(1 + \mu x^2) = f(t, \theta). \qquad (2)$$

Here, η is the damping ratio, ω_n denotes the natural frequency of the system and μ represents the nonlinear stiffness coefficient and x represents the pitching degree of freedom. Note that the nonlinearity in Eq.(2) is cubic and can be considered to be an approximation of the free play nonlinearity that typically exists in these systems. The coefficient μ determines the extent of nonlinearity. The excitation $f(t,\theta)$ is assumed to be a stationary Gaussian random process with the following auto-correlation function

$$R_{ff}(\tau) = \sigma_f^2 e^{-c_0\tau^2}, \qquad (3)$$

where, σf is the standard deviation of the process and c_0 denotes the inverse of the correlation length. The response of the system can be obtained by solving Eq.(2). As the excitations are random processes, the response are also random processes. However, as the equations of motion are nonlinear, even though the excitations are Gaussian, the response constitute non-Gaussian random processes. Estimating the fatigue damage due to these non-Gaussian response processes require characterization of the joint probability density of the response and its instantaneous time derivative. This is explained in the following section.

3 Rain Flow Cycle Counting Method

The rain flow cycle counting method is a method for extracting and counting equivalent load cycles from a random time history. It is a technique which enables us to estimate the fatigue damage using Palmgren- Miner's rule [6, 7]. It leads to the best estimate of fatigue life [9]. Let *Y (t)* be the load acting on the system and let it be a random process. The accumulated linear fatigue damage due to *Y(t)* is denoted by D_T . Since *Y (t)* is a random process, D_T will be a random variable. Therefore, expectation of D_T given by $E[D_T]$ is to be evaluated. The process of evaluating suitable approximations for $E[D_T]$ using rain flow count is presented in the following section.

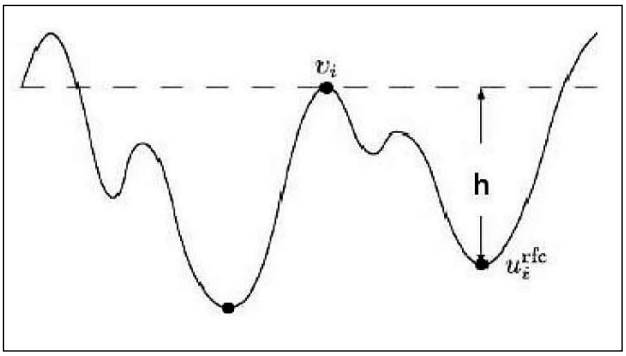

Figure 2: Definition of rain flow cycle [4]

3.1 Fatigue damage estimation using rain flow counting

A schematic of the rain-flow cycle counting as discussed in [4, 9] is presented through Fig.2. Here, each local maximum of the load process, say v_i, is paired with a particular local minimum, v_i, determined as follows:

- From the local maximum value (v_i), the lowest value is determined in forward and backward directions between the time point of the local maximum and the nearest points at which the load exceeds the value v_i.

- The larger of the two values determined above is the rain-flow minimum paired with v_i and is denoted by u_i^{rfc} in Fig.2. In other words, the rain-flow minimum is the least drop before reaching the value of local maximum (v_i) again on either side. Thus, the ith rain-flow pair is (u_i^{rfc} , v_i).
- The cycle range, *h*, is the difference between the local maximum and the paired rain-flow minimum.

In case the local minimum, u_i^{rfc} lies outside the time interval chosen, the incomplete cycle thus formed is known as the residual and it has to be handled separately.

Using the Palmgren-Miner's rule [6, 7], the accumulated linear rain-flow damage is expressed as

$$D_T = \sum f(u_i^{\mathrm{rfc}}, v_i) + D^{\mathrm{res}}, \tag{4}$$

where, $f(u_i^{rfc}, v_i)$ is the fatigue damage due to the rain-flow pair (u_i^{rfc} , v_i) and D^{res} is the damage due to the cycles constituting the residual. An alternative definition of rain-flow damage is as follows:

$$D_T = \int_{-\infty}^{\infty}\int_{-\infty}^{v} f_{12}(u,v)N(u,v)\mathrm{d}u\mathrm{d}v + \int_{-\infty}^{\infty} f_2(u,u)N(u)\mathrm{d}u. \tag{5}$$

Here, $f_2(u,v) = \frac{\partial f(u,v)}{\partial v}$ and $f_{12}(u,v) = \frac{\partial^2 f(u,v)}{\partial u \partial v}$. In the above equation, for a random time history *X(t)*, the number of up-crossings of level *u* by *X(t)*, $t \in [0, T]$ is given by *N(u)*. *N(u, v)* denotes the number of up-crossings of an interval *[u, v]* by *X(t)*.

As mentioned earlier, the quantity of interest, here, is the expected fatigue damage $\mathrm{E}[D_T]$, where, $\mathrm{E}[\cdot]$ is the expectation operator. This can be obtained by changing the order of integration in Eq.(5) as

$$\mathsf{E}[D_T] = \int_{-\infty}^{\infty}\int_{-\infty}^{\infty} f_{12}(u,v)\mathsf{E}[N(u,v)]\mathrm{d}u\mathrm{d}v. \tag{6}$$

The expected damage increase in period *T* can be shown to be proportional to loading time duration *T*, and is expressed as

$$\mathsf{E}[D_T] = T\int_{-\infty}^{\infty}\int_{-\infty}^{\infty} f_{12}(u,v)\mu(u,v)\mathrm{d}u\mathrm{d}v, \tag{7}$$

where, *μ(u, v)* is known as the intensity of interval up-crossings. As it is difficult to estimate *μ(u, v)*, bounds for intensity crossings can be evaluated. It can be shown that [9]

$$\mu(u,v) \le \min[\mu(u,u), \mu(v,v)] = \hat{\mu}(u,v), \tag{8}$$

where, *μ(u, u) = μ(u)*. Now, the bound for expected damage can be given as follows

$$\mathsf{E}[D_T] \le T\int_{-\infty}^{\infty}\int_{-\infty}^{v} f_{12}(u,v)\hat{\mu}(u,v)\mathrm{d}u\mathrm{d}v. \tag{9}$$

The mean crossing rate *μ(u)* can be easily computed using the Rice's formula [8], which is given by

$$\mu(u) = \int_0^{\infty} \dot{x}\, p_{X\dot{X}}(u,\dot{x})\mathrm{d}\dot{x}, \tag{10}$$

where, $p_{X\dot{X}}(x,\dot{x})$ is the joint probability density function (pdf) of the process, *X(t)*, and its instantaneous time derivative, $\dot{X}$ *(t)*. The focus of this study is on quantifying the joint pdf of the process, *X(t)* and its instantaneous time derivative. Analytical closed form expressions for $p_{X\dot{X}}(x,\dot{x})$ is not easy to estimate, especially if the governing differential equations of motion exhibit significant nonlinearities. An alternative procedure for estimating $p_{X\dot{X}}(x,\dot{x})$ would be to obtain approximations by Monte Carlo simulations. This would necessitate generating an ensemble of realizations of the excitations $\{f(t)_i\}_{i=1}^N$ compute an ensemble of the response state $\{X(t)_i\}_{i=1}^N$ and $\{\dot{X}(t)_i\}_{i=1}^N$ subsequently estimate $p_{X\dot{X}}(x,\dot{x})$ by statistical processing. To obtain reasonable accuracies at the tail regions of $p_{X\dot{X}}(x,\dot{x})$, *N* has to be large. This would imply *N* numerical solutions of the governing equations of motion. For more complicated forms of differential equations , such as Eq. (2), this would be computationally expensive. The focus of this study is on the development of a technique by which the computational effort could be minimized. To achieve this, we employ the polynomial chaos representation of the response. This is discussed further in the following sections.

4. Karhunen-Loeve Expansion(K-L Expansion)

A continuous random process can be represented as a series expansion involving sets of discrete random variables and deterministic basis functions. While there can be many such representations, for example, the spectral representation where the trigonometric functions are the basis functions [10], the Karhunen-Loeve expansion is the most optimal representation. The K-L expansion is based on the eigendecomposition of the auto-covariance function. The deterministic basis functions, which are orthonormal, are the eigenfunctions of the auto-covariance function and their magnitudes are the eigenvalues. The Karhunen-Loeve expansion converges in the mean-square sense for any distribution of the stochastic process [8]. A

K-L representation of a zero-mean stochastic process f(t, θ) can be represented in the form

$$f(t,\theta) = \sum_{i=0}^{\infty} \boldsymbol{\xi}_i(\theta)\sqrt{\lambda_i}\phi_i(t), \tag{11}$$

where, the coefficients λ_i and the functions $\phi_i(t)$ respectively are the eigenvalues and the eigenfunctions of the covariance function and are evaluated by solving the following Fredholm integral equation of the second kind:

$$\int_0^T R_{ff}(t,s)\phi_i(s)\mathrm{d}s = \lambda_i\phi_i(t). \tag{12}$$

The parameter 't' indicates time and θ represents the random sample. In Eq.(12), $R_{ff}(t, s)$ denotes the auto-correlation function of the process $f(t,\theta)$. In Eq.(11), $\{\xi_i(\theta)\}$ is a vector consisting of uncorrelated random variables with zero-mean and unit variance. The eigenfunctions are orthonormal and satisfy the identity

$$\int_0^T \phi_i(t)\phi_j(t)\mathrm{d}t = \delta_{ij} \tag{13}$$

where, δ_{ij} is the Kronecker-delta function defined as

$$\delta_{ij} = \begin{cases} 1 & \text{if } i = j \\ 0 & \text{otherwise.} \end{cases}$$

Since Eq.(11) is an infinite series, it becomes imperative to decide on the number of terms to be retained in the expansion of $f(t, \theta)$. It is seen that not all terms have a significant contribution in the expansion. The number of significant terms depend on various factors such as the form of auto-correlation function, length of the interval T and correlation length of the stochastic process [5]. Some of these issues have been considered in this paper to truncate the series expansion to appropriate number of terms. The K-L expansion is usually employed for a Gaussian process. For non-Gaussian process, a generalization of the K-L expansion is the polynomial chaos expansion also known as PCE. This is discussed in the following section.

5. Polynomial Chaos Expansion

Polynomial chaos expansion is a spectral representation of the random process in terms of orthonormal basis functions and deterministic coefficients. Wiener [11] introduced the homogeneous chaos theory based on Cameron andMartin theorem [1]. The homogeneous chaos theory, in its original form, employs Hermite polynomials with Gaussian random variables, from the Askey scheme, as orthonormal bases. The exponential convergence of the polynomial chaos expansion has been extended to several other types of commonly used probability distributions in the generalized polynomial chaos by Xiu and Karniadakis [12]. A random process X(t, θ) can be represented according to Cameron-Martin theorem as follows [1]:

$$X(t,\theta) = \hat{x}_0\Gamma_0 + \sum_{i_1=1}^{\infty}\hat{x}_{i_1}\Gamma_1(\xi_{i_1}(\theta)) + \sum_{i_1=1}^{\infty}\sum_{i_2=1}^{i_1}\hat{x}_{i_1 i_2}\Gamma_2(\xi_{i_1}(\theta),\xi_{i_2}(\theta)) + \ldots, \tag{14}$$

where, $\Gamma_n(\xi_{i1}, \xi_{i2}, \ldots, \xi_{in})$ denotes the Hermite polynomials of order n in terms of n-dimensional independent standard Gaussian random variables $\xi = (\xi_{i1}, \xi_{i2}, \ldots, \xi_{in})$ with zero mean and unit variance. The above equation is a discrete form representation of the Wiener polynomial chaos expansion. A generalization of Eq.(14) can be obtained by rewriting it in the form

$$X(t,\theta) = \sum_{i=0}^{\infty} x_i(t)\Psi_i(\boldsymbol{\xi}(\theta)), \tag{15}$$

where, ψ_i denotes the basis functions and $x_i(t)$ are the deterministic coefficients. The polynomials ψ_i's are mutually orthogonal and the satisfy the following identity:

$$\langle\Psi_i\Psi_j\rangle = \langle{\Psi_i}^2\rangle\delta_{ij}, \tag{16}$$

where, δ_{ij} is the Kronecker delta function and $\langle\cdot\rangle$ is the expectation operator of the form

$$\langle x\rangle = \int_\Omega xw(x)\mathrm{d}x. \tag{17}$$

Here, $w(x)$ is an appropriate weighting function. The one dimensional Hermite polynomials can be shown to be related in the recursive form

$$\Gamma_{n+1} = \xi\Gamma_{n-1} - (n-1)\Gamma_{n-2}, \tag{18}$$

where, the first few polynomials are of the form

$$\Gamma_0 = 1,\ \Gamma_1 = \xi,\ \Gamma_2 = \xi^2 - 1,\ \Gamma_3 = \xi^3 - 3\xi,\ \Gamma_4 = \xi^4 - 6\xi^2 + 3. \tag{19}$$

The two dimensional Hermite polynomials can be expressed as

$$\begin{aligned}
&\Psi_0(\boldsymbol{\xi}) = \Gamma_0(\xi_1)\Gamma_0(\xi_2) = 1,\\
&\Psi_1(\boldsymbol{\xi}) = \Gamma_1(\xi_1)\Gamma_0(\xi_2) = \xi_1,\\
&\Psi_2(\boldsymbol{\xi}) = \Gamma_0(\xi_1)\Gamma_1(\xi_2) = \xi_2,\\
&\Psi_3(\boldsymbol{\xi}) = \Gamma_2(\xi_1)\Gamma_0(\xi_2) = {\xi_1}^2 - 1,\\
&\Psi_4(\boldsymbol{\xi}) = \Gamma_1(\xi_1)\Gamma_1(\xi_2) = \xi_1\xi_2.
\end{aligned} \tag{20}$$

Truncating Eq.(15) to p terms, we approximate $X(t, \theta)$ as

$$X(t,\theta) = \sum_{i=0}^{p} x_i(t)\Psi_i(\boldsymbol{\xi}(\theta)). \tag{21}$$

The number of terms up to which the series is truncated, p, is known as the order of expansion. For n number of random variables and polynomial order n_p, p is given by the following :

$$p = \frac{(n+n_p)!}{n!n_p!} - 1. \tag{22}$$

A number of methods can be used for finding the coefficients in the polynomial chaos expansion, two of which are presented.

5.1 Galerkin PCE solution of the equation of motion

The solution of Eq.(2), by the Galerkin PCE approach is presented here. In this approach, a Galerkin projection of the orthogonal polynomials is performed to modify the governing equation to a system of deterministic coupled nonlinear equations in terms of the polynomial chaos coefficients. The governing equation is rewritten below for convenience:

$$\begin{aligned}
&\ddot{x} + 2\eta\omega_n\dot{x} + {\omega_n}^2 x(1+\mu x^2) = f(t,\theta),\\
&x(0) = \dot{x}(0) = 0.
\end{aligned} \tag{23}$$

As mentioned in the previous section, $f(t, \theta)$ is approximated as a K-L expansion, truncated up to M terms, as shown below:

$$f(t,\theta) = \sum_{i=0}^{M} \boldsymbol{\xi}_i(\theta)\sqrt{\lambda_i}\phi_i(t). \tag{24}$$

The solution to the governing equation is assumed to be in the form

$$X(t,\theta) = \sum_{i=0}^{N} x_i(t)\Psi_i(\boldsymbol{\xi}), \tag{25}$$

where, $x_i(t)$ are the deterministic functions to be evaluated and ψ_i represent the polynomial chaoses. Substituting Eq.(24) and Eq.(25) in Eq.(23), the governing equation of motion can now be written as

$$\begin{aligned}
&\sum_{i=0}^{N}(\ddot{x}_i(t)\Psi_i(\boldsymbol{\xi}) + 2\eta\dot{x}_i(t) + x_i(t)) + \mu\sum_{i=0}^{N}\sum_{j=0}^{N}\sum_{k=0}^{N}\\
&x_i(t)x_j(t)x_k(t)\Psi_i(\boldsymbol{\xi})\Psi_j(\boldsymbol{\xi})\Psi_k(\boldsymbol{\xi}) = \sum_{i=0}^{M} f_i(t)\xi_i,
\end{aligned} \tag{26}$$

where,

$$f_i(t) = \sqrt{\lambda_i}\phi_i(t). \tag{27}$$

Multiplying Eq.(26) by $\psi_m(\xi)$ and taking expectation, a set of nonlinear deterministic differential equations is obtained, which is of the form

$$\begin{aligned}
&\ddot{x}_m(t) + 2\eta\dot{x}_m(t) + x_m(t) + \mu\sum_{i=0}^{N}\sum_{j=0}^{N}\sum_{k=0}^{N}\frac{c_{ijkm}}{\langle\Psi_m^2\rangle}\\
&x_i(t)x_j(t)x_k(t) = f_m(t).
\end{aligned} \tag{28}$$

Here,

$$c_{ijkm} = \langle\Psi_i\Psi_j\Psi_k\Psi_m\rangle = \int_{-\infty}^{\infty}\Psi_i\Psi_j\Psi_k\Psi_m w(\boldsymbol{\xi})\mathrm{d}\boldsymbol{\xi} \tag{29}$$

The weight function, $w(\xi)$, in Eq.(29), is the Gaussian probability density function for Hermite polynomials and is of the form

$$w(\xi) = \frac{1}{\sqrt{2\pi}}e^{-(\frac{1}{2}\boldsymbol{\xi}^T\boldsymbol{\xi})} \tag{30}$$

It is to be noted that the orthogonality property of the Hermite polynomials given by Eq.(16) has been made use of while arriving at Eq. (28). Eq. (28) is solved for various values of m and the corresponding coefficients are obtained. Once the coefficients are evaluated, the solution is reconstructed by substituting them in Eq.(25).

Although the Galerkin method minimizes the error due to truncation accurately, it has some serious drawbacks. The process of evaluating the inner products and arriving at the set of nonlinear deterministic equations is computationally expensive and can become tedious. The complexity increases with type and extent of nonlinearity, the distribution of random variables used and the number of terms included in the expansion. In order to circumvent

these difficulties, several alternative methods are available in literature. One among those, known as the non-intrusive projection method, is used in this work. This is discussed in the following section.

5.2 Non-intrusive Projection Method

In the non-intrusive polynomial chaos method, the polynomial chaos coefficients are evaluated by solving the governing equation at certain collocation points and then substituting them in a projection formula. In contrast to the Galerkin method, the polynomial chaos expansions are not substituted in the governing equation and hence it is known as non-intrusive. It is also referred to as the pseudo Monte-Carlo approach as a number of runs of the deterministic equation are required, but not as large as in Monte-Carlo simulations [2]. A Galerkin projection of Eq.(15) by taking $\langle ., \Psi_j \rangle$ gives the following formula

$$x_j(t) = \frac{\langle X(t, \boldsymbol{\xi}(\theta)), \Psi_j \rangle}{\langle \Psi_j^2 \rangle}, \tag{31}$$

where, x_j is the PCE coefficient and the inner product in the numerator is given by the following multidimensional integral

$$\langle x(t, \boldsymbol{\xi}(\theta)), \Psi_j \rangle = \int_{-\infty}^{\infty} \ldots \int_{-\infty}^{\infty} X(t, \boldsymbol{\xi}(\theta)) \Psi_j w(\boldsymbol{\xi}) d\boldsymbol{\xi} \tag{32}$$

The dimension of the integral is equal to the dimension of the vector ξ. The above multidimensional integral can be solved by suitable quadrature rules. Since the weight is a Gaussian probability density function and the domain of integration is $(-\infty, \infty)$, Gauss-Hermite quadrature is used here. The multidimensional integral in Eq.(32) can now be approximated using the following expression:

$$\langle x(t, \boldsymbol{\xi}(\theta)), \Psi_j \rangle = \sum_{k_1=1}^{N_0} \ldots \sum_{k_n=1}^{N_0} X(t, \xi_{k_1}, \ldots, \xi_{k_n})(W_{k_1} \ldots W_{k_n}) \tag{33}$$

where, N_0 is the number of quadrature points and $W_{k1} \ldots W_{kn}$ are the weighting functions.

6. Numerical Results and Discussions

To decide the number of terms to be included in the K-L expansion, the magnitude of the eigenvalues is considered. The magnitude of the first few eigenvalues of the covariance function is given in Table 1. It is seen that the magnitude of eigenvalues quickly diminishes to zero and only the first few eigenvalues are significant. For the sake of simplicity, the number of terms in the K-L series has been fixed at 2. The resulting expansion is given by

$$f(t, \theta) = f_1(t)\xi_1(\theta) + f_2(t)\xi_2(\theta). \tag{34}$$

Table 1: Magnitude of eigenvalues

Eigenvalue	Magnitude
λ_1	7.2105
λ_2	4.5738
λ_3	2.1815
λ_4	0.8031
λ_5	0.2356
λ_6	0.0569
λ_7	0.0116
λ_8	0.0020
λ_9	0.0003
λ_{10}	0.0000

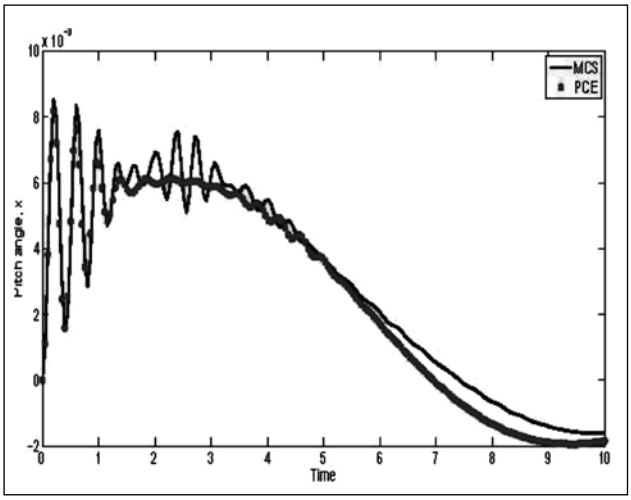

Figure 3: Mean response; μ = 2

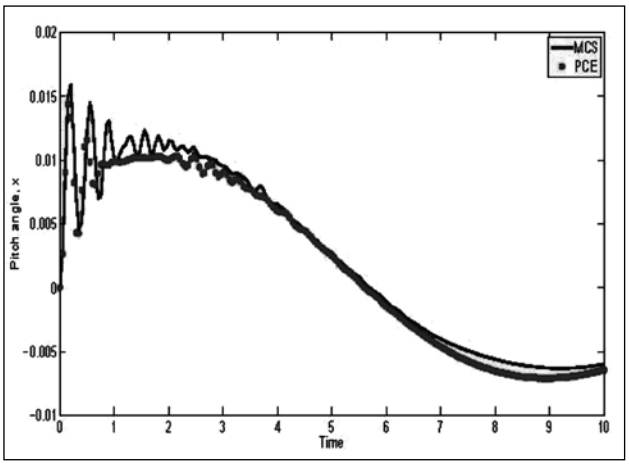

Figure 4: Mean response with; μ = 10

Now the numerator in Eq.(30) is evaluated as follows

$$\langle X(t,\boldsymbol{\xi}(\theta))\Psi_j\rangle = \sum_{k_1=1}^{N_0}\sum_{k_2=1}^{N_0} X(t,\xi_{1_{k_1}},\xi_{2_{k_1}}) \Psi(\xi_{1_{k_1}},\xi_{2_{k_1}})W_{1_{k_1}}W_{2_{k_2}}. \quad (34)$$

The coefficients thus evaluated are substituted i n Eq.(26) to obtain the response process. The number of quadrature points, N_0, is chosen to be 24 for each random variable making a total of 576 collocation points at which the deterministic equation is to be solved. This is much less than the number of deterministic runs performed in a Monte-Carlo simulation which is generally higher than 1000.

The analysis explained in the preceding sections is performed with the auto-correlation function given by Eq.(2) and for a duration of 10s. The excitation is represented in the form given by Eq.(24) and the response is obtained as a 12th order polynomial chaos expansion. A damping factor of η = 0.1 has been chosen and the inverse of correlation length, c_0, is 0.1.

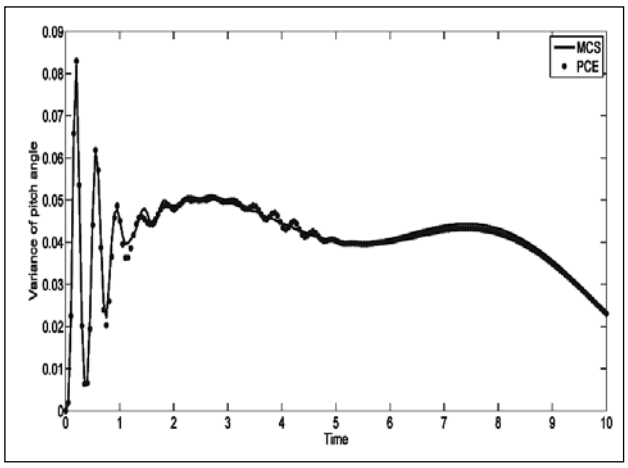

Figure 5: Variance of response; μ = 2

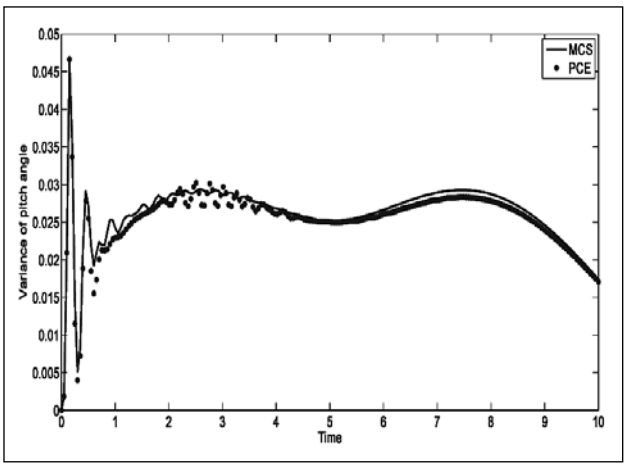

Figure 6: Variance of response; μ = 10

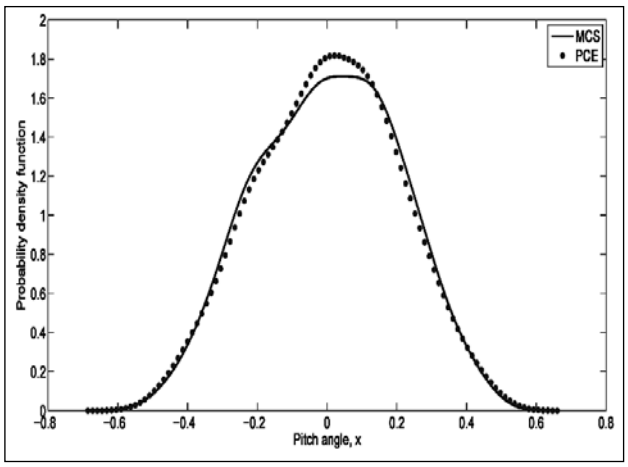

Figure 7: Marginal pdf of response X(t); μ = 2

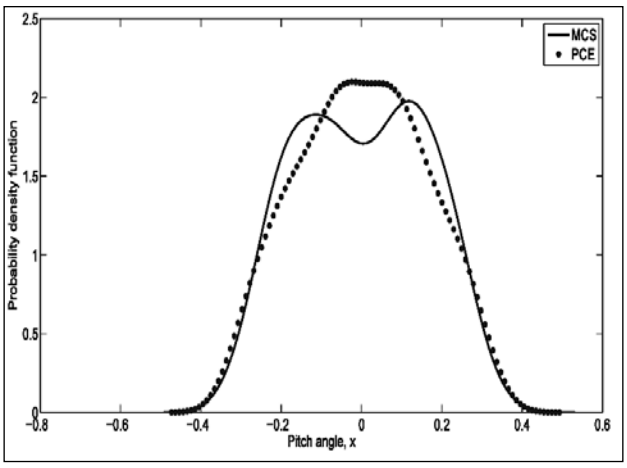

Figure 8: Marginal pdf of response X(t); μ = 10

The natural frequency of the system, ω_n, is 200rad/s. The deterministic differential equations are solved using an adaptive 4th order Runge- Kutta algorithm. The polynomial chaos expansion response has been compared with the Monte-Carlo simulation response. 1000 realizations of the response process are generated. Fig. 3 shows the mean of the response process calculated at each time instant from 0 to 10 with μ = 2 whereas Fig. 4 shows the mean response with μ = 10. The variance of the

response for the two levels of nonlinearities is shown in Fig. 5 and Fig. 6. The marginal probability density functions of response at 110th time step corresponding to the two cases are shown in Fig. 7 and Fig. 8. Figs. 9-10 show the joint pdf, $p_{X\dot{X}}(x,\dot{x})$ at time , t = 5.53s for different values of μ and these are compares with the corresponding joint pdfs obtained from MCS in Figs. 11-12. It is observed that a fairly good agreement between the results obtained from MCS and those from PCE are obtained. This lends promise for

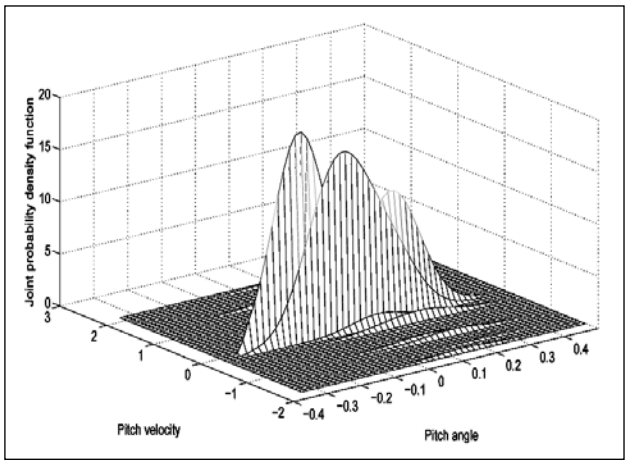

Figure 9: Joint pdf $p_{X\dot{X}}(x,\dot{x})$; μ = 2

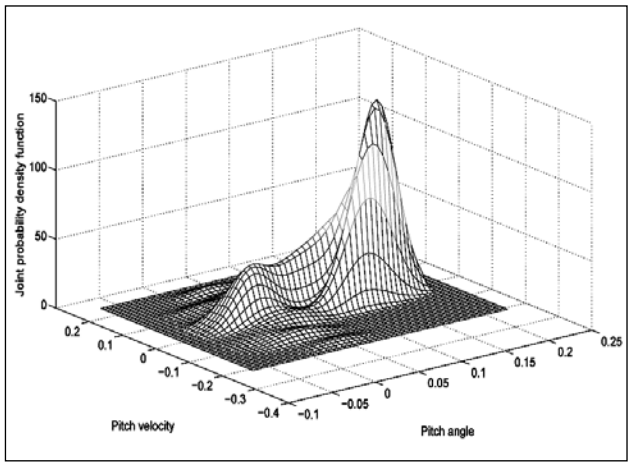

Figure 10: Joint pdf of $p_{X\dot{X}}(x,\dot{x})$; μ = 10

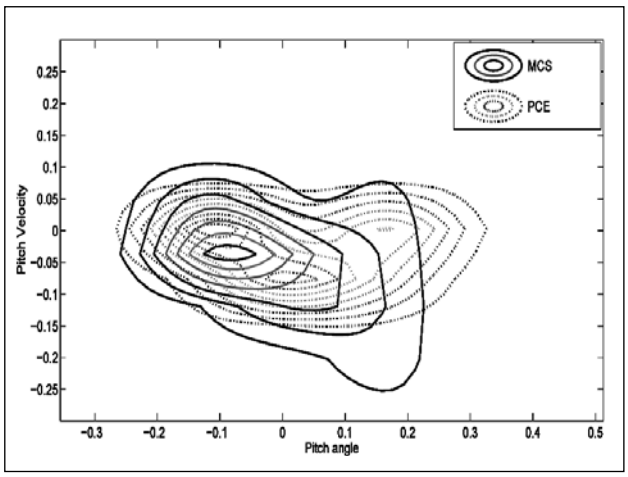

Figure 11: Contour plots for joint pdf $p_{X\dot{X}}(x,\dot{x})$; μ = 2

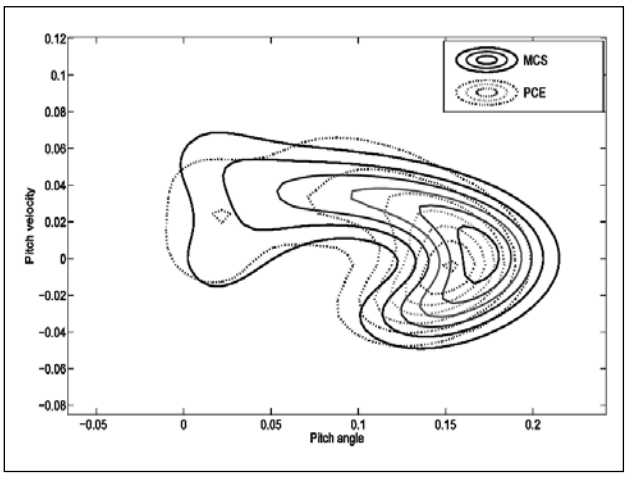

Figure 12: Contour plots for joint pdf $p_{X\dot{X}}(x,\dot{x})$; μ = 10

the developed methodology for estimating the expected fatigue damage in nonlinear vibrating problems. The efficiency of the developed method in terms of computational costs would obviously increase as the complexity and the nonlinearity of the method increases. This study is currently in progress.

7. Concluding Remarks

The response of a nonlinear vibrating oscillator has been analyzed using the polynomial chaos expansion approach. The application of PCE for approximating the response of nonlinear vibrating systems has been investigated. A non-intrusive method has been used to obtain the PCE coefficients. Numerical simulations on simple nonlinear oscillator show reasonable agreement in the mean, variance and marginal probability distribution functions of the response obtained from the PCE approximations and full scale MCS. The approximated probability density functions can be used to estimate mean rain-flow fatigue damage. More studies along these lines are currently in progress.

References

1. Cameron R.H., Martin W.T, The orthogonal development of nonlinear functionals in series of Fourier–Hermite

functionals, Annals of Mathematics 48:1947;385–392.
2. Desai A, Sarkar S, Analysis of a nonlinear aeroelastic system with parametric uncertainties using polynomial chaos expansion, Mathematical Problems in Engineering, 2010.
3. Fung YC, An Introduction to the Theory of Aeroelasticity. John Wiley Sons, Inc.,New York, 1955.
4. Gupta S, Rychlik I (2007), Rain-flow fatigue damage due to nonlinear combination of vector Gaussian loads.
5. Li R, Ghanem R (1998), Adaptive polynomial chaos expansions applied to statistics of extremes in nonlinear random vibration, Probabilistic Engineering Mechanics.
6. Miner MA, Cumulative damage in fatigue, Journal of Applied Mechanics 1945;12:A159-64.
7. Palmgren A, Die lebensdauer von kugellagern,VDI Z 1924;68:339-41.
8. Papoulis A, Pillai SU, Probability, Random Variables and Stochastic Processes, Tata-McGraw- Hill, 2002.
9. Rychlik I. On the "narrow-band" approximation for expected fatigue damage, Probabilistic Engineering Mechhanics, 1993;8:1–4.
10. Shinozuka M, Jan CM, Digital simulation of random processes and its applications, Journal of Sound and Vibration 1972;25(1),111-128.
11. Wiener N, The Homogeneous Chaos, American Journal of Mathematics,vol.60, no.4, 897-936.
12. Xiu D, GE Karniadakis. TheWiener-Askey polynomial chaos for stochastic differential equations. SIAM Journal on Scientific Computing,2002;24(2):619–644.

Life Cycle Reliability and Safety Engineering
Vol.1 Issue 4 (2012) 26-32

Structural Reliability Evaluation and Optimization of a Pressure Vessel Using Non-Linear Performance Functions

P Bhattacharjee[1] K Ramesh Kumar [2] Dr. T A Janardhan Reddy[3]
[1] *Reliability Engineering Division, DRDL Hyderabad,*
[2]*Production Planning Division, DRDL Hyderabad*
[3]*Mechanical Engineering, OU Hyderabad*
pradeep9_rqa@yahoo.com

Abstract

Structural safety is one of the most important factors of any aerospace product. Until recently, a design is considered to be robust if all the variables that affect its life has been accounted for and brought under control. The meaning of robustness is changing. Designer and engineers have traditionally handled variability with safety factors. In this paper, in the first phase, a pressure vessel made of titanium alloy is considered for safety index (structural reliability) study. The safety index is evaluated based on the data collected during manufacturing and operation. Various methods like mean value and moment methods are used for safety evaluation and same have been discussed. In the second phase of the paper, an attempt has been made to carry out multi objective design analysis taking into account the effect of variation of design parameters. Multiple objective of interest include structural weight, load induced stress, deflection and structural reliability. The design problem is formulated under nonlinear constrained optimization and has been solved. Nonlinear regression relations are used for various performance functions. Nonlinear regression model is validated & found to be in good agreement with experimental results. Finally, optimum design parameters are suggested for design operating conditions.

Keywords: Structural reliability, safety index, nonlinear regression, reliability optimization

1. Introduction

Probabilistic structural design evaluation method is fast growing in aerospace engineering. In this method, all uncertainties like variability in material properties, geometry and loads are considered during design which enables a product to have better reliability compared to deterministic design. The study of reliability engineering is also developing very rapidly. The desire to develop and manufacture a product with superior performance and reliability than its predecessor is a major driving force in engineering design. The design of any engineering system requires the assurance of its reliability and quality. Traditional deterministic method have accounted for uncertainties through empirical safety factor. Such safety factors do not provide a quantitative measure of safety margin in design and are not quantitatively linked to influence different design variables and their uncertainties on over all system performance. In this paper a Titanium Air bottle (pressure vessel) is identified for structural safety index study. These Air bottles are extensively used in Aerospace and ground operations. The detailed safety index evaluation is discussed in this paper.

Generally, the objective & constraint functions, load conditions, failure modes, structural parameters and design variables are treated in a deterministic manner. The problem with this approach is that, in many cases, deterministic optimization gives designs with higher failure probability than optimized structures. Therefore, since uncertainties are always present in the design for engineering structure, it is necessary to introduce reliability theory in order to achieve a balance between cost and safety for optimal design. A straightforward approach for the modeling and analysis of uncertainties is to introduce probabilistic models in which structural parameters and /or design variables are considered stochastic in nature. Then, by the combination of reliability based design procedures and optimization technique, it is possible to devise a tool to obtain optimal designs.

The aim of this work to establish a simple methodology, which will be useful to pressure vessel designer during design and development. The present paper deals with analysis of a typical Titanium pressure vessel that is used to store high-pressure air, nitrogen or inert gas to run turbine to generate power as well as for pneumatic actuation for

control system. These bottles have to be safe, reliable and shall be of lower weight. The optimum design problem formulated under nonlinear constrained optimization using nonlinear regression has been solved as "Nonlinear Constrained Minimization" optimization. Optimum parameters of Air bottle are suggested for design operating pressure.

2. Nomenclature

a,b,c	:	Regression Coefficient
g(x)	:	Performance Function
P	:	Pressure
p_f	:	Probability of Failure
R	:	Reliability
R^2_{adj}	:	Adjusted R-square
R^2	:	Regression Square
R_i	:	Internal Radius
R_0	:	External Radius
s,M	:	Material Strength
t	:	Thickness
U,u, Z	:	A Vector of Statistically Independent Random Variables with Zero Mean and Unit Standard Deviation
V	:	Volume
W	:	Weight
β	:	Safety Index
β_0	:	Design Safety Index Requirement
γ	:	Poisson's Ratio
δ	:	Deformation
μ_M	:	Mean Material Strength
μ_σ	:	Mean Induced Stress
ρ	:	Density
σ	:	Stress /Standard Deviation
σ_M	:	Standard Deviation of Material Strength
σ_σ	:	Standard Deviation of Induced Stress
Φ	:	Normal cdf

3. Problem Statement and Methodology Adapted

Weight optimization is one of the prime requirements of any aerospace product. Aerospace product has to be optimum in respect of weight, size, volume, cost etc. Any weight saving results in increase in pay load capacity. Similarly, packaging density can be increased with volume optimization. But all these design optimizations should not be at the cost of safety and reliability. In this paper we have identified a pressure vessel which has already been designed, developed and successfully used in various ground and space vehicles applications. These air bottles operate at very high pressure and are filled with dry air, nitrogen or inert gas. Due to its higher operating pressure, it has to be totally safe as ground personnel handle these bottles in fully charged condition.

In the first phase, safety index (structural reliability) is evaluated using Mean Value Method (MVM) and Advanced First Order Second Moment (AFOSM) Method, using data collected during manufacturing and testing. In the second phase an attempt is made to optimize the weight of the air bottle to meet the target reliability. Finite Element Analysis (FEA) is carried out to generate maximum stress, strain and deformation for various design parameters and operating conditions. Nonlinear performance functions (regression relations) are established for stress, and deflection.

4. Safety Index Evaluation

4.1 Mean value method

This method [1-3] is commonly referred to as the Mean Value First Order - Second Moment (MVFOSM or simply MV) method since it involves a first order expansion about the mean to estimate the first and second moments. MV method involves developing the Taylor series expansion of g(x) about the nominal or mean value of the individual random variables. The moments of the resulting approximating function are found using which approximate statements can be made regarding the probability of failure.

$$g(x) = g(x_1, x_2, \ldots x_n); \quad \textit{Safety Index} \quad \beta = \frac{\mu_g}{\sigma_g}$$

Where μ_g and σ_g are the mean and standard deviation of performance function.

4.2 Advanced first - order second -moment

Hasofer and Lind (HL) [4-6] proposed a method for evaluating the safety index (β). According to HL approach, the constraint is linearized by using Taylor Series expansion retaining up to the first order terms. The linearization point selected is that of maximum likelihood of occurrence and is known as the most probable failure point. This method is called Advanced First-Order Second-Moment (AFOSM) method. The most probable failure point is determined by transforming original random variables to normalized and independent set of reduced variables as shown in Fig.1.

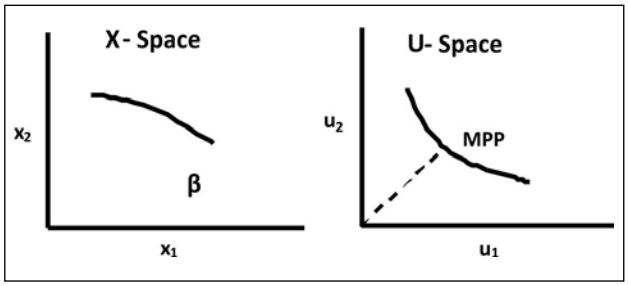

Fig: 1 Transformation of coordinate into Standard Space

$$U = \frac{x - x_\mu}{x_\sigma} \tag{1}$$

The failure surface is mapped onto the corresponding failure surface in the reduced space. The point on this surface with minimum distance from the origin is the most probable failure point and the geometric distance to the origin is equal to the safety index β. The failure surface is generally a nonlinear function and the point with minimum distance to the origin can be evaluated by solving the following optimization problem i.e.

$$\text{Minimize } \left(U^T U\right)^{1/2} = \beta \tag{2}$$
$$\text{Subject to } g(U) = 0$$

Where g(U) is the failure function or limit state equation in reduced space. Using AFOSM, this optimization can be solved by using nonlinear optimization or iterative algorithms.

5. Optimization Formulation

The present paper deals with a practical problem of high pressure air bottles. In the first phase of the study, we have evaluated the safety index (structural reliability) of these air bottles. After confirming that these air bottles have enough margins of safety, an attempt has been made to optimize the weight of the air bottle. These air bottles are at present under serial production and are being used in various ground and space applications. Static linear strength, deformation and safety index have been considered as design constraints. The brief optimization formulation of this problem is discussed below.

5.1 Nonlinear performance functions

Nonlinear Regression Relations

The regression relations [7] are established for induced stress and deformation due to internal load. In many engineering situations the relationship between dependent and independent variable may not be linear but exponential, Weibull, logarithmic or inverse type. These types of equations generally fall under the category of having nonlinear parameter. In order to apply the principles of least squares, the equation should be reduced to linear form. The process of transforming the nonlinear equation into a linear form is called linear transformation. It is observed from ANSYS output data Table 1, that the hoop stress and deflection have nonlinear relation with its wall thickness and outer radius. A logarithmic relation has been established and tested statistically for significance. The regression relations considered are as below

$$\log \sigma = a_1 + b_1 \log t + c_1 \log R_0 \tag{3}$$

$$\log \delta = a_2 + b_2 \log t + c_2 \log R_0 \tag{4}$$

The wall thickness of the hemispherical shell and outer radius of the air bottle are the main design geometrical parameters which accounts for weight. Hence these parameters are considered for weight optimization. The nonlinear performance function relations for stress and deformation are as given below

$$\sigma = a_1 t^{b_1} R_0^{c_1} \tag{5}$$

$$\delta = a_2 t^{b_2} R_0^{c_2} \tag{6}$$

Load induced stress and deformation under various operating load (pressures) is evaluated using finite element analysis (ANSYS), where a_1, a_2, b_1, b_2, c_1 & c_2 are the coefficients of above regression equations. The nonlinear regressions established are given in Table 2.

5.2 Optimization constraints

Static Linear Strength

The static linear strength [8] design criteria is based on load induced stress at the critical location in the spherical shell should be less than or equal to maximum allowable stress. In other words that the maximum stress generated due to internal pressure should not exceed the material strength as defined below

$$\frac{\sigma}{\sigma_{\max}} - 1 \le 0 \tag{7}$$

Deformation

The spherical air bottle will dilate radially outward due to internal pressure. In no case the airbottle shall deform beyond maximum allowable deflection, i.e.

$$\frac{\delta}{\delta_{max}} - 1 \le 0 \tag{8}$$

Safety Index (Structural Reliability)

The safety index β is defined as

Where $\beta = -\frac{\mu_M - \mu_\sigma}{\left(\sigma_M^2 + \sigma_\sigma^2\right)^{1/2}}$ (9)

$$\beta \ge \beta_0 \; ; \quad 1 - \frac{\beta}{\beta_0} \le 0$$

Where β_0 is design safety index requirement.

'β' is achieved safety index and is evaluated using strength-stress interference model. In this present paper both material strength and induced stress are considered normally distributed to be random variable.

5.3 Nonlinear constrained optimization

The main objective is to minimize the weight of the air bottle, without compromising the safety requirement. A nonlinear single objective constrained optimization method is adapted. The nonlinear regression equations as given in Table 2 are used for optimization formulation [9-11]. The optimization problem formulation is as under

Objective function

Minimize W = ρV

Subject to

$$\frac{\sigma}{\sigma_{\max}} - 1 \le 0; \quad \frac{\delta}{\delta_{max}} - 1 \le 0; \quad 1 - \frac{\beta}{\beta_0} \le 0$$

Where $\sigma = a_1 t^{b_1} R_0^{c_1}$; $\delta = a_2 t^{b_2} R_0^{c_2}$;

$$\beta = \frac{\mu_M - \mu_\sigma}{\left(\sigma_M^2 + \sigma_\sigma^2\right)^{1/2}} \; ; \; V = \frac{4}{3}\pi\left[3R_0^2 t - 3R_0 t^2 + t^3\right]$$

Bound constraints $t_l < t < t_u$ & $R_{01} < R_0 < R_{0u}$

l & u are lower and upper design limit

6. Nonlinear Performance Function Generation

6.1 Finite element analysis

To establish the performance function relations, the ANSYS output is generated for each set of design input parameters i.e. wall thickness and outer radius of spherical shell. The details of ANSYS output is given in Table 1.

Table –1: ANSYS Output

Thickness (t)	Outer radius (R_0)	Design Load 40 MPa	
		Hoop stress (σ) MPa	Deformation (δ) mm
2.5	152.0	1233	1.0555
3.0	152.5	1007	0.8819
3.5	153.0	885	0.7567
4.0	153.5	746	0.6644
4.5	154.0	665	0.5927
5.0	154.5	599	0.5353
5.5	155.0	544	0.4883
6.0	155.5	500	0.4492
6.5	156.0	461	0.4161
7.0	156.5	428	0.3877
7.5	157.0	399	0.3632
8.0	157.5	375	0.3417
8.5	158.0	358	0.3227

6.2 Nonlinear regression & regression statistics

The nonlinear regression of induced stress (σ) and deformation (δ) versus wall thickness (t) and outer radius (R_0) are established using ANSYS output as given in Table 1. These regression equations are used for optimization formulation. The nonlinear regression and regression statistics are given in Table 2 & Table 3.

Table –2: Nonlinear Regression Equations

Design Load	$\sigma = a_1 t^{b1} R_0^{c1}$	$\delta = a_2 t^{b2} R_0^{c2}$
40 (MPa)	$\sigma = 0.0059 t^{-1.0967} R_0^{2.6386}$	$\delta = 0.0037 t^{-1.0242} R_0^{1.7701}$

Table –3: Regression Statistics

Design Load	$\sigma = a_1 t^{b1} R_0^{c1}$	$\delta = a_2 t^{b2} R_0^{c2}$
40 (MPa)	R^2_{adj} = 0.9999 *rmse* = 0.0020 *mse* = 3.9 * 10^{-6}	R^2_{adj} = 1.0000 *rmse* = 0.0010 *mse* = 1.0377 * 10^{-6}

R^2_{adj}: Adjusted Regression Square; rmse: root mean square error; mse: mean square error R^2_{adj} as values are close to one and 'rmse' value is low indicating that the regression relations are fitting well.

7. Design Data

To evaluate safety index, initially design data are collected from design document. The important design parameters of the air bottle are given in Table -4.

Table –4: Design Parameter

Internal Radius (R_i)	:	149.5 mm
Wall Thickness (t)	:	8.0 mm
Design Pressure (P)	:	40 MPa
Material	:	Titanium alloy
Construction	:	Welded
Type of Welding	:	Electron Beam
Weight	:	10.5 kg

Table –5: Variability Observed

Parameter	Mean (μ)	Standard Deviation (σ)
Operating Pressure (P)	36 (Mpa)	1.98 (Mpa)
Internal Radius (R_i)	149.5 (mm)	0.5 (mm)
Wall Thickness (t)	7.91 (mm)	0.25 (mm)
Material Strength (M)	860 (Mpa)	8.6 (Mpa)

A systematic data collection is carried out during manufacturing at production centers starting from raw material to final product. Material mechanical properties are taken from test certificates provided by the suppliers which cover chemical compositions, heat treatment details, tensile strength and percentage elongation. Similarly, thickness mapping for wall thickness and internal radius are carried out before joining of each spherical shell. The statistical dispersion of various parameters is given in Table -5.

8. Design Safety Analysis

8.1 Safety index (structural reliability)

The structural safety [1] of the air bottle is evaluated considering the statistical variability from the data collected during manufacturing, testing and operation. The Safety Index (β) evaluated using Mean Value Method and Advanced First Order Second Moment Method as discussed in Safety Index Evaluation section is as follows

a) Mean value method

$$g = \left(s - \frac{PR_i}{2t}\right)$$

$$\mu_g = 484.84 \qquad (10)$$

$$\sigma_g = \left[\left(\frac{\partial g}{\partial s}\sigma_s\right)^2 + \left(\frac{\partial g}{\partial P}\sigma_P\right)^2 + \left(\frac{\partial g}{\partial R}\sigma_R\right)^2 + \left(\frac{\partial g}{\partial t}\sigma_t\right)^2\right]^{1/2} \quad \sigma_g = 23.2585$$

$$\beta = \frac{\mu_g}{\sigma_g}; \quad \mathbf{\beta = 20.8}$$

σ_g; **β = 20.8**

b) Advanced first order second moment method

Data from Table -5 is transformed to Normal space

$$Z_1 = \frac{s - s_\mu}{\sigma_s} = \frac{s - 860}{8.6}$$

$$Z_2 = \frac{P - P_\mu}{\sigma_P} = \frac{P - 40}{1.98}$$

$$Z_3 = \frac{R_i - R_\mu}{\sigma_R} = \frac{R_i - 149.5}{0.5}$$

$$Z_4 = \frac{t - t_\mu}{\sigma_t} = \frac{t - 7.91}{0.25}$$

$$s = 8.6Z_1 + 860$$
$$P = 1.98Z_2 + 40$$
$$R_i = 0.5Z_3 + 149.5$$
$$t = 0.25Z_4 + 7.91$$

Substituting s, P, Ri & t in Eq 10

$$g(Z) = (8.6Z_1 + 860) - \left[\frac{(1.98Z_2 + 40)(0.5Z_3 + 149.5)}{2(0.25Z_4 + 7.91)}\right]$$

Minimize $\beta = \sqrt{Z^T Z}$

Such that g(Z) = 0

Solving above optimization problem we get **β = 14.39**

9. Reliability Optimization

9.1 Non-linear constrained optimization

The main objective of this paper is to minimize the weight of the air bottle as thickness and outer radius

are the design parameters which contribute to the weight of titanium material. Hence these parameters are optimized so as to minimize the weight of the air bottle. The non-linear constrained optimization [10-12] is formulated as below.

Objective function

Minimize weight (W) = V * ρ

Subject to

$$\frac{\sigma}{\sigma_{\max}} - 1 \le 0, \quad \frac{\delta}{\delta_{max}} - 1 \le 0, \quad 1 - \frac{\beta}{\beta_0} \le 0$$

Where: $V(volume) = \frac{4}{3}\pi\left[3R_0^2 t - 3R_0 t^2 + t^3\right]$

β_0 (Target Safety Index) ≥ 4; R (Structural Reliability) ≥ 0.99996; R_i (Internal Radius) = 149.5; σ (Induced Stress) = $a_1 t^{b1} R_0^{c1}$; δ (deformation) = $a_2 t^{b2} R_0^{c2}$

$\beta = -\frac{\mu_M - \mu_\sigma}{\left(\sigma_M^2 + \sigma_\sigma^2\right)^{1/2}}$; $\sigma_\sigma = 25.91$ (Experimentally observed induced stress standard deviation)

$\mu_\sigma = \sigma$, $\mu_M = \sigma_{Max}$, σ_M = 8.6 *MPa* & P (design load) = 40 MPa

Rewriting the above optimization formulation

Objective function

Minimize weight (W) = $[55.67R_0^2 t - 55.67R_0 t^2 + 18.5t^3)$

Subject to

$$6.8604 * 10^{-6} t^{-1.0967} R_0^{2.6386} - 1 \le 0 \quad (11)$$

$$7.4 * 10^{-4} t^{-1.0242} R_0^{1.7701} - 1 \le 0 \quad (12)$$

$$5.4 * 10^{-5} t^{-1.0967} R_0^{2.6386} - 6.875 \le 0 \quad (13)$$

Inequality constraints

$3 < t < 8$ & $152.5 < R_0 < 157.5$

Solving above optimization problem using nonlinear programming technique, the optimized design parameters obtained are given in Table 6.

Table –6: Optimized Parameters

Parameter	Design	Optimized
Inner Radius 'R_i'	149.5 mm	149.5 mm
Thickness 't'	8.00 mm	5.3453 mm
Outer Radius 'R_0'	157.5 mm	154.8453 mm
Weight 'W'	10.5 Kg	6.8919 Kg
Safety Index 'β'	14.39	6.0949

10. Results and Discussion

The structural reliability (safety index) study has been carried out using moment methods, the safety index 'β' is found to be high. This indicates that titanium air bottle is over designed and these bottles are very safe at design operating pressure. Hence, this gives scope for weight optimization.

The nonlinear regression relation of performance functions established using ANSYS output is found to be useful for prediction of stress, strain and deformation. These relations are simple and help in optimization formulation. Many complex performance functions can be written in simple linear, nonlinear or polynomial forms.

Using above findings, the weight of the existing air bottle is optimized without compromising quality, design and safety requirements. A net weight reduction of 3.5 kg is possible which in turn helps in increasing payload capacity for aerospace mission. The optimized safety index is now β = 6.09, that is the probability of failure of this optimized air bottle is p_f = 0.522E-09.

11. Conclusion

A nonlinear constraint optimization for air bottle using regression model has been developed and found to be useful in their domain validity. This method accounts for effect of design variability while providing a realistic design model where conflicting and multi objectives viz; structural weight, operating load, induced stress, strain, deformation and structural reliability (safety index) exist. Suggested nonlinear regressions (nonlinear performance functions) are validated. In addition to design parameters, fatigue and fracture can also be considered in safety and optimization studies.

Acknowledgement

The constant encouragement and support extended by Director DRDL, and help rendered by Director R&QA are gratefully acknowledged.

References

1. Bhattacharjee, P., (2009). Structural Reliability Assessment of Pressure Vessel. Journal of Aerospace Quality and Reliability Vol. 5, 159-163.
2. David G Robinson, (1998)A Survey of Probabilistic methods used in Reliability, Risk and Uncertainty Analysis Analytical Techniques -1. SANDIA REPORT SAND 98 1189-1998.
3. Wong, Felix S., (1985). First Order Second Moment Methods Computer & Structure . 20 (4), 779-791.

4. Melchers, R E., (1987). Structural Reliability Analysis and Prediction Ellis Harwood Limited. 104 -141
5. Shu, Ho Dai & Ming.0 Wang., (1992).Reliability Analysis in Engineering Applications,61-132.
6. Sorensen, John Dalsgaard., (2004). Notes in Structural Reliability Theory and Risk Analysis. Aalborg
7. Montgomery, Douglas C., (2004). Design and Analysis of experiments John Wiley & Sons Inc
8. Mohamed E. El-Sayed., (1999). Structural Optimization for Reliability using Nonlinear Goal Programming. NAGI – 1837.
9. Seung Kyumchoi, Ramana V Grandhi and Robert A Canfield., (2006). Reliability - Based Structural Design. Springer.
10. Grandhi, Ramana V. and Liping Wang. (1999). Structural Reliability Analysis and Optimization: use of Approximations Wright State University,Ohio.NASA/ CR - 209154.
11. Bhattacharjee P., K Ramesh Kumar & Dr T A Janardhan Reddy,(2010). Reliability Design Evaluation and Optimization of a Nitrogen Gas Bottle using Response Surface Method. Int. Journal of Reliability, Quality and Safety Engineering. 17(2), 119-132..
12. Bhattacharjee P., Dr T A Janardhan Reddy & K Ramesh Kumar, (2009). Structural Reliability Evaluation Using Response Surface Method. Proceedings of International Conference on Reliability, Maintainability and Safety. IEEE ICRMS, 972-977.

Life Cycle Reliability and Safety Engineering
Vol.1 Issue 4 (2012) 33-38

On Reliability Evaluation of Structures using Hermite Polynomial Chaos

Sabarethinam Kameshwar and Arunasis Chakraborty
Department of Civil Engineering, Indian Institute of Technology Guwahati
E-mail: arunasis@iitg.ernet.in

Abstract

Reliability analysis using first and/or second order methods need to evaluate the slope of the limit surface near the most probable point (MPP) of failure which is often difficult for real life structures due to limited information of the failure plane. To avoid this problem, present study aims to use stochastic response surface method (SRSM) to evaluate the reliability index. In this method, implicit limit state is modeled using series expansion of standard normal random variables (i.e. polynomial chaos expansion). The coefficients of the polynomial chaos expansion are obtained by stochastic collocation which needs limited number of performance function evaluation. Once the order of the polynomial and subsequently the coefficients are evaluated, reliability index is obtained by gradient based approach. Numerical examples are presented to show the applicability of the proposed SRSM based reliability analysis.

Keywords: limit state, reliability index, polynomial chaos, stochastic response surface

Introduction

First order reliability methods have been extensively used for reliability analysis of structural systems [Lu *e.t al.* (1994), Rodriguez *et. al.* (2006), Griffiths (2011) *et. al.*] operating in random environment. For this purpose, Rackwitz-Fiessler algorithm is often used to find out the optimal distance (i.e. reliability index) of the limit surface from the origin in the standard normal space. In this method, the slopes (i.e. first derivative) of the limit surface are required to locate the most probable design point. However, limit surfaces are often unknown in close form (i.e. implicit) and hence their derivatives are difficult to evaluate. In this context, Bucher and Bourgand (1990) developed Response Surface Method (RSM) for reliability analysis. In RSM, the unknown limit surface is approximated by a multidimensional quadratic polynomial near the failure region. In the recent past, engineers and researchers have extensively used this method for various applications like performance evaluation, crash simulation and reliability based design optimization [Babu and Srivastava (2010), Minghao *et. al.* (2009), Gupta and Manohar (2004), and Deb *et. al.* (2009)]. However, as this polynomial approximation of the original limit state is valid near the failure region, it often faces difficulty to find out the optimal distance for limit states with multiple design points. Moreover, as this is a deterministic representation of the failure surface, it fails to capture the stochastic characteristics of the original limit state. To avoid this problem, Stochastic Response Surface Method (SRSM) was proposed by Isukapalli (1999). In this method, the stochastic signature of the original limit state is mapped in the standard normal space using Polynomial Chaos Expansion (PCE). Wiener (1938) first introduced PCE to model the turbulence where infinite ortho-normal functions in standard normal space were used to model the stochastic phenomenon. Ghanem and Spanos (1991) showed that Hermite polynomials form an orthogonal basis for PCE and is convergent in mean-square sense. However, this representation needs to evaluate the coefficients of the Hermite polynomials to model the original performance function. Tatang (1995) developed probabilistic collocation technique where Gauss quadrature points were used to evaluate the coefficients of the PCE. In his thesis, Isukapalli (1999) used the roots of the polynomial which were one order higher as the reference points and evaluated the coefficients by regression analysis. Gavin and Yau (2008) showed that SRSM works better for complex structures with low failure probability where Monte Carlo simulation (MCS) and approximate methods are either computationally intensive or inaccurate. It models the global stochastic nature of the limit surface as opposed to model the local nature near the failure region in RSM. This property may be exploited to identify the local minima where multiple design points exist. Due to these advantages, SRSM has gained

momentum in reliability analysis of civil engineering structures in the recent past. Li *et. al.* (2011) performed reliability analysis of rock slopes using SRSM with higher order polynomials. Mollon *et. al.* (2011) used collocation based SRSM to analyze the stability of a circular tunnel driven by a pressurized shield.

With these in view, present study aims to apply SRSM to analyze the reliability of a retaining wall against overturning. The results obtained from this method will be compared with Monte-Carlo simulations to check the efficiency and accuracy of the SRSM.

Stochstic Response Surface Methodology

The limit surface divides the probability space into safe and failure regions, which is symbolically represented as

$$g(X) = 0 \tag{1}$$

Where, X = [x_1, x_2, ..., x_n] are the random variables that describe the failure plane. In the above equation, $g(X) < 0$ represents the failure region. The probability of failure for a limit state described in Eq. 1 can be represented as

$$p_f = \int \dots\dots \int_{g(x)<0} f_{X_1,X_2,\dots\dots,X_n}(x_1, x_2, \dots\dots, x_n)$$
$$dx_1 dx_2 \dots\dots dx_n = P[g(X) \leq 0] \tag{2}$$

However, probability evaluation using above equation demands complete description of the joint probability distribution function *f* which is often unknown. The problem is more complex where the performance function described in Eq.1 is not available in explicit form. To evaluate the reliability for these cases either RSM or SRSM can be used. However, RSM often faces difficulties in highly non-linear failure planes with multiple local minima as only the polynomial approximation near the MPP is carried out in this method. In this situation, SRSM can be a better alternative as the stochastic nature of the failure plane, irrespective of the local minima are modeled using PCE. Reliability evaluation using SRSM involves following steps

a) Functional/Polynomial chaos representation of output
b) Evaluation of unknown coefficients
c) Representation of input random variables in terms of standard normal variables
d) Evaluation of reliability using FORM/SORM

Functional/Polynomial Chaos Representation of Output

Polynomial chaos is defined by an ortho-normal set of standard normal variables $\{z_i\}_{i=1}^{\infty}$. Therefore, PC of order *p* (i.e. Γ_p) is defined by the set of polynomials of order *p* which is orthogonal to all polynomials of order (*p* - 1). Using these ortho-normal set of standard normal variables, any function g can be represented as

$$g = \sum_{p\geq 0} \sum_{n_1+n_2+\dots+n_r=p} \sum_{\rho_1,\dots,\rho_r} a^{n_1,\dots,n_r}_{\rho_1,\dots,\rho_r} \Gamma_p (z_{\rho 1}, \dots\dots, z_{\rho r}) \tag{3}$$

In the above equation, *p* and *r* represent the order and the dimension respectively and $a^{n_1,\dots,n_r}_{\rho_1,\dots,\rho_r}$ represent the coefficients. Hermite polynomials are used to represent which is given by [Ghanem & Spanos (1991), Issukapalli (1999)]

$$\Gamma_p(z_{i_1}, \dots\dots, z_{i_r}) = e^{\frac{1}{2}z^t z}(-1)^p \frac{\partial^p}{\partial z_{i_1}, \dots\dots, z_{i_r}} e^{-\frac{1}{2}z^t z} \tag{4}$$

Where, Z_i is the standard normal random variable. Using Eq.3 and Eq.4 the limit state given in Eq.1 can be represented in standard normal space as

$$g_p(Z) = 0 \tag{5}$$

In the above expression, performance function is represented by the linear combination of *n*-dimensional polynomials involving unknown coefficients $a^{n_1,\dots,n_r}_{\rho_1,\dots,\rho_r}$ which can be evaluated using regression technique [Issukapalli (1999)].

Evaluation of Unknown Coefficients

Once the functional representation of Eq. 1 is decided, the next step is to evaluate the unknown coefficients. For this purpose, regression analysis is performed using collocation points which are the roots of the Hermite polynomial that are one order higher than the polynomial used to represent the limit surface. Therefore, the number of collocation points available for *n* dimensional p^{th} order PCE is $(p+1)^n$ [Isukapalli *et al* (1998)]. In this format, it can be shown that the numbers of collocation points are always more than the number of unknowns in Eq. 5.

Representation of Stochastic Inputs

The regression analysis mentioned in the previous sub-section needs to evaluate the performance function represented by Eq. 1 at $(p+1)^n$ collocation

points. However, as these collocation points are in standard normal space, the equivalent points in the original space need to be found by one to one mapping of cumulative distribution function (CDF) of the two random variables. For the details of this transformation one may refer to Isukapalli *et. al.* (1998).

Evaluation of Reliability

Once the coefficients in Eq. 5 are evaluated, gradient based approaches (either FORM or SORM) may be adopted to evaluate the reliability index. The details of these methods may be found in Melcher (1999). Using FORM, the reliability index is represented as

$$\beta = \left.\frac{\sum z_i \nabla_i g_p(Z)}{\|\nabla g(Z)\|}\right|_{z^*} \quad (6)$$

In the above equation, z^* zrepresents MPP in standard normal space and $\|.\|$ represents the Euclidian norm. It can be shown that the probability of failure is related to through the following relation

$$p_f = \Phi(-\beta) \quad (7)$$

Example Cases

The SRSM method described in the previous section is used to evaluate the reliability for two different limit surface.

Example 1: Non-linear Limit State

In the first problem, the following performance function is considered

$$g(X) = \frac{-1}{25}(X_1 - 1)^2 - \frac{X_2}{3} + 3 + \frac{sin(5X_1)}{5} \quad (8)$$

Where, x_1 and x_2 are the two random variables that describe the failure plane.

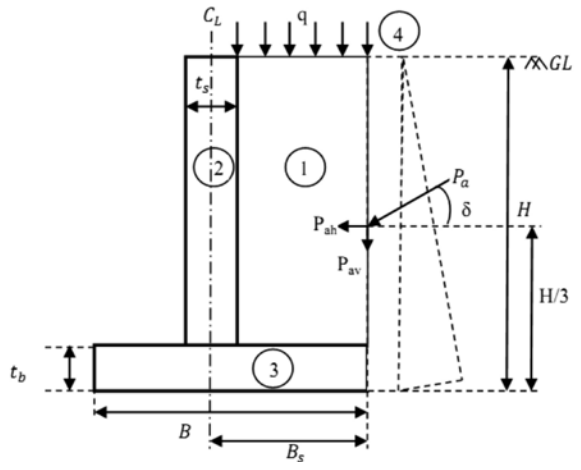

Figure 1: Retaining wall

Example 2: Retaining Wall against Overturning

In the second problem, the reliability analysis of a retaining wall as shown in Fig. 1 against overturning is considered.

The parameters in Fig. 1 and the details of the stabilizing and overturning moments are described in Appendix A. The limit state in this case is given by

$$g(X) = M_r - M_o \quad (9)$$

In the above equation, M_r represents the stabilizing moment and M_o represents the overturning moment about the toe of the wall. The random variables associated with this limit state are surcharge loading (q) unit weight of concrete (w_c), unit weight of soil (w_s), soil friction angle (φ) and wall friction angle (δ).

Numerical Results and Discussion

The proposed SRSM based reliability analysis discussed in the previous sections is used to solve example cases to evaluate the reliability. In Example 1, X_1 and X_2 are the two uncorrelated random variables with mean and standard deviation as 3.5 and 1 respectively. In this example, different combinations of normal and lognormal variables for X_1 and X_2 are considered and the results are compared with the Monte Carlo simulations. The unknown coefficients of the PCE are evaluated using collocation points. For this purpose, 4th order polynomials are used to model the limit surface. Hence, the total number of unknowns in Eq. 5 is 15. To generate the collocation points, roots of the 5th order are used. As the dimension of the problem is 2, the possible combinations using these roots are $(4+1)^2$ (i.e. 25.) Although, 25 collocation points are available for the regression analysis, only 23 (i.e. 1.5*15) points are used to evaluate the unknown coefficients. It has been observed that the convergence can be achieved with 1.5**N* collocation points where, *N* is the number of unknown coefficients in PCE representation. In this context, the points that are close to the origin were given priority. Fig 2 shows the cumulative distribution function (CDF) of the limit state using PCE and Monte-Carlo simulations. It can be observed from this figure that the 4th order polynomial estimates CDF satisfactorily. Using this 4th order PCE, Hasofer-Lind Reliability Index is evaluated as described in Eq. 6. Table 1 shows the reliability index and probability of failure for different combinations of random variables X_1 and X_2. From this table, it can be concluded that SRSM results match closely with simulations. In this context, $6*10^6$ samples were used in Monte-Carlo simulations.

Table 1: Reliability index and probability of failure in Example 1 (N: normal, LN: lognormal)

X_1	X_2	β		p_f	
		Monte Carlo	SRSM	Monte Carlo	SRSM
N	N	3.3692	3.4325	0.00037	0.00029
N	LN	2.8977	2.8094	0.00187	0.00248
LN	N	2.7879	2.8019	0.00265	0.00254
LN	LN	2.6461	2.8058	0.00407	0.00250

Table 2: Random variables in Example 2

Variable	Distribution	Statistics	
		μ	cov(%)
q	LN	20	10
w_c	N	24	7
w_s	N	18	7
φ	LN	30	7
δ	LN	10	7

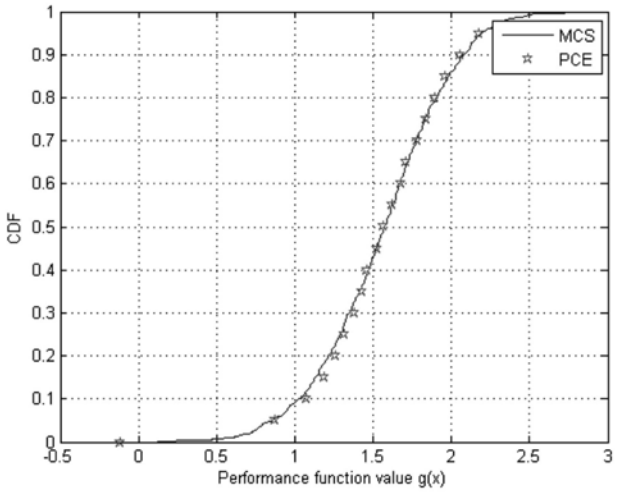

Figure 2: CDF of the limit state in Example 1

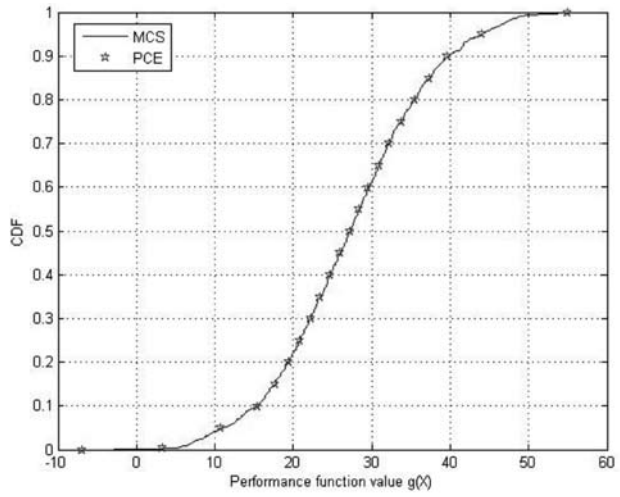

Figure 3: CDF of the limit state in Example 2

The SRSM based technique is further used for to evaluate the reliability of the retaining wall. Table 2 shows the distributions and the parameters of the random variables used in this model. It can be observed that the dimension of this problem is 5. Similar to example 1, 4th order PCE is used in this problem to model the limit state in the standard normal space. The total number of unknowns for this 5th dimensional and 4th order PCE representation is 126. Hence, the roots of the 5th order polynomial are used as the collocation points. As described in previous section, total number of collocation points available in this case is 3125 [i.e. $(4+1)^5$]. However, 183 collocation points (i.e. 1.5*126) which are closer to the origin are used for regression analysis. Using these collocation points CDF of the limit state are obtained and is shown in Fig. 3. In this case also, one can notice a close match between the PCE and the simulations. Fig 4 and 5 show the reliability index for different values of height and base width of the retaining wall. From these figures, one can conclude that the reliability index obtained by SRSM closely match with the simulations. Fig 6 shows the probability of failure for different values of height and base width. This design curve can be used to evaluate the reliability (i.e. 1 - p_f) for a given combination of height and base width of the retaining wall.

Conclusions

In this paper, stochastic response surface method is used to evaluate the reliability for different limit state functions. The random characteristics of the limit state is modeled by multidimensional polynomial chaos expansion whose coefficients are evaluated by regression analysis. For this purpose, the roots of

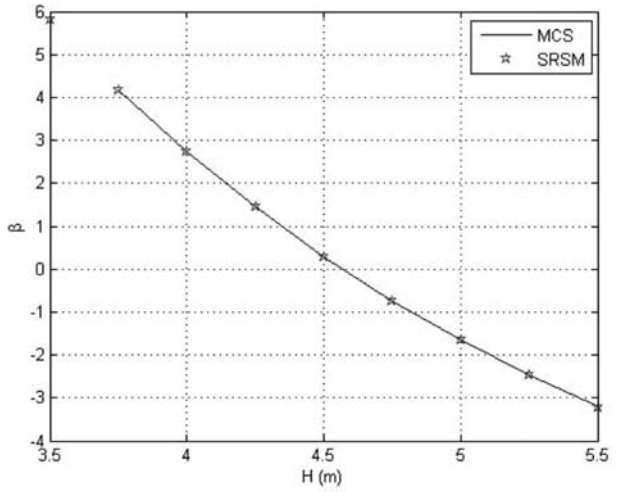

Figure 4: Change of β with height of the wall

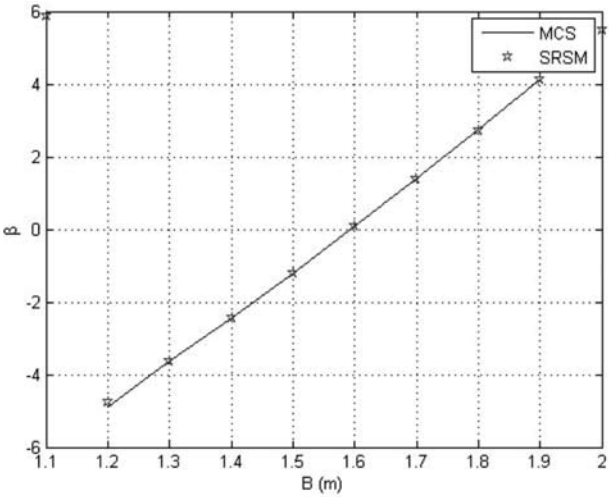

Figure 5: Change of β with base width

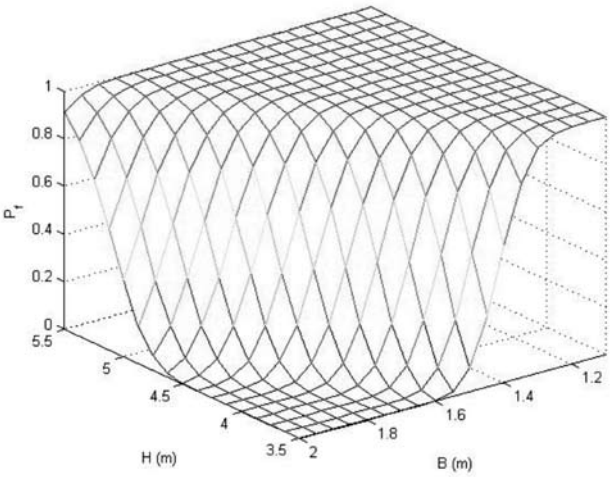

Figure 6: Variation of p_f for different height and base width

the polynomial of dimension one order higher than the original one are used to generate the collocation points. Once the coefficients are evaluated, the optimal distance in standard normal space (i.e. reliability index) is evaluated using Rackwitz-Fiessler algorithm. The example cases in the previous section show the accuracy and efficiency of the SRSM based reliability analysis.

Appendix

Fig 1 shows the retaining wall used in example 2. In this figure H, B, B_s, t_s and t_b are the height of the wall, length of the base, distance of the centerline of stem to heel, thickness of the stem and thickness of the base slab respectively. The thickness of the stem and the base are taken to be 0.45m. Further, q and δ represent the surcharge and the wall friction angle while P_a represents the active earth pressure which has horizontal and vertical components as P_{ah} and P_{av} respectively. M_1, M_2, M_3 and M_4 are the moments due to self weights of different components of the wall–soil combination marked 1, 2, 3 and 4 respectively, which are given by

$$M_1 = w_s \frac{\left(B_s - \frac{t_s}{2}\right)^2}{2}(H - t_b) \quad \text{(A1.a)}$$

$$M_2 = w_c t_s (H - t_b) B_s \quad \text{(A1.b)}$$

$$M_3 = w_c t_b \frac{B^2}{2} \quad \text{(A1.c)}$$

$$M_4 = \frac{q}{2}\left(B_s - \frac{t_s}{2}\right)^2 \quad \text{(A1.d)}$$

The total downward force due to the weights of different components (i.e. soil mass, stem of the wall, base of the wall and surcharge) is given by

$$W = w_s\left(B_s - \frac{t_s}{2}\right)(H - t_b) + w_c t_s (H - t_b) + w_c t_b B + q\left(B_s - \frac{t_s}{2}\right) \quad \text{(A2)}$$

The point of action of the total weight W can be obtained as

$$x_w = \frac{M_w}{W} \quad \text{(A3)}$$

Using Eq. A2 and A3, the total resisting moment about the toe of the wall can be expressed as

$$M_r = W(B - x_w) \quad \text{(A4)}$$

Thus, the active earth pressure acting on the wall due to the soil mass is given by

$$P_a = \frac{1}{2}K_a w_s H^2 + K_a q H \quad \text{(A5)}$$

Where, the active earth pressure coefficient K_a is defined as

$$K_a = \frac{\cos^2(\varphi - \alpha)}{\cos^2(\alpha)\cos(\alpha + \delta)\left[1 + \sqrt{\frac{\sin(\varphi + \delta)\sin(\varphi - \gamma)}{\cos(\alpha + \delta)\cos(\gamma - \alpha)}}\right]^2} \quad \text{(A6)}$$

In the above equation, φ, α and γ are the soil friction angle, the angle of the wall and the inclination of the backfill respectively. Using Eq. A5 and A6, one can estimate the total overturning moment acting on the wall as

$$M_o = \left(\frac{1}{2}K_a w_s \frac{H^3}{3} + K_a q \frac{H^2}{2}\right)\cos(\delta) \quad \text{(A7)}$$

In this paper, the wall is considered to be perfectly vertical while the backfill is considered to be perfectly horizontal.

References

1. Babu G. L. S. and Srivastava A. (2010) "Reliability Analysis of Earth Dams", Journal of Geo-technical and Geo-environmental Engineering, 136(7), 995 – 998.
2. Bucher C. G. and Bourgund U. (1990) "A Fast and Efficient Response Surface Approach for Structural Reliability Problems", Structural Safety, 7, 57 – 66.
3. Deb K., Gupta S., Daum D., Branke J., Mall A. K. and Padmanabhan D. (2009), "Reliability-Based Optimization Using Evolutionary Algorithms", IEEE Transactions on Evolutionary Computation, 13(5), 1054 – 1074.
4. Gavin H. P. and Yau S. C. (2008), "High-Order Limit State Functions in the Response Surface Method for Structural Reliability Analysis", Structural Safety, 30, 162 – 179.
5. Ghanem R. and Spanos P. (1991), "Stochastic Finite Elements: A Spectral Approach", Springer-Verlag, New York, USA.
6. Griffiths D. V., Huang J. and Fenton G. A. (2011), "Probabilistic Infinite Slope Analysis", Computers and Geotechnics, 38, 577 – 584.
7. Gupta S. and Manohar C. S. (2004), "Improved Response Surface Method for Structural Reliability Analysis", Structural Safety, 26, 123 – 139.
8. Isukapalli S. S. (1999), "Uncertainty Analysis of Transport –Transformation Models", Ph.D. Thesis, State University of New Jersey, USA.
9. Isukapalli S. S., Roy A. and Georgopoulos P. G. (1998). "Stochastic Response Surface Methods (SRSMs) for Uncertainty Propagation: Application to Environmental and Biological Systems," Risk Anal, 18(3), 351 – 363.
10. Li D., Chen Y., Lu W. and Zhou C. (2011), "Stochastic Response Surface Method for Reliability Analysis of Rock Slopes Involving Correlated Non-Normal Variables," Computers and Geotechnics, 38, 58 – 68.
11. Lu R., Luo Y., and Conte J. P. (1994), "Reliability Evaluation of Reinforced Concrete Beams", Structural Safety, 14, 277 – 298.
12. Melcher R. E. (1999), "Structural Reliability and Prediction", John Wiley and Sons, New York, USA.
13. Minghao L., Lam F. and Foschi R. O. (2009), "Seismic Reliability Analysis of Diagonal-Braced and Structural-Panel-Sheathed Wood Shear Walls," Journal of Structural Engineering, 135(5), 587 – 596.
14. Mollon G., Dias D. and Soubra A. H. (2011), "Probabilistic Analysis of Pressurized Tunnels against Face Stability Using Collocation-Based Stochastic Response Surface Method," Journal of Geotechnical and Geo environmental Engineering, 137(4), 385 – 397.
15. Rodriguez R. J., Sitar N. and Chacon J. (2006), "System Reliability Approach to Rock Slope Stability," International Journal of Rock Mechanics & Mining Sciences, 43, 847 – 859.
16. Tatang M. A. (1995), "Direct Incorporation of Uncertainty in Chemical and Environmental Engineering Systems". PhD thesis, Massachusetts Institute of Technology, USA.
17. Wiener N. (1938), "The Homogeneous Chaos", American Journal of Mathematics, 60, 897 – 936.

Life Cycle Reliability and Safety Engineering
Vol.1 Issue 4 (2012) 39-52

Past, Present and Future of Engineering under Uncertainty: Safety Assessment and Management

Achintya Haldar
Department of Civil Engineering and Engineering Mechanics
University of Arizona, Tucson, Arizona, U.S.A.
E-mail: Haldar@u.arizona.edu

Abstract

The author's perspective of engineering under uncertainty is presented. In the first part of the paper, past, present and future trend of reliability assessment methods, applicable to many branches of engineering are presented. The discussions cover the cases for both explicit and implicit limit state functions. Finite element based reliability evaluation methods for large structures satisfying underlying physics are emphasized. The necessity of estimating risks for both strength and serviceability limit states are documented. Concept of several energy dissipation mechanisms recently introduced to improve performance and reduce risk during seismic excitations can be explicitly incorporated in the formulation. Reliability evaluation of very large structures requiring over several hours of continuous running of a computer for one deterministic evaluation is briefly presented. Since major sources of uncertainty cannot be completely eliminated from the analysis and design of an engineering system, the risk needs to be managed appropriately. Risk management in the context of decision analysis framework is also briefly presented. In discussing future directions, the use of artificial neural networks and soft computing, incorporation of cognitive sources of uncertainty, developing necessary computer programs, and education-related issues are discussed.

Keywords: Reliability analysis; seismic analysis; nonlinear response, partially restrained connections, shear walls; post-Northridge connections; computer programs, education, uncertainty management

Introduction

Uncertainty must have been present from the beginning of time. Our forefathers must have experienced it through observations and experiences. In engineering practices, the probability concept is essentially an attempt to incorporate uncertainty in the formulation. The probability concept can be defined in two ways: (i) an expression of relative frequency and (ii) degree of belief. The underlying mathematics of probability are based on three axioms, well developed, and accepted by experts, however, sometimes it is used in a philosophical sense. Since the relative frequency concept is almost never used [1], a measure of confidence in expressing uncertain events leads to the degree of belief statements. Laplace (1749-1827), a famous mathematician in "A Philosophical Essay on Probabilities" wrote "It is seen in this essay that the theory of probabilities is at bottom only common sense reduced to calculus; it makes us appreciate with exactitude that which exact minds feel by a sort of instinct without being able of times to give a reason for it. It leaves no arbitrariness in the choice of opinions and sides to be taken; and by its use can always be determined the most advantageous choice. Thereby, it supplements most happily the ignorance and weakness of the human mind." [2].

These timeless remarks sum up the importance of probability, reliability and uncertainty concepts in human endeavor. In my way of thinking, I will try to give my understanding or assessment of "Engineering under Uncertainty – Past, Present and Future". Obviously, the time lines when past meets present and present becomes future are very difficult to establish. According to Albert Einstein "People like us, who believe in physics, know that the distinction between past, present, and future is only a stubbornly persistent illusion."

Although, the area of probability has a glorious past, I will try to emphasize the present and future in reliability assessment and management in this

paper. I believe that structural engineering provided leadership in developing these areas and I will emphasize it in my presentation.

Reliability Assessment - Past

Many brilliant scholars such as Einstein did not believe in probability. His famous comment that "I am convinced that He (God) does not play dice." is known to most present scholars. On the other hand, the Rev. Thomas Bayes (1702-1761), a Presbyterian Minister at Tunbridge Wells, wrote the Bayes' Theorem in 1763 in "An Essay towards Solving a Problem in the Doctrine of Chances." [3]. It has become one of the most important branches of statistics in the modern time. Please note that the paper was published two years after his death. One of Bayes' friends, Richard Price, sent the paper for publication by adding an introduction, examples and figures. Most likely, Bayes was not confident about the paper. At present, the Bayesian approach provides a mechanism to incorporate uncertainty information in cases of inadequate reliable data by combining experience and judgment.

It is reasonable to state that Freudenthal [4] formally introduced the structural reliability discipline. Obviously, it has gone through monumental developments since then under the leadership of many scholars 5-14 A more complete list can be found in [9].

Available Reliability Evaluation Methods

It will be informative to discuss very briefly how the reliability evaluation methods evolved in the past few decades. After four decades of extensive work in different engineering disciplines, several reliability evaluation procedures of various degrees of complexity and sophistication are now available. First-generation structural design guidelines and codes are being developed and promoted worldwide using some of these procedures. Obviously, depending upon the procedure being used, the estimated risk could be different. The engineering profession has not yet officially accepted a particular risk evaluation method. Thus, design of structures satisfying an underlying risk can be debated; even the basic concept of acceptable risk is often openly debated in the profession. Moreover, uncertainty introduced due to human error is not yet understood and thus cannot be explicitly introduced in the available reliability assessment methods. Also, risk or reliability estimated using these methods may not match actual observations. Sometimes, to be more accurate, scholars denote the estimated risk as the notional or relative risk. The main idea is if risk can be estimated using a reasonably acceptable procedure, the design alternatives will indicate different levels of relative risk. When the information is used consistently, it may produce a risk-aversive appropriate design.

Before introducing the reliability-based design concept, it may be informative to study different deterministic structural design concepts used in the recent past and their relationship with the reliability-based concept. The fundamental concept behind any design is that the resistance or capacity or supply should at least satisfy demand with some conservatism or safety factor built in it. The level of conservatism is introduced in the design in several ways depending on the basic design concept being used. In structural design using the allowable stress design (ASD) approach, the basic concept is that the allowable stresses should be greater than the unfactored nominal loads or load combinations expected during the lifetime of a structure. The allowable stresses are calculated using safety factors. In other words, the nominal resistance R_n is divided by a safety factor to compute the allowable resistance R_a, and safe design requires that the nominal load effect S_n is less than R_a. In the ultimate strength design (USD) method, the loads are multiplied by load factors to determine the ultimate load effects and the members are required to resist the ultimate load. In this case, the safety factors are used in the loads and load combinations. Since, the predictabilities of different types of load are expected to be different; the USD significantly improved the ASD concept. In the current risk-based design concept, widely known as the load and resistance factor design (LRFD), safety factors are introduced to both load and resistance under the constraint of an underlying risk, producing improved designs. It should be pointed out that LRFD-based designs are calibrated with the old time-tested ASD designs. Thus, the final design may be very similar but LRFD design is expected to be more risk-consistent.

Fundamental Concept of Reliability-Based Design

Without losing any generality, suppose R and S represent the resistance or capacity and demand or load effect, respectively, and both are random variables since they are functions of many other random variables. The uncertainty in R and S can be completely defined by their corresponding probability density functions (PDFs) denoted as $f_R(r)$ and $f_S(s)$, respectively. Then the probability of failure of the structural element

can be defined as the probability of the resistance being less than the load effect or simply $P(R < S)$. Mathematically, it can be expressed as [9]:

$$P(\text{failure}) = P(R < S) = \int_0^{\infty} \left[\int_0^{s} f_R(r)dr \right] f_S(s)ds = \int_0^{\infty} F_R(s) f_S(s)ds \quad (1)$$

where $F_R(s)$ is the cumulative distribution function (CDF) of R evaluated at s. Conceptually, (1) states that for a particular value of the random variable $S = s$, $F_R(s)$ is the probability of failure. However, since S is also a random variable, the integration needs to be carried out for all possible values of S, with their respective likelihood represented by the corresponding PDF. Equation 1 can be considered as the fundamental equation of the reliability-based design concept. It is shown in Fig. 1. In Fig. 1, the nominal values of resistance and load effect are denoted as R_n and S_n, respectively, and the corresponding PDFs of R and S are shown period. The overlapped (dashed area) between the two PDFs provides a *qualitative measure* of the probability of failure. Controlling the size of the overlapped area is essentially the idea behind reliability-based design. Haldar and Mahadevan [9] pointed out that the area could be controlled by changing the relative locations of the two PDFs by separating the mean values of R and S (μ_R and μ_S), the uncertainty expressed in terms of their standard deviations (σ_R and σ_S), and the shape of the PDFs [$f_R(r)$ and $f_S(s)$].

In general, the CDF and the PDF of S may not be available in explicit forms and the integration of (1) may not be practical. However, (1) can be evaluated, without performing the integration if R and S are both statistically independent normal [15] or lognormal [16] random variables. Considering the practical aspects of a design, since R and S can be linear and nonlinear functions of many other random variables, their normality or log normality assumptions can rarely be satisfied.

If the risk cannot be evaluated in close form, it needs to be evaluated in approximate ways. This led to the development of several reliability analysis techniques. Initially, in the late 1960s, the first-order second-moment (FOSM) method, also known as the mean value first-order second-moment (MVFOSM) was proposed neglecting the distributional information on the random variables present in the problem. This important deficiency was overcome by the advanced first-order second-moment (AFOSM) method applicable when all the variables are assumed to be normal and independent [13]. A more general formulation applicable to different types of distribution was proposed by Rackwitz and Fiessler [14]. In the context of AFOSM, the probability of failure can be estimated using two types of approximations to the limit state at the design point: first order (leading to the name FORM) and second order (leading to the name SORM). Since FORM is a major reliability evaluation technique commonly used in the profession, it is discussed in more detail below.

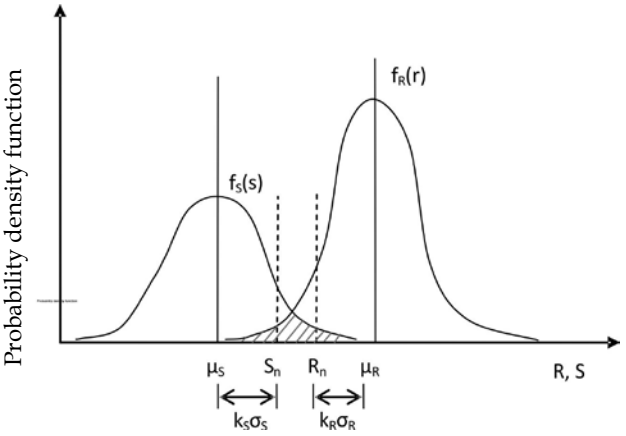

Figure 1. Reliability based design concept [9]

The basic idea behind reliability-based design is to design satisfying several performance criteria and considering the uncertainties in the relevant load and resistance-related random variables, called the basic variables X_i. Since the R and S random variables in (1) are functions of many other load and resistance-related random variables, they are generally treated as basic random variables. The relationship between the basic random variables and the performance criterion, known as the performance or limit state function, can be mathematically represented as:

$$Z = g(X_1, X_2, \ldots, X_n) \quad (2)$$

The failure surface or the limit state of interest can then be defined as $Z = 0$. The limit state equation plays an important role in evaluating reliability using FORM/SORM. It represents the boundary between the safe and unsafe regions and a state beyond which a structure can no longer fulfill the function for which it was designed. Assuming R and S are the two basic random variables, the limit state equation, and the safe and unsafe regions are shown in Fig. 2.

A limit state equation can be an explicit or implicit function of the basic random variables and can be linear or nonlinear. For nonlinear limit state functions, an iterative strategy is required to estimate the probability of failure as discussed by Haldar and Mahadevan [9], elsewhere. Two types of performance functions are generally used in engineering: strength and serviceability. Strength performance functions relate to the safety of the structures and serviceability performance functions are related to the serviceability (deflection, vibration, etc.) of the structure. The reliabilities underlying the strength and serviceability performance functions are expected to be different.

Reliability Assessment – Implicit Limit State Functions

Reliability evaluation using FORM is relatively simple if the limit state function is explicit in terms of design variables. In this case, the derivatives of the limit state functions with respect to design variables are readily available; the iterative process necessary for the reliability evaluation becomes very straight forward. However, in many cases of practical importance, particularly for complicated large systems, the explicit expressions for the limit state functions may not be available. For such systems, the required functions need to be generated numerically such as the finite element analysis. In such cases, the derivatives are not readily available. Their numerical evaluation could be time-consuming. Some alternatives are necessary.

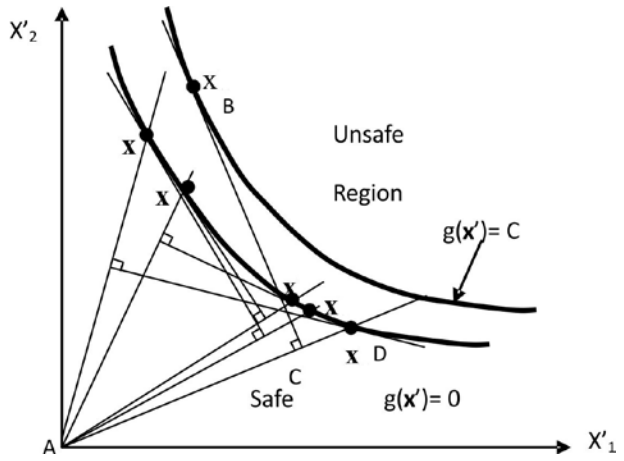

Figure 2. Limit state concept [9,10]

Several computational approaches can be pursued for reliability analysis of systems with implicit performance functions. They can be broadly divided in to three categories, based on their essential philosophy, as (1) Monte Carlo simulation (MCS), (2) response surface method (RSM), and (3) sensitivity-based analysis. Monte Carlo simulation uses randomly generated samples of input variables for each deterministic analysis. Its efficiency can be increased using intelligent schemes, as will be discussed later. It can be used for both explicit and implicit limit state functions. The RSM approximately constructs a polynomial (mainly first- or second-order) using a few selected deterministic analyses, and in some cases regression analysis of these results. The approximate closed-form expression thus obtained is then used to estimate reliability using FORM/SORM. In the sensitivity-based approach, the sensitivity of the structural response to the input variables is computed and it can be integrated with the FORM approach to extract the information on the underlying relaibility. The value of the performance function is evaluated using deterministic structural analysis. The gradient is computed using sensitivity analysis. When the limit state function is implicit, the sensitivities can be computed in three different ways: (i) through a finite difference approach, (ii) through classical perturbation methods that apply the chain rule of differentiation to finite element analysis, and (iii) through iterative perturbation analysis techniques [10]. The sensitivity-based reliability analysis approach is more elegant and in general more efficient than the simulation and response surface methods. Haldar and Mahadevan [10] suggested the use of the iterative perturbation technique in the context of the basic nonlinear stochastic finite element method (SFEM)-based algorithm.

Unified Stochastic Finite Element Method

Without losing any generality, the limit state function can be expressed in terms of the set of basic random variables **x** (e.g., loads, material properties and structural geometry), the set of displacements **u** and the set of load effects **s** (except the displacements) such as internal forces, stresses, etc. The displacement **u** = **QD**, where **D** is the global displacement vector and **Q** is a transformation matrix. The limit state function can be expressed as $g(\mathbf{x},\mathbf{u},\mathbf{s}) = 0$. For reliability computation, it is convenient to transform **x** into the standard normal space **y** = y**(x)** such that the elements of **y** are statistically independent and have a standard normal distribution. An iteration algorithm can be used to locate the design point (the most likely failure point) on the limit state function using the first-order approximation. During each iteration, the structural response and the response gradient vectors are calculated using finite element

models. The following iteration scheme can be used for finding the coordinates of the design point:

$$\mathbf{y}_{i+1}=\left[\mathbf{y}_i^t\alpha_i+\frac{g(\mathbf{y}_i)}{\left|\nabla g(\mathbf{y}_i)\right|}\right]\alpha_i \tag{3}$$

where

$$\nabla g(\mathbf{y})=\left[\frac{\partial g(\mathbf{y})}{\partial y_1},\ldots,\frac{\partial g(\mathbf{y})}{\partial y_n}\right]^t \text{ and } \alpha_i=-\frac{\nabla g(\mathbf{y}_i)}{\left|\nabla g(\mathbf{y}_i)\right|} \tag{4}$$

To implement the algorithm, the gradient $\nabla g(\mathbf{y})$ of the limit state function in the standard normal space can be derived as [10]:

$$\nabla g(\mathbf{y})=\left[\frac{\partial g(\mathbf{y})}{\partial \mathbf{s}}\mathbf{J}_{s,x}+\left(\mathbf{Q}\frac{\partial g(\mathbf{y})}{\partial \mathbf{u}}+\frac{\partial g(\mathbf{y})}{\partial \mathbf{s}}\mathbf{J}_{s,D}\right)\mathbf{J}_{D,x}+\frac{\partial g(\mathbf{y})}{\partial \mathbf{x}}\right]\mathbf{J}_{y,x}^{-1} \tag{5}$$

here $\mathbf{J}_{i,j}$'s are the Jacobians of transformation (e.g., $\mathbf{J}_{s,x}=\partial\mathbf{s}/\partial\mathbf{x}$) and y_i's are statistically independent random variables in the standard normal space. The evaluation of the quantities in Equation (5) will depend on the problem under consideration (linear or nonlinear, two- or three-dimensional, etc.) and the performance functions used. The essential numerical aspect of SFEM is the evaluation of three partial derivatives, $\partial g/\partial\mathbf{s}$, $\partial g/\partial\mathbf{u}$, and $\partial g/\partial\mathbf{x}$, and four Jacobians, $\mathbf{J}_{s,x}$, $\mathbf{J}_{s,D}$, $\mathbf{J}_{D,x}$, and $\mathbf{J}_{y,x}$. They can be evaluated by peocedures suggested by Haldar and Mahadevan [10] for linear and nonlinear, two- or three-dimensional structures. Once the coordinates of the design point $\mathbf{y}^*$ are evaluated with a preselected convergence criterion, the reliability index β can be evaluated as:

$$\beta=\sqrt{(\mathbf{y}^*)^t(\mathbf{y}^*)} \tag{6}$$

The evaluation of (5) will depend on the problem under consideration and the limit state functions used. The probability of failure, P_f can be calculated as:

$$P_f=\Phi(-\beta)=1.0-\Phi(\beta) \tag{7}$$

where Φ is the standard normal cumulative distribution function. Equation (7) can be considered as a notational failure probability. When the reliability index is larger, the probability of failure will be smaller. The author and his team published numerous papers to validate the above procedure.

Reliability Assessment - Present

Available Risk Evaluation Methods for Large Structures

As mentioned earlier, one of the alternatives for reliability analysis of large structures with implicit limit state functions is the use of the RSM [17]. The primary purpose of applying RSM in reliability analysis is to approximate the original complex and implicit limit state function using a simple and explicit polynomial [18,19,20]. Three basic weaknesses of RSM that limits its application potential are: (i) it cannot incorporate distribution information of random variables, (ii) if the response surface (RS) is not generated in the failure region, it may not be directly applicable, and (iii) for large systems, it may not give the optimal sampling points. Thus, a basic RSM-based reliability method may not be applicable for large structures.

Before suggesting strategies on how to remove deficiencies in RSM, it is necessary to briefly discuss other available methods to generate RS. In recent past, several methods with the general objective of approximately developing multivariate expressions for RS for mechanical engineering applications were proposed. One such method is High Dimensional Model Representation (HDMR) [21,22]. It is also referred to as "Decomposition method", "Univariate approximation", "Bivariate approximation", "S−variate approximation", etc. HDMR captures the high-dimensional relationships between sets of input and output model variables in such a way that the component functions of the approximation are ordered starting from a constant and adding terms such as first order, second order, and so on. The concept appears to be reasonable if higher-order variable correlations are weak, allowing the physical model to be captured by the first few lower-order terms.

Another major work is known as the Explicit Design Space Decomposition (EDSD). It can be used when responses can be classified into two classes, e.g., safe and unsafe. The classification is performed using explicitly defined boundaries in space. A machine learning technique known as Support Vector Machines (SVM) [23] is used to construct the boundaries separating distinct classes. The failure regions corresponding to different modes of failure are represented with a single SVM boundary, which is refined through adaptive sampling.

Improvement of RSM

To bring distributional information of random variables and to efficiently locate the failure region for large complicated systems, the author proposed to integrate RSM and FORM. The integration can be carried out with the help of following tasks.

Degree of Polynomial

The degree of polynomial used to generate a response surface (RS) should be kept to a minimum to increase efficiency. At present, second order polynomial without and with cross terms are generally used to generate response surfaces. Recently, Li et al. [24] proposed high-order response surface method (HORSM). The method employs Hermite polynomials and the one-dimensional Gaussian points as sampling points to determine the highest power of each variables. Considering the fact that higher order polynomial may result in ill-conditional system of equations for unknown coefficients and exhibit irregular behavior outside of the domain of samples, for complicated large systems, second-order polynomial, without and with cross terms can be used. They can be represented as:

$$\hat{g}(\boldsymbol{X}) = b_0 + \sum_{i=1}^{k} b_i X_i + \sum_{i=1}^{k} b_{ii} X_i^2 \tag{8}$$

$$\hat{g}(\mathbf{X}) = b_0 + \sum_{i=1}^{k} b_i X_i + \sum_{i=1}^{k} b_{ii} X_i^2 + \sum_{i=1}^{k-1} \sum_{j>1}^{k} b_{ij} X_i X_j \tag{9}$$

where X_i (i = 1, 2,…, k) is the i^{th} random variable, and b_0, b_i, b_{ii}, and b_{ij} are unknown coefficients to be determined; they need to be estimated using the response information at the sampling points by conducting several deterministic FE analyses and k represents the total number of sensitive random variables after making less sensitive variables constants at their mean values, by conducting sensitivity analyses [9]. The numbers of coefficients necessary to define (8) and (9) are $p = 2k+1$ and $= (k+1)(k+2)/2$, respectively. The coefficients can be fully defined either by solving a set of linear equations or from regression analysis using responses at specific data points called experimental sampling points around a centre point.

Detection of Failure Region

In the context of iterative scheme of FORM to locate the coordinates of the most probable failure point and the corresponding reliability index, the initial center point $\mathbf{X}c_1$ can be selected to be the mean values of the random variable X_i's. The response surface $\hat{g}(\mathbf{X})$ can be generated explicitly in terms of the random variables X_i's by conducting deterministic FE analyses at all the experimental sampling points, as will be discussed next. Once an explicit expression of the limit state function $\hat{g}(\mathbf{X})$ is obtained, the coordinates of the checking point $\mathbf{x}_{D_1}$ (iterative process to identify the coordinates of the most probable failure point) can be estimated using FORM, using all the statistical information on X_i's. The actual response can be evaluated again at the checking point $\mathbf{x}_{D_1}$, i.e., $g(\mathbf{x}_{D_1})$ and a new center point $\mathbf{x}_{C_2}$ can be selected using a linear interpolation [18,25] as: 0

$$\mathbf{x}_{C_2} = \mathbf{x}_{C_1} + (\mathbf{x}_{D_1} - \mathbf{x}_{C_1}) \frac{g(\mathbf{x}_{C_1})}{g(\mathbf{x}_{C_1}) - g(\mathbf{x}_{D_1})} \quad \text{if } g(\mathbf{x}_{D_1}) \geq g(\mathbf{x}_{C_1}) \tag{10}$$

$$\mathbf{x}_{C_2} = \mathbf{x}_{D_1} + (\mathbf{x}_{C_1} - \mathbf{x}_{D_1}) \frac{g(\mathbf{x}_{D_1})}{g(\mathbf{x}_{D_1}) - g(\mathbf{x}_{C_1})} \quad \text{if } g(\mathbf{x}_{D_1}) < g(\mathbf{x}_{C_1}) \tag{11}$$

A new center point $\mathbf{x}_{C_2}$ then can be used to develop an explicit performance function for the next iteration. This iterative scheme can be repeated until a pre-selected convergence criterion of $(\mathbf{x}_{C_{i+1}} - \mathbf{x}_{C_i}) / \mathbf{x}_{C_i} \leq \varepsilon$ is satisfied. ε can be considered to be $|0.05|$. The second deficiency of RSM will be removed by locating the failure region using the above scheme.

Selection of Sampling Points

Saturated design (SD) and central composite design (CCD) are the two most promising schemes that can be used to generate experimental sampling points around the centre point. SD is less accurate but more efficient since it requires only as many sampling points as the total number of unknown coefficients to define the response surface. CCD is more accurate but less efficient since a regression analysis needs to be carried out to evaluate the unknown coefficients. The details of experimental design procedures can be found in [17,20]. In any case, the use of SD or CCD will remove the third deficiency of RSM.

Since the proposed algorithm is iterative and the basic SD and CCD require different amount of computational effort, considering efficiency without compromising accuracy, several schemes can be followed. Among numerous schemes, one basic and two promising schemes are:

Scheme 0 – Use SD with 2nd order polynomial without the cross terms throughout all the iterations.

Scheme 1- Use (8) and SD for the intermediate iterations and (9) and full SD for the final iteration.

Scheme 2 – Use (8) and SD for the intermediate iterations and (9) and CCD for the final iteration.

To illustrate the computational effort required for the reliability evaluation of large structural system, suppose the total number of sensitive random variables present in the formulation is, $k = 40$. The total number of coefficients necessary to define Equation 8 will be $2 \times 40 + 1 = 81$ and to define Equation 9 will be $(40 + 1)(40 + 2) / 2 = 861$. It can also be shown that if Equation 8 and SD scheme are used to generate the response surface, the total number of sampling points, essentially the total number of deterministic FE-based response analyses will be 81. However, if Equation 9 and full SD scheme are used, the corresponding deterministic analyses will be 861. If Equation 9 and CCD scheme are used, the corresponding deterministic analyses will be $2^{40} + 2 \times 40 + 1 = 1{,}099{,}511{,}160{,}081$.

Mathematical Representation of Large Systems for Reliability Evaluation

The phrase "probability of failure" implies that the risk needs to be evaluated just before failure in the presence of several sources of nonlinearities. Finite element (FE)-based formulations are generally used to realistically consider different sources of nonlinearity and other performance enhancing features with improved energy dissipation mechanism now being used after the Northridge earthquake of 1994. Thus, for appropriate reliability evaluation, it is essential that structures are represented realistically by FEs and all major sources of nonlinearity and uncertainty are appropriately incorporated in the formulation.

To study the behavior of frame structures satisfying underlying physics, consideration of appropriate rigidities of connections is essential. In a typical design, all connections are considered to be fully restrained (FR), i.e., the angles between the girders and columns, before and after the application of loads, will remain the same. However, extensive experimental studies indicate that they are essentially partially restrained (PR) connection with different rigidities. In a deterministic analysis, PR connections add a major source of nonlinearity. In a dynamic analysis, it adds a major source of energy dissipation. In reliability analysis, it adds a major source of uncertainty. In general, the relationship between the moment M, transmitted by the connection, and the relative rotation angle θ, is used to represent the flexible behavior. Among the many alternatives (Richard model, piecewise linear model, polynomial model, exponential model, B-Spline model, etc.), the Richard four-parameter moment-rotation model is chosen here to represent the flexible behavior of a connection. It is expressed as [26]:

$$M = \frac{(k - k_p)\theta}{\left(1 + \left|\frac{(k - k_p)\theta}{M_0}\right|^N\right)^{1/N}} + k_p\theta \tag{12}$$

where M is the connection moment, θ is the relative rotation between the connecting elements, k is the initial stiffness, k_p is the plastic stiffness, M_0 is the reference moment, and N is the curve shape parameter. These parameters are identified in Fig. 3. To incorporate flexibility in the connections, a beam-column element can be introduced to represent each connection. However, its stiffness needs to be updated at each iteration since the stiffness representing the partial rigidity depends on θ. The tangent stiffness of the connection element, $K_C(\theta)$, can be shown to be:

$$K_C(\theta) = \frac{\mathrm{d}M}{\mathrm{d}\theta} = \frac{(k - k_p)}{\left(1 + \left|\frac{(k - k_p)\theta}{M_0}\right|^N\right)^{\frac{N+1}{N}}} + k_p \tag{13}$$

The Richard model discussed above represents only the monotonically increasing loading portion of the M-θ curves. However, the unloading and reloading behavior of the M-θ curves is also essential for any nonlinear seismic analysis [27]. Using the Masing rule and the Richard model, Huh and Haldar [28] theoretically developed the unloading and reloading parts of the M-θ curves. The tangent stiffness for the unloading and reloading behavior of a PR connection can be represented as:

$$K_C(\theta) = \frac{\mathrm{d}M}{\mathrm{d}\theta} = \frac{(k - k_p)}{\left(1 + \left|\frac{(k - k_p)(\theta_a - \theta)}{2M_0}\right|^N\right)^{\frac{N+1}{N}}} + k_p \tag{14}$$

As shown in Fig. 3, this represents hysteretic behavior at the PR connections. The basic FE formulation of the structure remains unchanged.

Pre- and post-Northridge PR connections

During the Northridge earthquake of 1994, several connections in steel frames fractured in a brittle and premature manner. A typical connection, shown in Fig. 4, was fabricated with the beam flanges attached to the column flanges by full penetration welds (field-welded) and with the beam web bolted (field-bolted) to single plate shear tabs [29], denoted hereafter as the pre-NC.

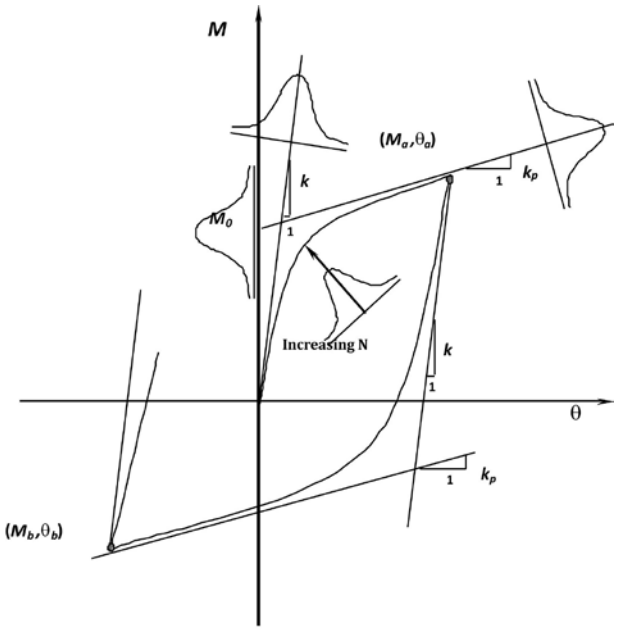

Figure 3. M-θ curve using the Richard Model, Masing rule and uncertainty

In the post-Northridge design practices, the thrusts were to make the connections more flexible than the pre-NC and to move the location of formation of any plastic hinge away from the connection and to provide more ductility to increase the energy absorption capacity. Several improved connections can be found in the literature including cover plated connections, spliced beam connections, side-plated connections, bottom haunch connections, connections with vertical ribs, and connections with a reduced beam sections (RBS) or Dog-Boned (FEMA 350-3). Seismic Structural Design Associates, Inc. (SSDA) proposed a unique proprietary slotted web (SSDA SlottedWeb™) moment connection [29], as shown in Fig. 5, denoted hereafter as the post-NC. The author was given access to some of the actual SSDA full-scale test results. Using the four parameters Richard model, the research team first proposed a mathematical model to represent moment-relative rotation (M-θ) curves for this type of connections [30].

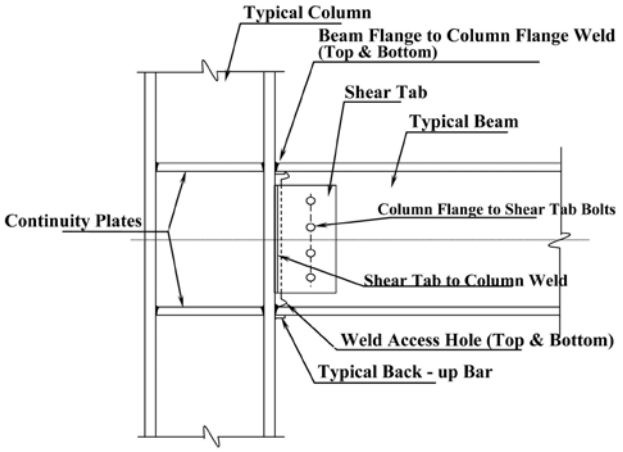

Figure 4. A typical pre-NC

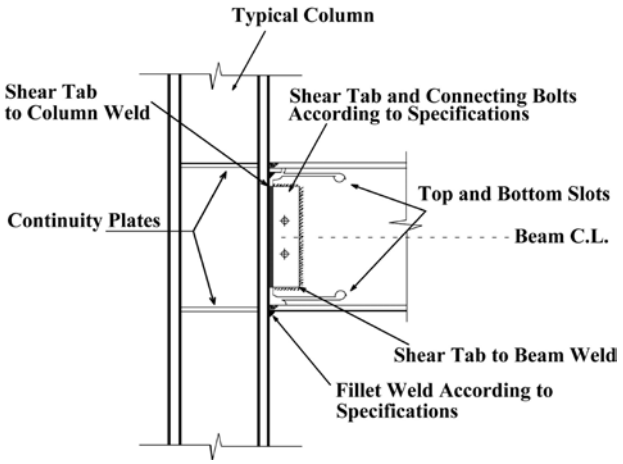

Figure 5. A typical post-NC

Examples

A three-story three-bay steel frame, as shown in Fig. 6, is considered. Section sizes of beams and columns, using A36 steel, are also shown in the figure. It was excited by a seismic time history shown in Fig. 7 [28,31].

The four parameters of the Richard model are calculated by PRCONN [32], a commercially available computer program for both Pre-NC and Post-NC connections. For the example under consideration, considering the sizes of columns and beams, three types of connection are necessary. They are denoted as Types A, B, and C, hereafter. Four Richard parameters for both Pre-NC and Post-NC connections are summarized in Table 1.

Limit states or performance functions

In structural engineering, both strength and serviceability limit states are used for reliability

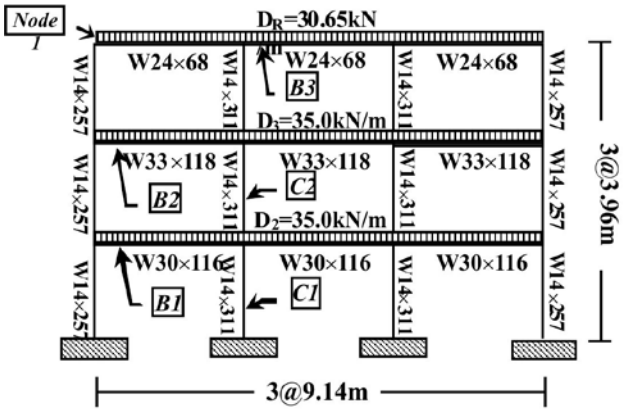

Figure 6. A 3-story 3-bay SMRF structure

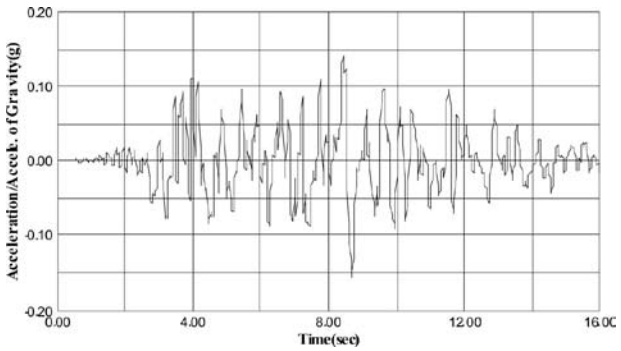

Figure 7. Earthquake time history

Table 1. Parameters of Richard Equation for M-θ Curves

Connection Assembly Type				Connection Parameters			
ID.		Beam	Column	k^1	k_p^1	M_0^2	N
Pre-NC	A	W24×68	W14×257	2.51E7	5.56E5	4.16E4	1.1
		W24×68	W14×311				
	B	W33×118	W14×257	5.08E7	1.14E5	6.79E4	1.1
		W33×118	W14×311				
	C	W30×116	W14×257	3.95E7	9.19E5	5.65E4	1.1
		W30×116	W14×311				
Post-NC	A	W24×68	W14×257	1.00E9	4.52E5	9.64E4	1.0
		W24×68	W14×311				
	B	W33×118	W14×257	2.34E9	4.52E5	2.44E5	1.0
		W33×118	W14×311				
	C	W30×116	W14×257	2.14E9	4.52E5	2.21E5	1.0
		W30×116	W14×311				
Note: ^{1}kN·cm/rad, ^{2}kN·cm							

Table 2. Statistical information on the design variables

	Item	Random Variable	Mean Value	COV	Dist.
Member	All	$E(kN/m^2)$	2.0 E+8	0.06	Ln
		$F_y(kN/m^2)$	2.48E+5	0.10	Ln
	Column W14×257	$I_x^{C1}(m^4)$	1.42E-3	0.05	Ln
		$Z_x^{C1}(m^3)$	7.98E-3	0.05	Ln
	Column W14×311	$A^{C2}(m^2)$	5.90E-2	0.05	Ln
		$I_x^{C2}(m^4)$	1.80E-3	0.05	Ln
	Beam W33×118	$I_x^{B2}(m^4)$	2.46E-3	0.05	Ln
	Beam W30×116	$I_x^{B3}(m^4)$	2.05E-3	0.05	Ln
		$Z_x^{B3}(m^3)$	6.19E-3	0.05	Ln
Seismic Load		ξ	0.05	0.15	Type I
		g_e	1.0	0.20	Type I
Connection	Richard Model Parameter	K^1	Refer to values in Table 3	0.15	N
		k_p^1		0.15	N
		M_0^2		0.15	N
		N		0.05	N
Shear Wall*		$E_C(kN/m^2)$	2.14E+7	0.18	Ln
		ν	0.17	0.10	Ln

Table 3. Reliability evaluation of FR frame

Limit State		Service-ability	Strength Limit State	
		Node at *1*	Beam (*B1*)	Column (*C1*)
MCS	P_f	0.08740	N/A*3	N/A*3
	$\beta \approx \Phi^{-1}(1-P_f)$	1.357	N/A	N/A
	NOS*1	20,000	30,000	30,000
Proposed Algorithm	No. of RV	8	6	6
	Scheme	1	2	2
	β	1.330	4.724	5.402
	Error w.r.t β	1.99%	N/A	N/A
	TNSP*2	79	103	103

*1 number of simulation for deterministic FEM analyses

*2 total number of sampling points (total number of deterministic FEM analyses)

*3 Not a single failure observed for 30,000cycles of simulation since large reliability indexes are expected in the strength limit state.

estimation. The strength limit states mainly depend on the failure modes. Most of the elements in the structural system considered are beam-columns. The interaction equations suggested by the American Institute of Steel Construction's *Load and Resistance Factor Design* (LRFD 2005) [33] manual for two dimensional structures are

used in this study. The serviceability limit states can be represented as:

$$g(\mathbf{X}) = \delta_{allow} - y_{max}(\mathbf{X}) = \delta_{allow} - \hat{g}(\mathbf{X}) \quad (15)$$

where δ_{allow} is the allowable inter-story drift or overall lateral displacement specified in codes and $y_{max}(\mathbf{X})$ is the corresponding the maximum inter-story drift or overall lateral displacement estimated.

Reliability Evaluations of Frame with Different Connection Conditions, without RC Shear Wall

The statistical characteristics of all the design variables used in the formulation are summarized in Table 2. The probabilities of failure of the frame for the lateral deflection at the top of the frame for serviceability limit state and the strength limit state of the weakest members are estimated assuming all the connections are of FR type. The results are summarized in Table 3. To verify the results, 20,000 MCS for the serviceability and 30,000 MCS for the strength limit states were carried out. The results clearly indicate that the bare steel frame will not satisfy the serviceability requirement. Then, the reliabilities of the frame are estimated assuming all the connections are Post-NC and Pre-NC types and the results are summarized in Table 4. The behaviour of the frame in the presence of FR and Post-NC for both serviceability and strength limit states are very similar. This was also observed during the full-scale experimental investigations. This observation clearly indicates that the method can predict realistic behaviour of complex structural systems. In any case, the lateral stiffness of the frame needs to be increased.

Reliability Evaluations of Frames with Different Connection Conditions with RC Shear Wall

To increase the lateral stiffness, the steel frame is strengthen with a reinforced concrete (RC) shear wall at the first floor level, as shown in Fig. 6. For the steel and concrete dual system, all the steel elements in the frame are modeled as beam-column elements. A four-node plane stress element is introduced for the shear wall in the frame. To consider the presence of RC shear wall, the modulus of elasticity, E_C, and the Poisson ratio of concrete,ν, are necessary in the deterministic formulation. Cracking may develop at a very early stage of loading. It was observed that the degradation of the stiffness of the shear walls occurs after cracking and can be considered effectively by reducing the modulus of elasticity of the shear walls [34]. The rupture strength of concrete, f_r, is assumed to be $f_r = 7.5 \times \sqrt{f_c'}$, where f_c' is the compressive strength of concrete. After the tensile stress of each shear wall exceeds the prescribed tensile stress of concrete, the degradation of the shear wall stiffness is assumed to be reduced to 40% of the original stiffness [34]. The uncertainty in all the variables considered for the bare steel frame will remain the same. However, two additional sources of uncertainty, namely in E_C and ν, need to be considered, as given in Table 2.

The frame is again excited by the same earthquake time history as shown in Fig. 7. The probabilities of failure for the combined dual system in presence of FR, Post-NC, and Pre-NC connections are calculated using the proposed algorithm for the strength and serviceability limit states. The results are summarized in Table 4. The results indicate that the presence of shear wall at the first floor level significantly improves both the serviceability and strength behavior of the steel frame. If the probabilities of failure need to be reduced further, RC shear walls can be added in the second and/or third floor. Again, this improved behavior can be observed and quantified by carrying out about hundred deterministic evaluations instead of thousands of MCS. The improved behavior of the frame in the presence of RC shear wall is expected, however, the proposed algorithm can quantify the amount of improvement in terms of probability of failure for different design alternatives.

Table 4. Reliability evaluations of frame without and with shear wall

Steel Frame without Shear Wall					Steel Frame with Shear Wall			
		Connection Type				Connection Type		
		FR	Post-NC	Pre-NC		FR	Post-NC	Pre-NC
Serviceability Limit State (Node 1)								
	β	1.330	1.329	0.463	β	3.667	3.534	1.685
	$P_f \approx \Phi(-\beta)$	0.092	0.092	0.322	$P_f \approx \Phi(-\beta)$	1.2E-4	2.0E-4	4.6E-2
	No. of R.V.	8	20	20	No. of R.V.	10	22	22
	TNSP	79	313	313	TNSP	108	366	366

Strength Limit State								
	β	4.724	4.756	3.681	β	6.879	6.714	4.467
Beam	$P_f \approx \Phi(-\beta)$	1.16E-6	9.87E-7	1.16E-4	$P_f \approx \Phi(-\beta)$	3.01E-12	9.477E-12	3.97E-6
	No. of R.V.	6	18	18	No. of R.V.	8	20	20
	TNSP	103	264	264	TNSP	79	313	313
Column	β	5.402	5.376	4.154	β	6.879	6.714	4.467
	$P_f \approx \Phi(-\beta)$	3.30E-8	3.81E-8	1.63E-5	$P_f \approx \Phi(-\beta)$	3.01E-12	9.47E-12	3.97E-6
	No. of R.V.	6	18	18	No. of R.V.	8	20	20
	TNSP	103	264	264	TNSP	79	313	313

Reliability Assessment - Future

Reliability Evaluation of Large Structural Systems

In some studies considered by the author, one deterministic nonlinear dynamic analysis of large structures may take over 10 hours of computer time. If one has to use very small, say only 100 simulations, it may take 1,000 hours or over 41 days of uninterrupted running of a computer. The author proposed to estimate reliability of such systems using only tens instead of hundreds or thousands of deterministic evaluations at intelligently selected points to extract the reliability information. The procedure is still under development. The concept is briefly discussed below.

Scheme M1: To improve the efficiency of Scheme 1 discussed earlier, the cross terms (edge points), *k (k-1)*, are suggested to be added only for the most important variables in the last iteration. Since the proposed algorithm is an integral part of FORM, all the random variables in the formulation can be arranged in descending order of their sensitivity indexes $\alpha(X_i)$, i.e., $\alpha(X_1) > \alpha(X_2) > \alpha(X_3) \ldots\ldots\ldots > \alpha(X_k)$. The sensitivity of a variable X, $\alpha(X)$ is the directional cosines of the unit normal vector at the design point. In the last iteration, the cross terms are added only for the most sensitive random variables, *m* and the corresponding reliability index is calculated. The total number of FEM analyses required for Scheme 1 and *M1* are $(k+1)(k+2)/2$ and $2k+1+m(2k-m-1)/2$, respectively. For an example, suppose for a large structural system, $k = 40$ and $m = 3$. The total number of required FEM analyses will be 861 and 195, respectively, for the two schemes.

Scheme M2: Instead of using full factorial plan in CCD, Myers et al. [35] recently proposed quarter factorial plan. This improved and efficient version of Scheme 2 will be denoted hereafter as Scheme M2. In Scheme M2, it is proposed that only quarter of the factorial points corresponding to the most sensitive random variables are to be considered. In other words, in the last iteration, the variables are to be arranged in descending order according to their sensitivity indexes $\alpha(X_i)$, i.e., $\alpha(X_1) > \alpha(X_2) > \alpha(X_3) \ldots\ldots\ldots > \alpha(X_k)$. Then, the factorial sampling points are determined by using the values +1 and -1, in the coded space, for X_1, X_2, X_3, … , until the number of quarter of factorial sampling = $0.25 \times 2^k = 2^{k-2}$.

Risk Management

Since risk cannot be completely eliminated in engineering analysis and design, it needs to be managed appropriately. It is undesirable and uneconomical, if not impossible, to design a risk-free structure. According to Raiffa [36], the decision or management can be subdivided in to risk or data analysis, inference, and decision. Risk analysis is discussed in the first part of the paper. Inference attempts to incorporate additional scientific knowledge in the formulation that may have been ignored in the previous data analysis. The decision is the final outcome of any risk-based engineering design. For a given structure, the risks for different design alternatives can be estimated. The information on risk and the corresponding consequences of failure, including the replacement cost, can be combined using a decision analysis frame work to obtain the best alternative. Thus, the probability concept provides a unified framework for quantitative analysis of risk as well as the formulation of trade-off studies for decision making, planning, and design considering economic aspects of the problem.

The relevant components of a decision analysis are generally described in the form of a decision tree [37]. The decision tree helps to organize all necessary information in a systematic manner suitable for analytical evaluation of the optimal alternative. A decision making process starts by choosing an action, a, from among the available alternatives actions (a1,

a2, …, an), called decision variables. They branch out from a square node or a decision node. Once a decision has been made, a natural outcome θ from among all possible states, θ1, θ2, …, θn, would materialize. All possible states are beyond the control of a decision maker; they are shown to originate from a circular node, called the chance node. Each natural outcome based on the action taken is expected to have a different risk of success or failure and expressed in terms of probability $P(\theta i \mid ai)$ period. As a result of having taken action a and having found true state θ, a decision maker will obtain a utility value u(a, θ), a numerical measure of the consequences of this action-state pair. A general decision analysis frame work may contain the following necessary components: (1) decision variables, (2) consequence, (3) risk associated with each alternative, and (4) identification of the decision maker and the decision criteria.

Future Directions

Artificial Neural Networks and Soft Computing

The application of artificial neural networks (ANN), the more generic term used by the research community as soft computing, in civil engineering has been significant in the very recent past [38]. In addition to ANN, the other soft computing techniques include Genetic Algorithm, Evolutionary computation, Machine learning, Organic computing, Probabilistic reasoning, etc. The applicability of these techniques could be problem specific, some of them can be combined, or one technique can be used when another failed to meet the objectives of the study. Soft computing differs from conventional hard computing. Unlike hard computing, soft computing is tolerant of imprecision, uncertainty, partial truth, and approximation. To some extent, it essentially plays a role similar to human mind.

Incorporation of Cognitive Sources of Uncertainty

Being a reliability person, I feel I should address this subject very briefly. Most of the works on reliability-based structural engineering incorporate noncognitive (quantitative) sources of uncertainty using crisp set theory. Cognitive or qualitative sources of uncertainty are also important. They come from the vagueness of the problem arising from the intellectual abstractions of reality. To incorporate cognitive sources of uncertainty, fuzzy set theory is generally used.

Education

Lack of education could be a major reason for avoidance of using the reliability based design concept by the profession. If closed form relibaility analysis is not possible and the design codes do not cover the design of a particular structure, at the minimum "simulation" can be used to satisfy the intent of the codes. In Europe, highway and railway companies are using simulation for assessment purposes. In the U.S., the general feeling is that we are safe if we design according to the design code. Designers should use all available means to satisfy performance requirements, according to a judge. The automotive industry satisfied the code requirements in one case. However, according to a judge, they should have used simulation to address the problem more comprehensively.

Some of the developments in the risk based design using simulation are very encouraging. Simulation could be used in design in some countries, but it is also necessary to look at its legal ramification. Unlike in Europe, in the U.S.A., a code is not a government document. It is developed by the profession and its acceptance is voted by the users and developers. It was pointed out that in some countries, code guidelines must be followed to the letters, and other countries permit alternative methods if they are better. In Europe, two tendencies currently exist: Anglo-Saxon – more or less free to do anything, and middle-European – fixed or obligatory requirements. Current Eurocode is obligatory. We need to change the mentality and laws to implement simulation or reliability based design concept in addressing real problems.

In the context of education of future structural engineers, the presence of uncertainty must be identified in design courses. Reliability assessment methods can contribute to the transition from deterministic to probabilistic way of thinking of students as well as designers. In the U.S., the Accreditation Board of Engineering and Technology (ABET) now requires that all civil engineering undergraduate students demonstrate knowledge of the application of probability and statistics to engineering problems, indicating its importance in civil engineering education. Most of the risk based design codes are the by-product of education and research at the graduate level. In summary, the profession is moving gradually in accepting the reliability based design concept.

Computer programs

The state-of-the-art in reliability estimation is quite advanced; however, it is not popular with the practicing engineers. One issue could be the lack of availability of the user friendly software. Two types of issues need to be addressed at this stage. Reliability based computer software should be developed for direct applications or the reliability based design feature should be added to the commercially available deterministic software. Some of the commercially available reliability based computer software is briefly discussed next.

NESSUS (numerical evaluation of stochastic structures under stress) was developed by the Southwest Research Institute (SWRI, 1991) [39] under the sponsorship of NASA Lewis Research Center. It combines probabilistic analysis with a general-purpose finite element/boundary element code. The probabilistic analysis features an advanced mean value (AMV) technique. The program also includes techniques such as fast convolution and curvature-based adaptive importance sampling.

PROBAN (PROBability ANalysis) was developed at Det Norske Veritas, Norway, through A.S. Veritas Research (1991) [40]. PROBAN was designed to be a general purpose probabilistic analysis tool. It is capable of estimating the probability of failure using FORM and SORM for a single event, unions, intersections, and unions of intersections. The approximate FORM/SORM results can be updated through importance sampling simulation scheme. The probability of general events can be computed by Monte Carlo simulation and directional sampling.

CALREL (CAL-RELiability) is a general purpose structural reliability analysis program designed to compute probability integrals [41]. It incorporates four general techniques for computing the probability of failure: FORM, SORM, directional simulation with exact or approximate surfaces, and Monte Carlo simulation. It has a library of probability distributions of independent as well as dependent random variables.

Under the sponsorship of the Pacific Earthquake Engineering Research (PEER), McKenna et. al. [42] has developed a finite element reliability code within the framework of OpenSees.

Structural engineers without formal education in risk based design may not be able to use the computer programs mentioned above. They need to be retrained with very little effort. They may be very knowledgeable using exiting deterministic analysis software including commercially available finite element packages. This expertise needs to be integrated with risk based design concept. Thus, probabilistic features may need to be added to the deterministic finite element packages. Proppe et al. [43] discussed the subject in great detail. For proper interface of deterministic software, they advocated for graphical user interface, communication interface which must be flexible enough to cope with different application programming interfaces and data format, and the reduction of the problem sizes before undertaking reliability analysis. COSSAN [44] software attempted to implement the concept.

The list of computer programs given here may not be exhaustive. However, they are being developed and are expected to play a major role in implementing reliability based engineering analysis and design in the near future.

Conclusions

Engineering under uncertainty has evolved in the past several decades. It has attracted multidisciplinary research interest. A brief overview of the past, present, and future, in the author's assessment is given here. Albert Einstein stated that "The important thing is not to stop questioning. Curiosity has its own reason for existing." The profession is very curious on the topic and there is no doubt that future analysis and design of engineering structures will be entirely conducted using probability concept.

Acknowledgments

I would like to thank all my teachers for teaching me subjects that helped to develop my career and understanding of my life in a broader sense. I also would like to thank all my former and current students who taught me subjects for which I did not have any formal education. They helped me explore some of the unchartered areas. I also appreciate financial supports I received from many funding agencies to explore several challenging and risky research areas. I would also like to thank the organizing committee of the International Symposium on Engineering under Uncertainty: Safety Assessment and Management (ISEUSAM- 2012) for inviting me to give the inaugural keynote speech.

References

1. Richard RM Allen CJ and Partridge J E (1997) Proprietary slotted beam connection designs. Modern Steel Construction.
2. Jeffreys, H. (1961). *Theory of Probability*, Oxford University Press.

3. Laplace, P.S.M. (1951). *A Philosophical Essay on Probabilities*, (translated from the sixth French edition by F.W. Truscott and F.L. Emory), Dover Publications, New York.
4. Fisher, R.A. (1959). *Statistical Methods and Scientific Inference*, Hafner, N.Y.
5. Freudenthal, A.M. (1947). Safety of Structures, Transactions, ASCE, Vol. 112, pp. 125-180.
6. Ang, A.H-S., and Cornell, C.A. (1974). Reliability Bases of Structural Safety and Design, Journal of Structural Engineering, ASCE, Vol. 100, No. ST9, pp. 1755-1769.
7. Ang, A.H-S and Tang, W.H. (1975). *Probability Concepts in Engineering Design, Vol. I: Basic Principles*, Wiley, N.Y.
8. Benjamin, J.R., and Cornell, C.A. (1970). *Probability, Statistics, and Decision for Civil Engineers*, McGraw-Hill, N.Y.
9. Ellingwood, B.R., Galambos, T.V., MacGregor, J.G., and Cornell, C.A. (1980). *Development of Probability Based Load Criterion for American National Standard A58*, NBS Special Publication 577, U.S. Department of Commerce, Washington, D.C.
10. Haldar, A., and Mahadevan, S. (2000a). *Probability, Reliability and Statistical Methods in Engineering Design*, John Wiley & Sons, New York, NY.
11. Haldar, A. and Mahadevan, S. (2000b). *Reliability Assessment Using Stochastic Finite Element Analysis*, John Wiley & Sons, New York, NY.
12. Shinozuka, M. (1983). Basic Analysis of Structural Safety, Journal of Structural Engineering, ASCE, Vol. 109, No. 3, pp. 721-740.
13. Rackwitz, R. (1976). Practical Probabilistic Approach to Design, Bulletin No. 112, Comite European du Beton, Paris, France.
14. Hasofar, A.M. and Lind, N.C. (1974). Exact and invariant second moment code format, J. *of Engineering Mechanics, ASCE,* 100(EM1), 111-121.
15. Rackwitz, R., and Fiessler, B. (1978). Structural Reliability under Combined Random Load Sequences, Computers and Structures, Vol. 9, No. 5, pp. 484-494.
16. Cornell, C.A. (1969). A Probability-Based Structural Code, Journal of the American Concrete Institute, Vol. 66, No. 12, pp. 974-985.
17. Rosenbleuth, E., and Esteva, L. (1972). Reliability Bases for Some Mexican Codes, ACI publication SP-31, pp. 1-41.
18. Box, G. P. William, G. H. & Hunter, J. S. (1978). *Statistics for Experimenters: An Introduction to Design, Data Analysis and Modeling Building*, John Wiley & Sons, New York.
19. Bucher, C.G. and Bourgund, U. (1990). A fast and efficient response surface approach for structural reliability problems, Structural Safety, 7, 57-66.
20. Yao, T. H.-J., and Wen, Y.K. (1996). Response surface method for time-variant reliability analysis, Journal of Structural Engineering, ASCE, 122(2): 193-201.
21. Khuri A.I. and Cornell, C.A. (1996). *Response Surfaces Designs and Analyses*, Marcel Dekker, New York, N.Y, 1996.
22. Rao, B.N. and Chowdhury, R. (2009). Enhanced high dimensional model representation for reliability analysis, International J. for Numerical Methods in Engineering, 77(5): 719 –750.
23. Xu, H., and Rahman, S. (2005). Decomposition methods for structural reliability analysis, Probabilistic Engineering Mechanics 20: 239–250.
24. Basudhar, A. Missoum, S. and Harrison Sanchez, A. (2008). Limit state function identification using support vector machines for discontinuous responses and disjoint failure domains, Probabilistic Engineering Mechanics, 23(1): 1-11.
25. Li, H. Lu, Z. and Qiao, H. (2008). A new high-order response surface method for structural reliability analysis, 2008, personal communication.
26. Rajashekhar, M.R. and Ellingwood, B.R. (1993). A new look at the response surface approach for reliability analysis, Structural Safety, 12: 205-220.
27. Richard, R. M. and Abbott, B.J. (1975). Versatile elastic-plastic stress-strain formula. *Journal of Engineering Mechanics, ASCE*, 101(EM4), 511-515.
28. Colson, A. (1991). Theoretical modeling of semi-rigid connection behavior, Journal of the Constructional Steel Research, 19: 213-224.
29. Huh, J., And Haldar, A. (2011). A Novel Risk Assessment Method for Complex Structural Systems, IEEE Transactions on Reliability, Vol. 60, No. 1, pp. 210-218.
30. Richard, R.M., and Radau, R.E., (1998). Force, Stress and Strain Distribution in FR Bolted Welded Connections,"Proceedings of Structural Engineering Worldwide, San Francisco, CA.
31. Mehrabian, A., Haldar, A., and Reyes, A. S. (2005). Seismic Response Analysis of Steel Frames with Post-Northridge Connection, *Steel and Composite Structures*, Vol. 5, No. 4, pp. 271-287.
32. Haldar, A., Farag, R., and Huh, J. (2010). Reliability Evaluation of Large Structural Systems, Keynote Lecture, International Symposium on Reliability Engineering and Risk Management (ISRERM2010), Shanghai, China, pp. 131-142.
33. Richard, R. M., 1993, *PRCONN Manual*, RMR Design Group, Tucson, Arizona
34. American Institute of Steel Construction. (2005). *Manual of Steel Construction: Load and Resistance Factor Design*, Chicago, Illinois.
35. Lefas, D. Kotsovos, D. and Ambraseys, N. (1990). Behavior of reinforced concrete structural walls: strength, deformation characteristics, and failure mechanism, ACI Structural Journal, 87(1): 23-31.
36. Myers, R.H. Montgomery, D.C. and Anderson-Cook, C.M. (2009). *Response Surface Methodology: Process and product optimization using designed experiments*, John Wiley & Sons, New York, NY.
37. Raiffa, H. (1968). *Decision Analysis*, Addison-Wesley, Reading, Mass.
38. Haldar, A. (1980). Liquefaction Study – A Decision Analysis Framework, Journal of the Geotechnical Engineering Division, ASCE, Vol. 106, No. GT12, pp. 1297-1312.
39. Kartam, N., Flood, I., and Garrett, J.H. (1997). *Artificial Neural Networks for Civil Engineers*, American Society of Civil Engineers, New York, N.Y.
40. Southwest Research Institute. (1991). NEUSS, San Antonio, Texas.
41. Veritas Sesam Systtems, *PROBAN*, Houston, Texas, 1991.
42. Liu, P.-L., Lin, H.-Z., and Der Kiureghian, A. (1989). *CALREL*, University of California, Berkeley, California.
43. McKenna, F., Fenves, G.L., and Scott, M.H., *Open System for Earthquake Engineering Simulation,* http://opensees.berkeley.edu/, Pacific Earthquake Engineering Research Center, Berkeley, CA., 2002.
44. Proppe, C., Pradlwarter, H.J., and Schueller, G.I. (2001). Software for stochastic structural analysis – needs and requirements," in *Proc. 4th Int. Conf. on Structural Safety and Reliability "AA Balkema Publishers,* The Netherlands", Corotis, R.B., Schueller, G.I., and Shinizuka, M., Eds.
45. COSSAN (Computational Stochastic Structural Analysis) – Stand – Alone Toolbox, (1996). *User's Manual*, IfM – Nr: A, Institute of Engineering Mechanics, Leopold – Franzens University, Innsbruck, Austria.

Life Cycle Reliability and Safety Engineering
Vol.1 Issue 4 (2012) 53-63

Past, Present, and Future of Structural Health Assessment

Achintya Haldar and Ajoy Kumar Das
Department of Civil Engineering and Engineering Mechanics
University of Arizona, Tucson, Arizona, U.S.A.
E-mail: Haldar@u.arizona.edu

ABSTRACT

Past, present, and future of structural health assessment (SHA) concepts and related areas, as envisioned by the authors, are briefly reviewed in this paper. The growth in the related areas has been exponential covering several engineering disciplines. After presenting the basic concept, the authors discussed its growth from infancy, i.e., hitting something with a hammer and listening to sound to the use of most recent development of wireless sensors and the associated advanced signal processing algorithms. Available SHA methods are summarized in the first part of this paper. The works conducted by the research team of the authors are emphasized. Later, some of the future challenges in SHA areas are identified. Since it is a relatively new multi-disciplinary area, the education component is also highlighted at the end.

Keywords: structural health assessment, Kalman filter, substructure, system identification, uncertainty analysis, sensors

Introduction

The nature and quality of infrastructure have always been one of the indicators of sophistication of a civilization. There is no doubt that we are now at a historical peak. However, keeping the infrastructure at its present level has been a major challenge due to recent financial strain suffered by the global community. We do not have adequate resources to build new infrastructure or replace the aged ones that are over their design lives. The most economical alternative is found to be extending the life of existing infrastructure without compromising our way of living and without exposing public to increased risk. This has been one of the major challenges to the engineering profession and attracted multi-disciplinary research interests. The main thrust has been to locate defects in structures at the local element level and then repair them or replace the defective elements, instead of replacing the whole structure. Several advanced theoretical concepts required to detect defects have been proposed. At the same time, improved and smart sensing technologies, high-resolution data acquisition systems, digital communications and high-performance computational technologies have been developed for implementing these concepts. The general area is now commonly known as structural heath assessment (SHA) or structural health monitoring (SHM). In spite of these developments in analytical and sensor technologies, the implementations of these concepts in assessing structural health have been limited due to several reasons. An attempt has been made here to identify some of the major works (emphasizing analytical), their merits and demerits, contributions made by the research team of the authors, and future challenges.

Concept of structural health assessment

All civil engineering structures, new and old, may not totally satisfy the intents of the designers. Minor temperature cracks in concrete or lack of proper amount of pre-tension in bolts cannot completely be eliminated. In that sense, all structures can be assessed as defective. Our past experiences indicate that presence of minor defects that do not alter the structural behavior may not be of interest to engineers. Considering only major defects, all of them are not equally important. Their locations, numbers, and severities will affect the structural behavior. Thus, the concept behind SHA can be briefly summarized as locating major defects, their numbers and severities in a structure at the local element level. For the sake of completeness of this discussion, available SHA procedures are classified into four levels as suggested by Rytter (1993). They are: Level 1 - determination if damage is present in a

structure, Level 2 - determination of geometric location of the damage, Level 3 - assessment of severity of the damage, and Level 4 - prediction of remaining life of the structure.

Structural health assessment - past

Structural health assessment has been practiced for centuries. Ever since pottery was invented, cracks and cavities in them were detected by listening to the sound generated when tapped by fingers. A similar sonic technique was used by blacksmiths to establish the soundness of the metals they were shaping. Even today, it is not uncommon to observe that inspectors assess structural health by hitting structures with a hammer and listening to the sounds they produce. These types of inspections, with various levels of sophistication, can be broadly termed as nondestructive evaluation (NDE) of health of a structure.

Early developments in SHA

Although the awareness of the scientific concepts of many NDE technologies began during 1920s, they experienced major growth during and after the Second World War. However, there had been always problems in the flow of NDE research to everyday use (Bray, 2000). Besides the use of Visual Testing (VT), early developments of instrument-based nondestructive detection of defects include Penetrate Testing (PT), Magnetic Particle Testing (MPT), Radiographic Testing (RT), Ultrasonic Testing (UT), Eddy Current Testing (ET), Thermal Infrared Testing (TIR), and Acoustic Emission Testing (AE). Many of them required the damage/irregularity to be exposed to the surface or within small depth from the open surface. Some of them required direct contact of sensors with the test surface (Hellier, 2003). They mainly focused on the "hot spot" areas or objects readily available for testing. For instance, RT has been routinely used for detection of internal physical imperfections such as voids, cracks, flaws, segregations, porosities, and inclusions in material at selective location(s). Most of these methods are non-model based, i.e., the structure need not be mathematically modeled to identify location and severity of defects.

Transition from past to present: new challenges

For most large civil infrastructure, the location(s), numbers, and severity of defect(s) may not be known in advance, although sometimes they can be anticipated using past experiences. Also, sometimes defects may be hidden behind obstructions, for an example, cracks in steel members hidden behind fire-proofing materials. Thus, instrument-based nondestructive testing (NDT) may not be practical if the inspector does not know what to inspect or the location of defect is not known *a priori*. During 1970s, detection of cracks was a major thrust. Subsequently, determination of crack size in order to compare with the critical crack size added another level of challenge to the engineering profession. In any case, inspection of "hot spot" areas limited their application potential. Subsequently, a consensus started developing about the use of measured responses to assess current structural health, as discussed next.

Model-based SHA

Some of the deficiencies in non-model based approaches can be removed by using model-based techniques. The aim of this approach is to predict the parameters of the assumed mathematical model of a physical system, i.e., the system is considered to behave in predetermined manner represented in algorithmic form using the governing differential equations, finite element (FE) discretization, etc. The changes in the parameters should indicate the presence of defects. To implement the concept, responses need to be measured by exciting the structure statically or dynamically.

SHA using static responses

Because of its simplicity, initially SHA using static responses were attempted. Static responses are generally measured in terms of displacements, rotations, or strains and the damage detection problems are generally formulated in an optimization framework employing minimization of error between the analytical and measured quantities. They mostly use FE model for structural representation. Three classes of error functions are reported in the literature: displacement equation error function, output error function, and strain output error function (Sanayei et al., 1997). Recently Bernal (2002) proposed flexibility-based damage localization method, denoted as the Damage Locating Vector (DLV) method. The basic approach is the determination of a set of vectors (i.e. the DLVs), which when applied as static forces at the sensor locations, no stress will be induced in the damaged elements. The method can be a promising damage detection tool as it allows locating damages using limited number of sensor responses. It was verified for truss elements, where axial force remains constant through its length. However, the verification of the procedure for real structures using noise-contaminated responses has yet to be completed.

There are several advantages of SHA using static responses including that the amount of data needed to be stored is relatively small and simple, and no assumption on the mass or damping characteristics is required. Thus, less errors and uncertainties are introduced into the model. However, there are several disadvantages including that the number of measurement points should be larger than the number of unknown parameters to assure a proper solution. Civil engineering structures are generally large and complex with extremely high overall stiffness. It may require extremely large static load to obtain measurable deflections. Fixed reference locations are required to measure deflections which might be impractical to implement for bridges, offshore platforms, etc. Also, static response-based methods are sensitive to measurement errors (Aditya and Chakraborty, 2008; Anh, 2009).

SHA using dynamic responses

Recent developments in SHA are mostly based on dynamic responses. There are several advantages of this approach. It is possible to excite structures by dynamic loadings of small amplitude relative to static loadings. In some cases, ambient responses caused by natural sources, e.g., wind, earthquake, moving vehicle, etc. can be used. If acceleration responses are measured, they eliminate the need for fixed physical reference locations. They perform well in presence of high measurement errors (Das et al., 2012).

Earlier works on SHA using dynamic responses are mostly modal information-based (Doebling et al. 1996; Sohn et al., 2004; Carden and Fanning, 2004; Montalvao, 2006; Fan and Qiao, 2010). Changes in modal properties, i.e., natural frequencies, damping, and mode shape vectors, or properties derived from these quantities are used as damage indicators. Doebling et al. (1996) presented various methods for damage identification including methods based on changes in frequency, mode shapes, mode shape curvature, and modal strain energy. Sohn et al. (2004) updated the above report and discussed procedures based on damping, anti-resonance, Ritz vectors, a family of autoregressive moving average (ARMA) models, canonical variate analysis, nonlinear features, time-frequency analysis, empirical mode decomposition, Hilbert transform, singular value decomposition, wave propagation, autocorrelation functions, etc. More complete information on them can be found in the literature cited above.

Natural frequency-based methods use change in the natural frequency as the primary feature for damage identification. They are generally categorized as forward problem or inverse problem. The forward problems deal with determination of changes in frequency based on location and severity of damage, whereas the inverse problems deal with determination of damage location and size based on natural frequency measurement. Among the mode shape-based procedures for damage detection, the mode shape/curvature methods generally use two approaches: traditional analysis of mode shape or curvature and modern signal processing methods using mode shapes or curvature. Modal strain energy-based procedures consider fractal modal energy for damage detection (Fan and Qiao, 2010). Methods based on damping have the advantage that a larger change in damping can be observed due to small cracks. Also, it is possible to trace nonlinear, dissipative effects produced by the cracks. However, damping properties have not been studied as extensively as natural frequencies and mode shapes (Sohn et al., 2004). Methods based on dynamically measured flexibility detect damages by comparing flexibility matrix synthesized using the modes of damaged structure to that of undamaged structure or flexibility matrix from FE analysis. The flexibility matrix is most sensitive to changes in the lower frequencies (Doebling, 1996).

Modal-based approaches have many desirable features. Instead of using enormous amount of data, the modal information can be expressed in countable form in terms of frequencies and mode shape vectors. Since structural global properties are evaluated, there may be an averaging effect, reducing the effect of noise in the measurements. However, the general consensus is that modal-based approaches fail to evaluate the health of individual structural elements; they indicate overall effect, i.e., whether the structure is defective or not (Ibanez, 1973; McCann, et al., 1998; Ghanem and Ferro, 2006). For complicated structural systems, the higher order calculated modes are unreliable and the minimum numbers of required modes to identify the system parameters is problem dependent, limiting their applicability. The mode shape vectors may be more sensitive to defects than the frequencies, but the fact remains that they will be unable to predict which element(s) caused the changes. It was reported that even when a member breaks, the natural frequency may not change more than 5%. This type of change can be caused by the noises in the measured responses. A time domain approach will be preferable.

Damages initiated during observations

A considerable amount of work is also reported on damages initiation time, commonly known as time-frequency methods for damage identification. The time-frequency localization capability has been applied for damage feature extractions from sudden changes, breakdown points, discontinuity in higher derivatives of responses, etc. They circumvent the modeling difficulty as they do not require the system to be identified and the health assessment strategy often reduces to the evaluation of symptoms reflecting the presence and nature of defect (Ceravolo, 2009). Extensive study on Short Time Fourier Transform (STFT), Wigner-Ville Distribution (WVD), Pseudo Wigner-Ville Distribution (PWVD), Choi-Williams Distribution (CWD), Wavelet Transform (WT), Hilbert Transform (HT), and Hilbert-Huang Transform (HHT) for analyzing any non-stationary events localized in time domain have been reported in the literature. STFT is an extension of the Fourier transform allowing for the analysis of non-stationary signals by dividing it into small time windows and analyzing each using the Fast Fourier Transform (FFT). The formulation provides localization in time as well as capturing frequency information simultaneously. WT has greater flexibility than STFT in terms of choosing different basis functions or mother wavelets. The Wavelets have finite duration and their energy is localized around a point in time. The WVD gives the energy distribution of a signal as a function of time and frequency; however, it has major shortcoming for multi-component signals in terms of cross-terms. The CWD provides filtered/smoothed version of the WVD by removing the cross-terms (Sajjad et al., 2007).

These studies are very interesting but there is no general consensus about the most suitable technique. Recently Yadav et al. (2011) studied some of the time-frequency procedures for defect characterization in a wave-propagation problem. However, the fundamental limitation of STFT, WVD, PWVD, CWD, and CWT is due to the fact that they are based on Fourier analysis and can accommodate only non-stationary phenomena in the data driven from linear systems; they are not suitable to capture nonlinear distortion. In this context, the HT and HHT are suitable for nonlinear and non-stationary data. Application of Hilbert Transform to nonlinear data requires the signal to be decomposed to 'mono-component' condition without any smaller, riding waves. The real advantage of HT is implemented in HHT proposed by Huang et al. (1998). The procedure consists of empirical mode decomposition (EMD) and Hilbert spectral analysis (HSA). HHT clearly define nonlinearly deformed waveforms; this definition can be the first indication of the existence of damage (Huang et al., 2005). They applied the concept for bridge health monitoring using two criteria: nonlinear characteristics of the intra-wave frequency modulations of the bridge response and frequency downshift as an indication of structural yield. Yang et al. (2004) proposed two HHT based procedures for identifying damage time instances, damage locations, and natural frequencies and damping ratios before and after occurrence of damage.

Structural health assessment – present

In an attempt to develop an ideal SHA technique for the rapid assessment of structural health, the research team at the University of Arizona identified several desirable features considering theoretical as well as implementation issues. The team concluded that a system identification (SI)-based approach using measured dynamic response information in time domain will have the most desirable attributes. A basic SI-based approach has three essential components: (a) the excitation force(s), (b) the system to be identified, generally represented by some equations in algorithmic form such as by FEs, and (c) the output response information measured by sensors. Using the excitation and response information, the third component i.e., the system can be identified. The basic concept is that the dynamic responses will change as the structure degrades. Since the structure is represented by FEs, by tracking the changes in the stiffness parameter of the elements, the location and severity of defects can be established.

For a structure with N dynamic degrees of freedom (DDOF), the dynamic governing equation can be written as:

$$\mathbf{M}\ddot{\mathbf{x}}(t) + \mathbf{C}\dot{\mathbf{x}}(t) + \mathbf{K}\mathbf{x}(t) = \mathbf{f}(t) \quad (1)$$

where $\mathbf{K}$, $\mathbf{M}$, $\mathbf{C}$ are $N \times N$ stiffness, mass, and damping matrix, respectively; $\mathbf{x}(t)$, $\dot{\mathbf{x}}(t)$, $\ddot{\mathbf{x}}(t)$, and $\mathbf{f}(t)$ are $N \times 1$ displacement, velocity, acceleration, and load vector, respectively, at time t. The acceleration time histories at the FE node points are expected to be measured by accelerometers. The velocity and displacement time histories can be generated by successively integrating the acceleration time histories, as suggested by Vo and Haldar (2003). Assuming mass is known, $\mathbf{K}$ matrix at the time of inspection can

be evaluated. Using the information on the current elements' stiffness properties and comparing them with the "as built" or expected properties, or deviation from the previous values if periodic inspections were conducted, the structural health can be assessed.

General challenges in time-domain SHA

Referring to the SI concept discussed earlier, structural stiffness parameters will be estimated by using information on excitation and measured responses. It is interesting to point out that according to Maybeck (1979) deterministic mathematical model and control theories do not appropriately represent the behavior of a physical system and thus the SI-based method may not be appropriate for SHA. He correctly pointed out three basic reasons: (a) a mathematical model is incapable of incorporating various sources of uncertainties and thus does not represent true behavior of a system, (b) dynamic systems are driven not only by controlled inputs but also by disturbances that can neither be controlled nor modeled using deterministic formulations, and (c) sensors used for data measurements cannot be perfectly devised to provide complete and perfect data about a system. These concerns and other implementation issues must be addressed before developing a SI-based SHA procedure.

Outside the controlled laboratory environment, measuring input excitation force(s) can be very expensive and problematic during health assessment of an existing structure. In the context of a SI-based approach, it will be desirable if a system can be identified using only measured response information, and completely ignoring the excitation information. This task is expected to be challenging since two of the three basic components of SI process will be unknown. Responses, even measured by smart sensors, are expected to be noise contaminated. Depending on the amount of noise, the SI-based approach may be inapplicable. The basic concept also assumes that responses will be available at all DDOFs. For large structural systems, it may be practically impossible or uneconomical to instrument the whole structure; only a part can be instrumented. Thus, the basic challenge is to identify stiffness parameters of a large structural system using limited noise-contaminated response information measured at a small part of the structure. The research team successfully developed such a method in steps, as discussed next.

SHA using responses at all DDOFs

Using noisy responses measured at all DDOFs, Wang and Haldar (1994) proposed a procedure, popularly known as Iterative Least-Squares with Unknown Input (ILS-UI). They used viscous damping and verified it for shear buildings. The efficiency of the numerical algorithm was improved later by introducing Rayleigh-type proportional damping; known as Modified ILS-UI or MILS-UI (Ling and Haldar, 2004). Later, Katkhuda et al. (2005) improved the concept further and called it Generalized ILS-UI or GILS-UI. All these are least-squares procedures. They were extensively verified using computer generated response information for shear buildings, two dimensional trusses, and frames. They added artificially generated white noises in the computer generated noise-free responses and showed that the methods could assess health of defect-free and defective structures. Recently, the concept has been verified for three dimensional (3D) structures; denoted as 3D-GILS-UI (Das and Haldar, 2010a, 2010b).

For the sake of completeness, other recently proposed least-squares based SHA procedures need a brief review. Yang et al. (2007) proposed a recursive least-squares estimation procedure with unknown inputs (RLSE-UI) for the identification of stiffness, damping, and other nonlinear parameters, and the unmeasured excitations. They implemented an adaptive technique (Yang and Lin, 2005) in RLSE-UI to track the variations of structural parameters due to damages. Then, Yang et al. (2006) proposed a new data analysis method, denoted as the sequential nonlinear least-square (SNLSE) approach, for the on-line identification of structural parameters. Later Yang and Huang (2007) extended the procedure for unknown excitations and reduced number of sensors (SNLSE-UI-UO). They verified the procedures for simple linear and nonlinear structures. Several other methods based on least-squares can be found in Chio et al. (2001), Chase et al. (2005a, b), Garrido and Rivero-Angeles (2006).

After analytically establishing the concept that a structure can be identified using only noise-contaminated response information, completely ignoring the excitation information, the research team at the University of Arizona tested a one dimensional beam (Vo and Haldar, 2004) and a two dimensional frame built to one-third scale in the laboratory (Martinez-Flores and Haldar, 2007; Martinez-Flores et al., 2008). The test setups for the two studies are

shown in Figs. 1 and 2, respectively. Both studies conclusively confirmed the validity of the basic the SI concept without excitation information.

SHA using limited response information – measured at a small part of the structure

It is now established that least-squares concept can be used for SHA without using excitation information but response information must be available at all DDOFs. This led the team to study cases when response information is available only at a part of the structure. Kalman filter-based algorithm is commonly used when the system is uncertain and the responses are noise-contaminated and not available at all DDOFs.

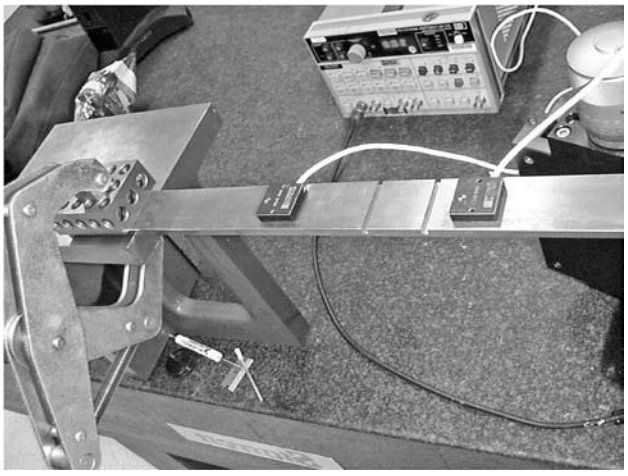

Figure 1. Laboratory Test of Defective Beams

Kalman filter

Application of Kalman Filter (KF) for assessing health for civil engineering structures is relatively recent. Various forms of Kalman Filter can be found in the literature including Extended Kalman Filter (EKF), Unscented Kalman Filter (UKF), Particle Filter (PF), Ensemble Kalman Filter (EnKF), etc. In mathematical sense, the basic KF is a non-deterministic, recursive computational procedure to provide best estimate of the states by minimizing the mean of squared error for a process governed by linear stochastic differential equation expressed as (Welch and Bishop, 2006):

$$\mathbf{x}(k+1) = \mathbf{F}(k)\mathbf{x}(k) + \mathbf{G}(k)\mathbf{u}(k) + \mathbf{w}(k) \tag{4}$$

with the measurement model of the form:

$$\mathbf{z}(k+1) = \mathbf{H}(k+1)\mathbf{x}(k+1) + \mathbf{v}(k+1) \tag{5}$$

where $\mathbf{x}(k+1)$ and $\mathbf{x}(k)$ are the state vectors at time instant k+1 and k, respectively, vectors $\mathbf{w}(k)$ and $\mathbf{v}(k)$ represent the process and measurement noises, respectively, $\mathbf{F}(k)$ relates the two state vectors in absence of either a driving function or process noise, $\mathbf{G}(k)$ relates the optimal control input $\mathbf{u}(k)$ to the state, and $\mathbf{H}(k+1)$ in the measurement model relates the state vector to the measurement vector $\mathbf{z}(k+1)$. $\mathbf{w}(k)$ and $\mathbf{v}(k)$ are considered to be independent, zero-mean, white random vectors with normal probability distributions. Kalman filter is very powerful in several ways. It incorporates the (i) knowledge of the system, (ii) statistical description of the system noises, measurement errors and uncertainty in the dynamic models, and (iii) any available information on the initial conditions of the variables of interest (Maybeck, 1979).

Figure 2. Experimental Verification of a Scaled 2D frame

The basic KF is essentially applicable for linear structural behavior. For SHA of civil engineering structures, the behavior may not be linear. Moderate to high level of excitation may force the structure to behave nonlinearly. Presence of defects may also cause nonlinearity, even when the excitation is at the low level. This leads to the development of the extended Kalman filter (EKF) concept. For EKF, Eqs. (4) is expressed in the following form (Welch and Bishop, 2006):

$$\mathbf{x}(k+1) = f\left[\mathbf{x}(k), \mathbf{u}(k), \mathbf{w}(k)\right] \tag{6}$$

and the measurement equation, Eq. (5) is modified as:

$$\mathbf{z}(k+1) = h\left[\mathbf{x}(k+1), \mathbf{v}(k+1)\right] \quad (7)$$

where nonlinear function f relates the states at time k to the current states at time k+1, and it includes the state vector $\mathbf{x}(k)$, driving force $\mathbf{u}(k)$ and process noise $\mathbf{w}(k)$. The nonlinear function h relates the state vector $\mathbf{x}(k+1)$ to the measurement vector $\mathbf{z}(k+1)$. Again, $\mathbf{w}(k)$ and $\mathbf{v}(k)$ are the independent, zero-mean, white random vectors with normal distribution, representing the process and measurement noises, respectively. The EKF estimates the state by linearizing the process and measurement equations about the current states and covariances. KF or EKF attempts to predict responses and the model parameters, and then updates them at each time point using current measurements. The procedure involving prediction and updating at each time point is generally known as *local iteration*. Completion of local iteration processes covering all time instances in the entire time-history of responses is generally known as first *global iteration*. The global iterations need to be repeated to satisfy the pre-selected convergence criterion of system parameters. Hoshiya and Saito (1984) proposed a Weighted Global Iteration (WGI) procedure with an objective function after the first global iteration to obtain convergence in an efficient way. The entire procedure is denoted as EKF-WGI. Recently, several researchers have improved computational aspects of EFK-WGI (Das et al., 2012). Koh and See (1994) proposed an adaptive EKF (AEKF) to estimate both the parameter values and associated uncertainties in the identification. Yang et al. (2006) proposed an adaptive tracking technique based on EKF to identify structural parameters and their variation during damage events. Ghosh et al. (2007) developed two novel forms of EKF-based parameter identification techniques; these are based on variants of the derivative-free locally transversal linearization (LTL) and multi-step transverse linearization (MTrL) procedures. Liu et al. (2009) proposed multiple model adaptive estimators (MMAE) that consists of bank of EKF designed in the modal domain (MOKF) and incorporated fuzzy logic-based block in EKF to estimate variance of measurement noise.

When KF or EKF is used to identify a structure using dynamic response information satisfying the governing equation represented by Eq. (1), it requires that the excitation information and the initial values of unknown state vector. As mentioned earlier, to improve implementation potential, the proposed approach needs to identify a structure without using excitation information and the information on the state vector will be available only at the completion of the identification, not at the beginning. The discussions clearly indicate that the basic KF or EKF cannot be used to identify a structure. To overcome these challenges, the research team proposed a two-stage approach by combining GILS-UI and EKF-WGI procedures. Based on the available measured responses, a substructure can be selected that will satisfy all the requirements to implement the GILS-UI procedure in Stage 1. At the completion of Stage 1, the information on the unknown excitation and the damping and stiffness parameters of all the elements in the substructure will be available. The identified damping can be assumed to be applicable for the whole structure. Structural members in a structure are expected to have similar cross sectional properties. Suppose the substructure consists of one beam and one column. The identified stiffness parameters of the beam in the substructure can be assigned to all the beams in the structure. Similarly, the identified stiffness parameters of the column can be assigned to all the columns. This will give information on the initial state vector. With the information on initial state vector and excitation information, the EKF-WGI procedure can be initiated to identify the whole structure in Stage 2. This novel concept was developed in stages; they are known as ILS-EKF-UI (Wang and Haldar, 1997), MILS-EKF-UI (Ling and Haldar, 2004), and GILS-EKF-UI (Katkhuda and Haldar, 2008). These procedures were successfully verified using analytically generated responses, primarily for two dimensional structures (Katkhuda, 2004; Haldar and Das, 2010). Martinez-Flores et al. (2008) then successfully verified GILS-EKF-UI in the laboratory for a two dimensional frame shown in Fig. 2. They considered defect-free and several defective states with different levels of severities, including broken members, loss of cross sectional area over the entire length of members, loss of area over small length of a member, presence of one or multiple cracks in a member, etc. Das and Haldar (2012) recently extended the method to assess structural health for 3D structures.

Future of structural health assessment

Future directions of the SHA area, as foreseen by the authors, are presented in the following sections. In the previous sections, the authors emphasized analytical concepts used for SHA and their contributions. In developing their methods, they observed many challenges yet to be resolved. Some issues are related to explicit consideration of uncertainty in describing the system and noises in the

measured responses. Selection of initial state vector for large structure is also expected to be challenging. Although EKF can be used in presence of nonlinearity, the threshold nonlinearity is not known, i.e., when it will fail to identify a structure. The methods proposed by the authors can identify structures with less information, but the absolute minimum number of required responses for acceptable identification needs further study. Issues related to the stability, convergence, and acceptable error in prediction need further works. Although the information of excitation is not required, characteristics of excitations need some attentions.

At the beginning of the paper, the authors mentioned that SHA is a multidisciplinary research area. This paper will not be complete without the discussions on sensors, intelligent sensing technologies and signal processing, next generation structural health monitoring strategies, etc. Since SHA is a relatively new area and not covered in the existing curriculum of major branches of engineering, it is necessary to emphasize education aspect of SHA. The authors are not expert in some of these areas; however, they expect that the discussions will prompt future engineers to explore them. The first author is in the process of editing a book with contributions from experts covering all these areas (Haldar, 2012).

Transition from present to future: local level sha using global responses

SHA procedures are developed generally assuming that measured responses will be altered in presence of defects. Obviously, minor defects may not alter the responses and thus cannot be detected. A structure is expected to be inspected several times during its lifetime. Minor defects such as initiation and development of cracks, corrosion of reinforcements in concrete, etc., are expected to grow over time. The basic assumption is that when they become major, they will be detected during the periodic inspections. Environmental influences on structural behavior, for example, effect of temperature on measured responses is not completely understood at this time. Similar comments can be made for exposure to chemicals or high pressure gradients. Smart sensors are now being developed to detect damage for various applications. Not all sensors are equally sensitive and noises in the measurements cannot be avoided. Depending upon to noise to signal ratios, the output of a sensor can be misleading. The discussions clearly indicate that besides analytical developments, industrial research is also going to be critical in implementing a particular health assessment strategy. Hopefully, advances in technologies, digital computing and data processing will remove some of these hurdles.

SHA in presence of nonlinearity

One major assumption in most SI-based SHA procedures is that the responses are linear or mildly nonlinear. Major nonlinearities are not expected to show up in the responses during ambient excitation or when the level of excitation is relatively small. However, in real situations, the nonlinearity in the responses cannot be avoided. To understand and develop robust mathematical model of the dynamical system, the distinct effects of nonlinearities must be realistically accounted for. At the same time, it will be important to use the available resources in a very systematic manner for successful implementation of the SHA procedures. To identify a highly nonlinear structure, it is important first to identify the level of nonlinearity and establish whether available methods are appropriate or not. Next, it will be important to determine the location, type, and form of nonlinearity and how to model them in the optimum way. Another important task will be the selection of parameters/ coefficients that need to be tracked for damage assessment. The area of nonlinear system identification is still in its infancy. An extensive discussion on the related areas and future directions in nonlinear SI is discussed by Kerschen et al. (2006).

Intelligent sensing technologies and signal processing

Development of new sensor technologies for various applications is expanding in an exponential scale. Use of smart wireless sensors is becoming very common. The placements of sensors, density, sources of power for their operation, calibration for maintaining them in good operating condition, acquisition of signals, advanced signal processing algorithms considering increased signal-to-noise ratio, well-developed numerical procedure for post-processing of signal, integration of software and hardware, realistic mathematical model for structures and their components, etc., are being actively studied by various researchers. Smart sensors are wireless and equipped with on-board microprocessors; they are small in size and can be procured at a lower cost. However, there are several hardware aspects such as efficient data acquisition, synchronization, limited memory, encryption and secured data transmission, limited bandwidth need further attention. They should

be operational throughout the life of the structure, if continuous-time SHA is performed (Chang et al., 2003). It is expected that distributed computational framework and use of agents-based architecture will expand the possibility of intelligent infrastructure maintenance in future (Spencer et al., 2004).

Next generation structural health monitoring strategy

Structural systems always change due to inevitable deterioration processes. Assessment of current state of a structure cannot be complete without taking into account the uncertainties at every step of the assessment process. Even ignoring uncertainties, monitoring a structure continuously throughout its life, may not be an optimum use of available resources. Next generation structural health monitoring research needs to be performance-based. Using information from the most recent assessment, mathematical model to represent the structure, placement of sensors, data collection and interpretation methods need to be modified or updated. The integration of past and present information on structural health needs to be carried out for the cost-efficient assessment. Risk-based nondestructive evaluation concept is expected to optimize the frequency of inspection.

SHA Curriculum in education

The authors sincerely hope that the previous discussions provided a flavor of multi-disciplinary nature of SHA areas. Both authors are civil engineers. Their formal education in civil engineering did not train them to undertake the research discussed here. Most engineering colleges do not offer courses related to SHA. NDE mostly belongs to mechanical engineering, whereas sensors and signal processing belong to electrical engineering. So far the SHA/SHM education for professional engineers is limited to web-based resources or short course modules. Recently, several universities in Europe are collaboratively offering an Advanced Master's in Structural Analysis of Monuments and Historical Constructions (SAMHC) funded by the European Commission. In the U.S., University of California, San Diego has started M. S. program with specialization in SHM.

There is no doubt that the SHA/SHM areas will grow exponentially in near future all over the world. Trained engineers will be essential to carry out the necessary works. A severe shortage of trained professionals is expected. It will be highly desirable if we introduce a multi-disciplinary engineering discipline in SHA/SHM by integrating civil, electrical, material, and mechanical engineering departments.

Conclusions

Structural health assessment has become an important research topic and attracted multi-disciplinary research interests. Its growth has been exponential in the recent past. Past and present developments in the related areas are briefly reviewed in this paper. Because of their academic background, the authors emphasized the structural health assessment for civil infrastructures. Some of the future challenges are also identified. Advancements in sensor technology and signal processing techniques are also reviewed briefly. An upcoming edited book on the subject by the first author is expected to provide more information on the related areas. Because of the newness of the area, there is a major gap in current engineering curriculum. In the near future a severe shortage is expected for experts with proper training in SHA/SHM. The authors advocate for a new multi-disciplinary engineering discipline in SHA/SHM by integrating, civil, electrical, material, and mechanical engineering departments.

References

1. Aditya, G. and S. Chakraborty (2008). "Sensitivity Based Health Monitoring of Structures with Static Responses," Scientia Iranica, **15**(3), 267-274.
2. Anh, T.V., 2009. Enhancements to the damage locating vector method for structural health monitoring, Ph. D. Dissertation, National University of Singapore, Singapore.
3. Bernal, D. (2002). "Load Vectors for Damage Localization," J. Engrg. Mech., ASCE, **128**(1), 7-14.
4. Bray, D.E. (2000). "Historical Review of Technology Development in NDE," 15th World Conference on Nondestructive Testing, Roma, Italy, 15-21 October.
5. Carden, E.P. and P. Fanning (2004). "Vibration Based Condition Monitoring: A Review," Struct. Health Monitoring, **3**(4), 355-377.
6. Ceravolo, R. (2009). "Time–Frequency Analysis," Chapter 26, Encyclopedia of Structural Health Monitoring, Ed. C. Boller, F-K. Chang, and Y. Fuzino, John Wiley & Sons, Ltd.
7. Chang, P.C., A. Flatau, and S.C. Liu (2003). "Review Paper: Health Monitoring of Civil Infrastructure," Struct. Health Monitoring, **2**(3), 257-267.
8. Chase, J.G., H.A. Spieth, C.F. Blome, and J.B. Mandler (2005b). "LMS-based Structural Health Monitoring of a Non-linear Rocking Structure," Earthquake Engrg. and Struct. Dyn., **34**, 909-930.
9. Chase, J.G., V. Begoc, and L.R. Barroso (2005a). "Efficient Structural Health Monitoring for Benchmark Structure using Adaptive RLS Filters," Comp. and Struct., **83**, 639-647.

10. Choi, Y.M., H.N. Cho, Y.B. Kim, and Y.K. Hwang (2001). "Structural Identification with Unknown Input Excitation," KSCE J Civil Engrg., **5**(3), 207-213.
11. Das, A.K. and A. Haldar (2010a). "Structural Integrity Assessment under Uncertainty for Three Dimensional Offshore Structures," Int. J. Terraspace Sc. and Engrg. (IJTSE), **2**(2), 101-111.
12. Das, A.K. and A. Haldar (2010b). "Structural Health Assessment of Truss-type Bridges using Noise-contaminated Uncertain Dynamic Response Information," Int. J. Engrg. under Uncertainty: Hazards, Assessment, and Mitigation, **2**(3-4), 75-87.
13. Das, A.K. and A. Haldar (2012). "Health Assessment of Three Dimensional Large Structural Systems – A Novel Approach," Int. J. Life Cycle Reliability and Safety Engineering, to be published in January, 2012.
14. Das, A.K., A. Haldar, and S. Chakraborty (2012). "Health Assessment of Large Two Dimensional Structures using Minimum Information – Recent Advances," Advances in Civil Engrg., **2012**, Article ID 582472, doi:10.1155/2012/582472.
15. Doebling, S.W., C.R. Farrar, M.B. Prime, and D.W. Shevitz, 1996. Damage Identification and Health Monitoring of Structural and Mechanical Systems from Changes in their Vibration Characteristics: A Literature Review, Los Alamos National Laboratory, Report No. LA-13070-MS.
16. Fan, W. and P. Qiao (2010). "Vibration-based Damage Identification Methods: A Review and Comparative Study," Struct. Health Monitoring, **0**(0), 1-29.
17. Garrido, R. and F.J. Rivero-Angeles (2006). "Hysteresis and Parameter Estimation of MDOF Systems by a Continuous-Time Least-Squares Method," J. Earthquake Engrg., **10**(2), 237-264.
18. Ghanem, R. and G. Ferro (2006). "Health Monitoring for Strongly Non-linear Systems using the Ensemble Kalman Filter," Struct. Control and Health Monitoring, **13**, 245-259.
19. Ghosh, S., D. Roy, and C.S. Manohar (2007). "New Forms of Extended Kalman Filter via Transversal Linearization and Applications to Structural System Identification," Comp. Methods in App. Mech. and Engrg., **196**, 5063-5083.
20. Haldar, A. and A.K. Das (2010). "Prognosis of Structural Health – Nondestructive Methods," Int. J. Performability Engrg., Special Issue on Prognostics and Health Management (PHM), **6**(5), 487-498.
21. Haldar, A., editor, (2012). Health Assessment of Engineered Structures: Bridges, Buildings and Other Infrastructures, World Scientific Publishing Co.
22. Hellier, C.J., (2003). Handbook of Nondestructive Evaluation, The McGraw-Hill Companies, Inc.
23. Hoshiya, M. and E. Saito (1984). "Structural Identification by Extended Kalman Filter," J. Engrg. Mech., ASCE, **110**(12), 1757-1770.
24. Huang, N.E., K. Huang, and W-L. Chiang (2005). "HHT-Based Bridge Structural-Health Monitoring," Chapter 12, Hilbert-Huang Transform and Its Applications, Ed. N.E. Huang and S.S.P. Shen, World Scientific Publishing Co. Pte. Ltd., Singapore.
25. Huang, N.E., Z. Shen, S.R. Long, M.C. Wu, H.H. Shih, Q. Zheng, N-C. Yen, C.C. Tung, and H.H. Liu (1998). "The Empirical Mode Decomposition and the Hilbert Spectrum for Nonlinear and Non-stationary Time Series Analysis," Proc. R. Soc. Lond. A., **454**, 903-995.
26. Ibanez, P. (1973). "Identification of Dynamic Parameters of Linear and Non-linear Structural Models from Experimental Data," Nucl. Engrg. and Design, **25**, 30-41.
27. Katkhuda, H. and A. Haldar (2008). "A Novel Health Assessment Technique with Minimum Information," Struct. Cont. & Health Monitoring, **15**(6), 821-838.
28. Katkhuda, H., 2004. In-service health assessment of real structures at the element level with unknown input and limited global responses, Ph. D. Thesis, University of Arizona, Tucson, USA.
29. Katkhuda, H., R. Martinez-Flores, and A. Haldar (2005). "Health Assessment at Local Level with Unknown Input Excitation," J. Struct. Engrg., ASCE, **131**(6), 956-965.
30. Kerschen, G., K. Worden, A.F. Vakakis, and J.C. Golinval (2006). "Past, Present and Future of Nonlinear System Identification in Structural Dynamics," Mech. Sys. and Sig. Processing, **20**(3), 505-592.
31. Koh, C.G. and L. M. See, "Identification and Uncertainty Estimation of Structural Parameters," J. Engrg. Mech., **120**(6), 1219-1236.
32. Ling, X. and A. Haldar (2004). "Element Level System Identification with Unknown Input with Rayleigh Damping," J. Engrg. Mech., ASCE, **130**(8), 877-885.
33. Liu, X., P.J. Escamilla-Ambrosio, and N.A.J. Lieven (2009). "Extended Kalman Filtering for the Detection of Damage in Linear Mechanical Structures," J. Sound and Vib., **325**, 1023-1046.
34. Martinez-Flores, R. and A. Haldar (2007). "Experimental Verification of a Structural Health Assessment Method without Excitation Information," J. Struct. Engrg., **34**(1), 33-39.
35. Martinez-Flores, R., H. Katkhuda, and A. Haldar (2008). "A Novel Health Assessment Technique with Minimum Information: Verification," Int. J. Performability Engrg., **4**(2), 121-140.
36. Maybeck, P.S., (1979). Stochastic Models, Estimation, and Control Theory, Academic Press, Inc., UK.
37. McCaan, D., N.P. Jones, and J.H. Ellis (1998). "Toward Consideration of the Value of Information in Structural Performance Assessment," Paper No. T216-6, Structural Engineering World Wide, CD-ROM.
38. Montalvao, M., N.M.M. Maia, and A.M.R. Ribeiro (2006). "A Review of Vibration-Based Structural Health Monitoring with Special Emphasis on Composite Materials," Shock and Vib. Digest, **38**(4), 295-324.
39. Rytter, A., 1993. Vibration based inspection of civil engineering structures, Ph. D. Dissertation, Department of Building Technology and Structural Engineering, Aalborg University, Denmark.
40. Sajjad.S., H. Zaidi, W.G. Zanardelli, S. Aviyente, and E.G. Strangas (2007). "Comparative Study of Time-Frequency Methods for the Detection and Categorization of Intermittent Fault in Electrical Devices," Diagnostics for Electric Machines, Power Electronics and Drive, SDEMPED, IEEE Symp., Sept 6-8, 39-45.
41. Sanayei, M., G.R. Imbaro, J.A.S. McClain, and L.C. Brown (1997). "Structural Model Updating using Experimental Static Measurements," J. Struct. Engrg, ASCE, **123**(6), 792-798.

42. Sohn, H., C.R. Farrar, F.M. Hemez, D.D. Shunk, D.W. Stinemates, B.R. Nadler, and J.J. Czarnecki, 2004. A review of structural health monitoring literature: 1996-2001, Los Alamos National Laboratory, LA-13976-MS.
43. Spencer Jr., B.F., M.E. Ruiz-Sandoval, and N. Kurata (2004). "Smart Sensing Technology: Opportunities and Challenges," Struct. Control and Health Monitoring, **11**, 349-368.
44. Vo, P.H. and A. Haldar (2003). "Post Processing of Linear Accelerometer Data in System Identification," J. Struct. Engrg., **30**(2), 123-130.
45. Vo, P.H. and A. Haldar (2004). "Health Assessment of Beams - Theoretical and Experimental Investigation," J. Struct. Engrg., Special Issue on Advances in Health Monitoring/Assessment of Structures Including Heritage and Monument Structures, **31**(1), 23-30.
46. Wang, D. and A. Haldar (1994). "An Element Level SI with Unknown Input Information," J. Engrg. Mech., ASCE, **120**(1), 159-176.
47. Welch, G. and G. Bishop, 2006. An Introduction to the Kalman Filter, Tech. Rep. TR95-041 2006, Department of Computer Science, University of North Carolina at Chapel Hill, NC.
48. Yadav, S.K., S. Banerjee, and T. Kundu (2011). "Effective Damage Sensitive Feature Extraction Methods for Crack Detection using Flaw Scattered Ultrasonic Wave Field Signal," Proceedings of the 8th International Workshop on Structural Health Monitoring, Stanford, USA, September 13-15.
49. Yang J.N., S. Lin, H.W. Huang, and L. Zhou (2006). "An Adaptive Extended Kalman Filter for Structural Damage Identification," J. Struct. Cont. and Health Monitoring, **13**, 849–867.
50. Yang, J.N. and H. Huang (2007). "Sequential Non-linear Least-square Estimation for Damage Identification of Structures with Unknown Inputs and Unknown Outputs," Int. J. Non-lin. Mech., **42**, 789-801.
51. Yang, J.N. and S. Lin (2005). "Identification of Parametric Variations of Structures Based on Least Squares Estimation and Adaptive Tracking Technique," J. Engrg. Mech., **131**(3), 290-298.
52. Yang, J.N., H. Huang, and S. Lin (2006). "Sequential Non-linear Least-square Estimation for Damage Identification of Structures," Int. J. Non-lin. Mech., **41**, 124-140.
53. Yang, J.N., S. Pan, and S. Lin (2007). "Least-Squares Estimation with Unknown Excitations for Damage Identification of Structures," J. Engrg. Mech., **133**(1), 12-21.
54. Yang, J.N., Y. Lei, S. Lin, and N. Huang (2004). "Hilbert-Huang Based Approach for Structural Damage Detection," J. Engrg. Mech., **130**(1), 85-95.
55. Wang, D. and A. Haldar (1997), "System Identification with Limited Observations and without Input," J. Engrg. Mech., ASCE, 123(5), 504-511.

SRESA JOURNAL SUBSCRIPTION FORM

Subscriber Information (Individual)

_____ _____ _____ _____

Title First Name Middle Name Last Name

_____ _____

Street Address Line 1 Street Address line 2

_____ _____ _____ _____ _____

City State/Province Postal Code Country

_____ _____ _____

Work Phone Home Phone E-mail address

Subscriber Information (Institution)

Name of Institution/ Library _____

Name and Designation of Authority for Correspondence _____

Address of the Institution/Library _____

Subscription Rates

	Subscription Quantity	Rate	Total
Annual Subscription (in India)	_____	Rs 10,000	_____
(Abroad)	_____	$ 500	_____
	_____		_____
	_____		_____

Payment mode (please mark)

Cheque ☐ Credit Card ☐ Master Card ☐ Visa ☐ Online Banking ☐ Cash ☐ De mand Draft ☐

Credit card Number _____

Credit Card Holders Name _____

Credit Card Holde _____

Guidelines for Preparing the Manuscript

A softcopy of the complete manuscript should be sent to the Chief-Editors by email at the address: editor@sresa.org.in. The manuscript should be prepared using 'Times New Roman' 12 font size in double spacing, on an A-4 size paper. The illustrations and tables should not be embedded in the text. Only the location of the illustrations and tables should be indicated in the text by giving the illustration / table number and caption.

The broad structure of the paper should be as follows: a) Title of the paper – preferably crisp and such that it can be accommodated in one or maximum two lines with font size of 14 b) Name and affiliation of the author(s), an abstract of the paper in ~ 100 words giving brief overview of the paper and d) Five key words which indicates broad subject category of the paper. The second page of the paper should start with the title followed by the Introduction

A complete postal address should be given for all the authors along with their email addresses. By default the first author will be assumed to be the corresponding author. However, if the first author is not the corresponding author it will be indicated specifically by putting a star superscript at the end of surname of the author.

The authors should note that the final manuscript will be having double column formatting, hence, the size of the illustration, mathematical equations and figures should be prepared accordingly.

All the figures and tables should be supplied in separate files along with the manuscript giving the figure / table captions. The figure and table should be legible and should have minimum formatting. The text used in the figures and tables should be such that after 30% reduction also it should be legible and should not reduced to less than font 9.

Last section of the paper should be on list of references. The reference should be quoted in the text using square bracket like '[1]'in a chronological order. The reference style should be as follow:

1. Pecht M., Das D, and Varde P.V., "Physics-of-Failure Method for Reliability Prediction of Electronic Components", Reliability Engineering and System Safety, Vol 35, No. 2, pp. 232- 234, 2011.

After submitting the manuscript, it is expected that reviews will take about three months; hence, no communication is necessary to check the status of the manuscript during this period. Once, the review work is completed, comments, will be communicated to the author.

After receipt of the revised manuscript the author will be communicated of the final decision regarding final acceptance. For the accepted manuscript the author will be required to fill the copy right form. The copy right form and other support documents can be down loaded from the SRESA website: http://www.sresa.org.in

Authors interested in submitting the manuscript for publication in the journal may send their manuscripts to the following address:

Society for Reliability and Safety
RN 68, Dhruva Complex
Bhabha Atomic Research Centre,
Mumbai – 400 085 (India)
e-mail : editor@sresa.org.in

The Journal is published on quarterly basis, i.e. Four Issues per annum. Annual Institutional Subscription Rate for SAARC countries is Indian Rupees Ten Thousand (Rs. 10,000/-) inclusive of all taxes. Price includes postage and insurance and subject to change without notice. For All other countries the annual subscription rate is US dollar 500 ($500). This includes all taxes, insurance and postage.

Subscription Request can be sent to SRESA Secretariat (please visit the SRESA website for details)

SRESA Journal of

Life Cycle Reliability and Safety Engineering

Contents

Vol. 1 Issue No. 4 Oct – December 2012 ISSN – 2250 0820

1. **Seismic Fragility Analysis of a Primary Containment Structure Using IDA**
Tushar K. Mandal, Siddhartha Ghosh, Ajai S Pisharady (India)..... 1

2. **Refined Modeling of Crack Tortuousness to Predict Pressurized Air Flow Through Concrete Cracks**
L.R. Bishnoi, R.P. Vedula, S.K. Gupta (India) 10

3. **Estimating the Rain-Flow fatigue Damage in wind Turbine Blades Using Polynomial Chaos**
N Ganesh, Sayan Gupta (India)…….. 17

4. **Structural Reliability Evaluation and Optimization of a Pressure Vessel Using Non-Linear Performance Functions**
P Bhattacharjee, K Ramesh Kumar,Dr. T A Janardhan Reddy (India).....26

5. **On Reliability Evaluation of Structures using Hermite Polynomial Chaos**
Sabarethinam Kameshwar, Arunasis Chakraborty (India)…….....33

6. **Past, Present and Future of Engineering under Uncertainty: Safety Assessment and Management**
Achintya Haldar (USA) …….....39

7. **Past, Present, and Future of Structural Health Assessment**
Achintya Haldar and Ajoy Kumar Das (USA) …….....53